

INVESTIGATIONS OF UPSCALING EFFECTS FOR AERODYNAMIC
DESIGN OF LARGE WIND TURBINE ROTORS BY USING BEM THEORY
AND OPTIMIZATION

A THESIS SUBMITTED TO
THE GRADUATE SCHOOL OF NATURAL AND APPLIED SCIENCES
OF
MIDDLE EAST TECHNICAL UNIVERSITY

BY

OZAN KESİKBAŞ

IN PARTIAL FULFILLMENT OF THE REQUIREMENTS
FOR
THE DEGREE OF MASTER OF SCIENCE
IN
AEROSPACE ENGINEERING

DECEMBER 2019

Approval of the thesis:

**INVESTIGATIONS OF UPSCALING EFFECTS FOR AERODYNAMIC
DESIGN OF LARGE WIND TURBINE ROTORS BY USING BEM THEORY
AND OPTIMIZATION**

submitted by **OZAN KESİKBAŞ** in partial fulfillment of the requirements for the degree of **Master of Science in Aerospace Engineering Department, Middle East Technical University** by,

Prof. Dr. Halil Kalıpçılar
Dean, Graduate School of **Natural and Applied Sciences**

Prof. Dr. İsmail Hakkı Tuncer
Head of Department, **Aerospace Engineering**

Assoc. Prof. Dr. Nilay Sezer Uzol
Supervisor, **Aerospace Engineering, METU**

Examining Committee Members:

Assist. Prof. Dr. Mustafa Perçin
Aerospace Engineering, METU

Assoc. Prof. Dr. Nilay Sezer Uzol
Aerospace Engineering, METU

Assist. Prof. Dr. Munir Elfarra
Aerospace Engineering, Ankara Yıldırım Beyazıt University

Assist. Prof. Dr. Ozan Keysan
Electrical and Electronics Engineering, METU

Assist. Prof. Dr. Elif Oğuz
Civil Engineering, METU

Date: 13.12.2019

I hereby declare that all information in this document has been obtained and presented in accordance with academic rules and ethical conduct. I also declare that, as required by these rules and conduct, I have fully cited and referenced all material and results that are not original to this work.

Name, Surname: Ozan KESİKBAŞ

Signature:

ABSTRACT

INVESTIGATIONS OF UPSCALING EFFECTS FOR AERODYNAMIC DESIGN OF LARGE WIND TURBINE ROTORS BY USING BEM THEORY AND OPTIMIZATION

KESİKBAŞ, Ozan

Master of Science, Aerospace Engineering
Supervisor: Assoc. Prof. Dr. Nilay Sezer Uzol

December 2019, 96 pages

In recent years, wind power has become one of the most preferred and accepted renewable energy sources. However, there are still design challenges of new wind turbines especially upscaling problems as the size of rotor blades gets larger and larger. The main objective of this research is to understand scaling effects on wind turbine design by investigating and developing new design and scaling methodologies. For the design studies, the 5 MW NREL wind turbine is used as the baseline rotor. For the upscaling studies, this selected 5 MW baseline wind turbine is scaled up to 10, 15 and 20 MW wind turbines by using the classical upscaling method which is a linear scaling rule. For the optimization studies based on the blade element momentum theory and multipurpose genetic algorithm, the 5 MW NREL wind turbine blade which is taken as the reference blade is first optimized and analyzed. Then, the aerodynamic shape and blade mass of the upscaled 10 MW, 15 MW and 20 MW wind turbines are optimized. The optimization studies are conducted to maximize power generation and minimize blade mass. The aerodynamic and structural parameters of the rotor blades such as chord length, twist angle, blade mass and blade stiffness are compared. Then, the aerodynamic and structural performance analyses are done by using the FAST software and the results are compared for the reference blade,

upscaled blades, and optimized blades. Finally, based on the results for the optimized wind turbines, new scaling trends are formulated as a function of rotor diameter to understand the re-sizing effects on wind turbines.

Keywords: Wind Turbine, Upscaling Effects, Genetic Algorithm, Optimization, Blade Element Momentum Theory, Aerodynamic and Structural Analyses

ÖZ

PALA ELEMANI MOMENTUM TEORİSİ VE OPTİMİZASYON KULLANARAK BÜYÜK RÜZGAR TÜRBİNİ ROTORLARININ AERODİNAMİK TASARIMI İÇİN YUKARI ÖLÇEKLENDİRME ETKİLERİNİN İNCELENMESİ

KESİKBAŞ, Ozan
Yüksek Lisans, Havacılık ve Uzay Mühendisliği
Tez Danışmanı: Doç. Dr. Nilay Sezer Uzol

Aralık 2019, 96 sayfa

Son yıllarda, rüzgar enerjisi en çok tercih edilen ve kabul edilen yenilebilir enerji kaynaklarından biri haline gelmiştir. Bununla birlikte, yeni rüzgar türbinlerinin tasarım zorlukları hala vardır, özellikle de yukarı ölçeklendirme problemleri, çünkü rotor kanat büyüklükleri gittikçe artmaktadır. Bu araştırmanın temel amacı, yeni tasarım ve ölçeklendirme yöntemlerini araştırarak ve geliştirerek, rüzgar türbini tasarımında ölçeklendirme etkilerini anlamaktır. Tasarım çalışmaları için, 5 MW NREL rüzgar türbini temel rotor olarak kullanılmıştır. Yukarı ölçeklendirme çalışmaları için, seçilen bu 5 MW temel rüzgar türbini, doğrusal ölçeklendirme kuralı olan klasik ölçeklendirme yöntemini kullanarak, 10, 15 ve 20 MW'lık rüzgar türbinlerine ölçeklendirilmiştir. Pala elemanı momentum teorisi ve çok amaçlı genetik algoritmaya dayalı optimizasyon çalışmaları için, ilk olarak referans olarak alınan 5 MW NREL rüzgar türbini kanadı optimize edilmiş ve analiz edilmiştir. Daha sonra, yukarı ölçeklendirilmiş 10 MW, 15 MW ve 20 MW rüzgar türbinlerinin aerodinamik şekli ve kanat kütlesi optimize edilmiştir. Enerji üretimini en üst düzeye çıkarmak ve kanat kütlesini en aza indirmek için optimizasyon çalışmaları yapılmıştır. Rotor palalarının aerodinamik ve yapısal parametreleri, veter uzunluğu, burğu açısı, pala kütlesi ve pala katılığı gibi parametreler karşılaştırılmıştır. Aerodinamik ve yapısal

performans analizleri FAST yazılımı kullanılarak yapılmıştır ve referans kanat, optimum kanatlar ve ölçeklendirilmiş kanatlar için sonuçlar karşılaştırılmıştır. Son olarak, rüzgar türbinlerinde yeniden boyutlandırma etkilerini anlamak için, optimize edilen rüzgar türbinlerinin sonuçlarından rotor çapının bir fonksiyonu olarak yeni ölçeklendirme eğilimleri formüle edilmiştir.

Anahtar Kelimeler: Rüzgar Türbini, Yukarı Ölçeklendirme Etkileri, Genetik Algoritma, Optimizasyon, Pala Elemanı Momentum Teorisi, Aerodinamik ve Yapısal Analizler

To my family

ACKNOWLEDGEMENTS

First of all, I would like to express my sincere gratitude to my supervisor Assoc. Prof. Dr. Nilay Sezer Uzol for giving me an opportunity to work with her, allowing me to benefit from her invaluable comments and experiences and her support in completing my study.

I am completely indebted to my whole family for their endless patience, encouragement and love. Especially, I would like to thank to my brother Kemal Kesikbaş for being a friend who helps in every time of need.

TABLE OF CONTENTS

ABSTRACT	v
ÖZ	vii
ACKNOWLEDGEMENTS	x
TABLE OF CONTENTS	xi
LIST OF TABLES	xiv
LIST OF FIGURES	xv
CHAPTERS	
1. INTRODUCTION	1
1.1. Objective of the Thesis	3
1.2. Literature Research.....	4
1.3. Scope of the Thesis.....	6
2. CLASSICAL SCALING METHODS FOR WIND TURBINE BLADE DESIGN	7
2.1. Introduction	7
2.2. Approach- I: Linear Scaling Rules	7
2.3. Approach-II: Existing Scaling Trends.....	8
2.4. Comparison of Scaling Approaches	10
3. INVESTIGATION OF LINEAR UPSCALING EFFECTS ON WIND TURBINE	
BLADE DESIGN.....	13
3.1. Introduction	13
3.1.1. Linear Upscaling with NREL 5 MW Reference Turbine Blade.....	13
3.2. Reference Rotor Model and Rotor Modeling.....	16

3.2.1. NREL 5 MW Reference Turbine Model	16
3.2.2. Scaled Turbine Models.....	18
3.2.3. Performance Analysis of Scaled Wind Turbines	21
3.2.3.1. Results of Aerodynamic Analysis	21
3.2.3.2. Results of Structural Analysis	25
3.3. Optimum Wind Speed for 20 MW Rotor.....	29
3.4. Summary	31
4. OPTIMIZATION AND DESIGN OF LARGE SCALE WIND TURBINES ...	33
4.1. Introduction.....	33
4.2. Optimization Methodology	33
4.3. Blade Element Momentum Theory (BEM)	36
4.3.1. Momentum Theory (Actuator Disk Model)	36
4.3.1.1. Angular Momentum Theory	38
4.3.1.2. Blade Element Theory	39
4.3.1.3. Tip Loss Correction	41
4.3.1.4. Blade Element Momentum Theory	42
4.3.2. Design Optimization of 5 MW NREL Wind Turbine	42
4.3.3. Comparison of Original NREL 5 MW Blade with the Optimized NREL 5 MW Blade	45
4.3.4. Performance Comparison of Original NREL 5 MW Rotor with the Optimized 5 MW Rotor.....	49
4.4. Multi-purpose Optimization of the 10, 15 and 20 MW Wind Turbines	50
4.4.1. Properties of the Optimized 10, 15 and 20 MW Wind Turbines	54
4.4.2. Performance Analysis of the Optimized 10, 15 and 20 MW Wind Turbines	61

4.4.3. Scaling Trends	66
4.5. Summary	69
5. CONCLUSION.....	71
5.1. Future Recommendations.....	72
REFERENCES.....	75
APPENDICES	
A. Fast Inputs File For 10, 15 and 20 MW Optimized Rotor.....	77

LIST OF TABLES

TABLES

Table 2-1 Classical Scaling Rules [15].....	8
Table 3-1 General characteristics of the NREL 5 MW reference turbine [15]	17
Table 3-2 The chord length, twist angle distribution and airfoil distribution of the aerodynamic performance of the NREL 5 MW [5].....	17
Table 3-3 The thicknesses of the airfoil sections used in NREL 5MW Reference Turbine.....	18
Table 3-4 The blade parameters for the scaled models	21
Table 4-1 Design inputs of the optimization of the 5 MW wind turbine	43
Table 4-2 The gross properties of the optimized blade	60

LIST OF FIGURES

FIGURES

Figure 1.1. Wind turbine upscaling pattern [1]	1
Figure 2.1. Flapwise Bending Moment [16]	9
Figure 2.2. Edgewise Bending Moment [16]	9
Figure 2.3. Mass – Diameter trends from existing data[15]	10
Figure 2.4. Power output vs rotor diameter [15]	10
Figure 3.1 Mass Distribution per Length for Scaled Models	19
Figure 3.2 Stiffness Distribution in Flap-wise Direction for Scaled Models	19
Figure 3.3 Stiffness Distribution in Edge-wise Direction for Scaled Models	20
Figure 3.4 Chord Length Distribution for Scaled Models	20
Figure 3.5 Time-dependent Power Coefficient (C_p) for Scaled Models	23
Figure 3.6 Time-dependent Thrust Coefficient (C_t) for Scaled Models	24
Figure 3.7 Bending Moment-Rotor Diameter Relationship in Flap-wise Direction ..	25
Figure 3.8 Bending Moment-Rotor Diameter Relationship in Edge-wise Direction ..	26
Figure 3.9 Bending Moments in Edgewise Direction for Scaled Models	27
Figure 3.10 Bending Moments in Flap-wise Direction for Scaled Models	28
Figure 3.11 Power Coefficient Variation for Wind Speed for 20 MW rotor	29
Figure 3.12 Flapwise and Edgewise Bending Moment for 20 MW at 5 m/s	30
Figure 3.13 Power Coefficient, Rotor Power and Thrust Coefficient for 20 MW at 5 m/s	31
Figure 4.1 HARP Optimization Multi-objective design algorithm	35
Figure 4.2 Wind turbine blade cross section showing centroidal axes, centroid and locations of strain gauges. [17]	36
Figure 4.3. The Actuator Disc Model [18]	37
Figure 4.4. Rotating Annular Stream tube	39
Figure 4.5. Schematic view of Blade Element Model [18]	40

Figure 4.6. Blade geometry for analysis of a horizontal axis wind turbine [18]	40
Figure 4.7 Annual Energy Production vs Blade Mass Relationship for 5 MW blade	44
Figure 4.8 Comparison of Blade Chord length (m) of Original and Optimized blade.	46
Figure 4.9 Comparison of Blade Twist of Original and Optimized Blade.....	46
Figure 4.10 Mass per unit span (kg/m) distribution	47
Figure 4.11 Flap-wise stiffness distribution along span	48
Figure 4.12 Edge-wise stiffness distribution along span	48
Figure 4.13 Comparison of Time-dependent Power Coefficient Value (C_p)	49
Figure 4.14 Annual Energy Production vs Blade Mass Relationship for 10 MW blade	51
Figure 4.15 Upper and Lower Limits of chord and twist angle for 10MW.....	51
Figure 4.16 Annual Energy Production vs Blade Mass Relationship for 15 MW blade	52
Figure 4.17 Upper and Lower Limits of chord and twist angle for 15 MW.....	52
Figure 4.18 Annual Energy Production vs Blade Mass Relationship for 20 MW blade	53
Figure 4.19 Upper and Lower Limits of chord and twist angle for 20 MW.....	53
Figure 4.20 Chord Length Comparison for 10 MW Blade.....	54
Figure 4.21 Chord Length Comparison for 15 MW Blade.....	55
Figure 4.22 Chord Length Comparison for 20 MW Blade.....	55
Figure 4.23 Twist Angle Comparison for 10 MW Blade	56
Figure 4.24 Twist Angle Comparison for 15 MW Blade	56
Figure 4.25 Twist Angle Comparison for 20 MW Blade	57
Figure 4.26 Structural Properties Comparison for 10 MW blade.....	58
Figure 4.27 Structural Properties Comparison for 15 MW blade.....	59
Figure 4.28 Structural Properties Comparison for 20 MW blade.....	60
Figure 4.29 Time dependent power coefficient (C_p) for optimized wind turbine blade	62

Figure 4.30 Time dependent Rotor Power for optimized wind turbine blade	63
Figure 4.31 Time dependent thrust coefficient (C_t) for optimized wind turbine blade	64
Figure 4.32 Edge-wise Bending Moment for Optimized Wind Turbine Blade.....	65
Figure 4.33 Flap-wise Bending Moment for Optimized Wind Turbine Blade	66
Figure 4.34 Curve fit graph for mass trend for the optimized blade.....	67
Figure 4.35 Curve fit graph for edge-wise bending moment trend for the optimized blade	68
Figure 4.36 Curve fit graph for flapwise bending moment trend for the optimized blade	68
Figure A. 1 Fast Input File for optimized 10 MW rotor	78
Figure A. 2 Aerodyn Input File for 10 MW Optimized Blade.....	80
Figure A. 3 Elastodyn Input File for 10 MW Optimized Rotor.....	84
Figure A. 4 Aerodyn Blade Input File for 10 MW Optimized Blade	86
Figure A. 5 Elastodyn Blade Input File for 10 MW Optimized Blade	88
Figure A. 6 Aerodyn Blade Input File for 15 MW Optimized Blade	90
Figure A. 7 Elastodyn Blade Input File for 15 MW Optimized Blade	92
Figure A. 8 Aerodyn Blade Input File for 20 MW Optimized Blade	94
Figure A. 9 Elastodyn Blade Input File for 20 MW Optimized Blade	96

CHAPTER 1

INTRODUCTION

Due to the rapid loss of non-renewable energy resources on earth, such as but not limited to; fossil fuels, coal, petroleum, alternative energy resources are being sought after; wind energy is one of these alternative resources that is widely used.

Nonetheless, population density and natural areas limit the expansion of wind energy installation and vast electricity generation in and around Europe. Setting up large scale wind turbines would not only provide a solution to this issue, but also lead to cost reduction. Additionally, as illustrated in Figure 1.1, to reduce the cost of energy, our intention is to enhance the rotor diameter of the turbine, which would add further height and turbine power. Thus, extraction of more energy from larger wind turbines means decrease in the overall cost of energy.

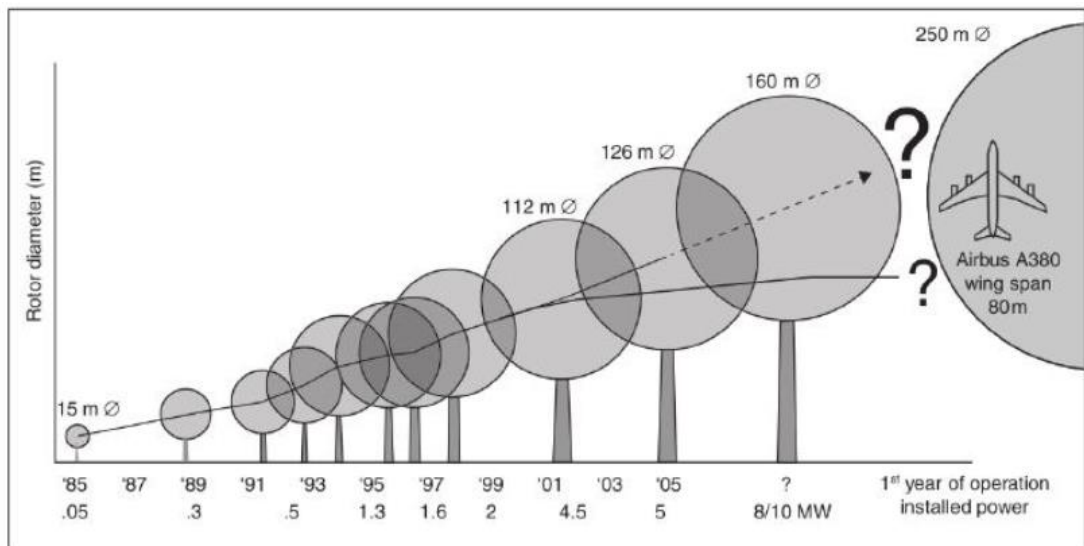


Figure 1.1. Wind turbine upscaling pattern [1]

However, looking at the market analysis of the use of large-scale wind turbines, it can be seen that there are many difficulties associated with technical feasibility. The

increase in blade size also means an increase in blade mass and other components of the turbine. For these reasons, it can be said that it would be difficult to develop large turbines using the classical upscaling method. Therefore, instead of using the classical upscaling method, to obtain a more efficient wind turbine design, a lot of research is being done to develop a new design method that is considered in every aspect.

Projects such as WINDPACT, UPWIND, and DOWEC each focus on a different feature of the new upscaling methods. Between the years 1997-2003, a 64.5 m DOWEC [2], [3] blade was studied. It also included the distributed geometric properties, stiffness and blade mass properties. The Upwind project [4] and the NREL 5 MW model [5] used the blade characteristics which is obtained from DOWEC project.

On the other hand, WINDPACT [6], [7] project studied the impact of enhanced turbine size and cost of energy through the development of cost and mass models of the components of a wind turbine.

The UPWIND project focused on identifying major technological and economic barriers to large-scale wind turbines. However, instead of achieving optimal wind turbine designs through optimization, the UPWIND project used linear scaling rules and engineering knowledge from experience.

Even though past research shows that many significant improvements have been made in upscaling, it is necessary to do more research before fully understanding and providing solutions to the technical characteristics such as chord length, twist angle and blade mass that correlate with upscaling.

For the reasons mentioned above, the focus of this thesis is the effect of scaling on wind turbine blade characteristics, as well as, examining new upscaling approaches beyond the classical upscaling method. Upscaling a 5 MW wind turbine to larger sizes up to 10, 15 and 20 MW and studying the effect of scaling on the aerodynamic

perspective. Also, scaling trends are used to identify size-related problems and detect the possible limiting causes.

1.1. Objective of the Thesis

Considering the methods for the effects of size on characteristics of a wind turbine, the most frequently used ones are the linear scaling rules or the extrapolation of existing data. The linear scaling rules, under some assumptions, examine the analytical relationships formed by formulating linearly scaled geometric parameters as a function of rotor diameter.

The existing data trends use the correlations between rotor diameter and other parameters of wind turbine characteristics. The existing data trends approach needs real data to be collected and the scaling trends can be gained by interpolation or extrapolation of the collected data. Nevertheless, to study larger wind turbines using the existing data trends approach, an extrapolation must be used. To obtain large scale wind turbines, extrapolation will go outside the data range and this will result in more uncertainty in the trend rules.

In order to overcome the disadvantages of the first two methods, in this study, wind turbine blades are designed and optimized for several different sizes by using the basic aerodynamic theories. The relation between different wind turbine parameters and rotor diameter can be obtained by using these optimized wind turbines and these relations can be used in order to develop new trends.

For the design studies in this thesis, the 5 MW NREL wind turbine is used as the baseline rotor. For the upscaling studies, the 5 MW NREL baseline wind turbine is scaled up to 10, 15 and 20 MW wind turbines by using the classical upscaling method which is a linear scaling rule. The scaled wind turbine rotors are analyzed and evaluated in terms of aerodynamic and structural characteristics by using the FAST software. For the design optimization studies, the 5 MW NREL wind turbine blade which is taken as the reference blade is first optimized and analyzed. Then, the aerodynamic shape and blade mass of the upscaled 10 MW, 15 MW and 20 MW wind

turbines are optimized. These larger optimized wind turbines are analyzed and evaluated in terms of aerodynamic and structural characteristics by using the FAST software. The results of optimized designs are also compared with the results which are obtained from the linearly scaled wind turbines.

1.2. Literature Research

In recent years, there have been several studies on scaling wind turbines. Ashuri *et al.* [8] investigated the non-linear upscaling approach for wind turbine blades based on stress levels. The aim was keeping the stresses in the upscaled blade the same as the reference blade which was NREL 5 MW. The reference blade was upscaled to 20 MW wind turbine blade by using the non-linear upscaling method. On the other hand, with the linear scaling methods, it has been seen that an increase in the total stress of %80 occurs. It was concluded that the design with the non-linear upscaling approach decreases the aerodynamic loads and the weight induced stresses compared to the design with the linear upscaling approach.

Nijssen *et al.* [9] studied the application of scaling rules on wind turbine design. The aim was to show the effects of scaling laws on reaching to the optimum blade design.

Sieros *et al.* [10] studied the upscaling of wind turbines and especially the theoretical and practical effects of upscaling on the aerodynamic loads and weight. The theoretical implications showed unfavorable increases in the weight and loads due to upscaling.

Griffin A. [6] studied scaling effects on the composite blades for 80 to 120 m diameter rotors. To obtain a blade-scaling model by using direct design calculations, the structural properties of the blade were calculated for different aerodynamic designs and rotor sizes. This structural design model was used to obtain some scaling trends. For a given blade design, the scaling model indicates that blade mass and costs scale as a near-cubic of rotor diameter. In contrast, the commercial blade designs have maintained a scaling exponent closer to 2.4 for lengths ranging between 20 and 40

meters. From this study, it was indicated that obtaining lower scaling exponent on cost and mass has required significant evolution of the aerodynamic and structural designs.

Ashuri *et al.* [11] performed the multidisciplinary design optimizations of large wind turbines of 5, 10 and 20 MW. Based on the design data and the properties of these large wind turbines, the scaling trends for loading, mass, and cost were developed. The results showed the technical feasibility of wind turbines up to 20 MW, but the design of such large upscaled turbine was cost prohibitive. The results of this research support the development of alternative lightweight materials to overcome mass problem. The results also showed that the upscaling without changing the concept, the materials, and the technology was not feasible.

Peeringa *et al.* [4] studied the pre-design of Upwind 20 MW Wind Turbine. In this study, the classical upscaling rules were used to obtain a starting point for 20 MW wind turbine design which was based on the Upwind 5 MW reference wind turbine.

Kazacoks R. and Jamieson P. [12] showed the scaling effects on the hub loads of a horizontal axis wind turbine. The general fatigue load trends of several wind turbines were generated. The aim was to investigate how loads (especially the fatigue loads) change for four wind turbines: 2 MW SuperGen (based on the NREL 2MW turbine), 3 MW Generic, 3.6 MW Generic, 5 MW SuperGen (based on the NREL 5MW turbine). The edge-wise and the flap-wise bending moment at the blade root were investigated. They showed that the structural modes and frequencies of rotor decrease with the wind turbine size.

Ashuri T. and Zaaijer [13] studied the size effects on the design drivers and discussed the critical issues for very large scale wind turbine blades. A classical upscaling law and a finite element model were used to perform the assessment. The structural responses such as the stresses and the displacements due to aerodynamic and inertial loadings were analyzed for 5, 10, 15 and 20 MW blades. Based on the results of the simulations, the challenges for design of very large blades and some design guidelines were presented and the use of light-weight materials were also stated as necessary.

1.3. Scope of the Thesis

In Chapter 1, the introduction on the design of large scale wind turbines are given, the motivation and objectives of the thesis are presented.

In Chapter 2, the classical upscaling methods and the existing data trends are explained in detail. These two methods are compared with each other in terms of advantages and disadvantages. A new alternative approach based on an aerodynamic design of large-scale wind turbine rotors is described.

In Chapter 3, NREL 5 MW wind turbine was taken as a reference rotor and three different turbine blades are obtained for 10 MW, 15 MW and 20 MW rotors by using the classical upscaling rules. The aeroelastic behavior of the turbine blades are examined and compared with each other by using the FAST [14] software of NREL for four different wind turbine rotors, including the reference baseline turbine blade.

In Chapter 4, the aerodynamic shape and blade mass of the 5 MW, 10 MW, 15 MW and 20 MW wind turbines are optimized by using a Multipurpose Genetic Algorithm and Blade Element Momentum (BEM) theory, with reference to the NREL 5MW wind turbine rotor and scaled rotors. The optimization studies have been conducted to maximize the power generation and minimize the blade mass. The blade shape design parameters are obtained from the genetic algorithm optimization, and then, the optimized 10, 15 and 20 MW wind turbine rotors are modelled and analyzed by using the FAST software. Aerodynamic and structural performances are compared with each other.

All results which are obtained in previous chapters, are discussed and summarized, and conclusions and future recommendations are given in Chapter 5.

CHAPTER 2

CLASSICAL SCALING METHODS FOR WIND TURBINE BLADE DESIGN

2.1. Introduction

Scaling laws can be used to extrapolate existing model properties to larger turbine sizes and predict the effect of blade length on design trends such as mass and energy production. In this section we consider general scaling trends.

Two classical scaling methods are used in the literature: the linear scaling rule and the extrapolation of existing data trends, to understand the effects of scaling on aerodynamic and structural characteristics of wind turbines.

In this study, it is aimed to find the best method for scaling by making a short review of the existing classical design methods. The two classical methods for upscaling are presented in this chapter. Scaling of wind turbines is done by using the linear scaling relations or the extrapolation of existing data where usually there is a relation between the rotor diameter and the important parameters of wind turbine design.

2.2. Approach- I: Linear Scaling Rules

The classical linear upscaling rules are based on the following assumptions:

1. The number of blades and their structural concepts are the same
2. Constant tip speed
3. Geometrical parameters are related linearly with blade diameter.

In 2001, Nijssen et al. [9] enlarged the linear scaling laws and, as a case study, applied this law in the process of upscaling a wind turbine. In the UPWIND project, in order to see the various effects of wind turbine scaling, linear scaling law has been applied to most components of the wind turbine by Chaviaropoulos et al. [10].

Different wind turbine sizes become possible by using the scaling laws and the relations between blade radius and turbine parameters. For a rotor blade, the classical linear scaling rules are presented in Table 2-1.

Table 2-1 *Classical Scaling Rules* [15]

Symbol	Description	Size dependency
L	Blade length	R
ω_{rot}	Rotor rotational speed	R^{-1}
$\omega_{rot} \cdot L$	Tip speed	I
$c_{bld}(x)$	Blade chord distribution	R
$t_{bld}(x)$	Blade thickness distribution	R
$\theta_{bld}(x)$	Blade twist distribution	I
M_{flp}	Flapwise moment	R^3
M_{edg}	Edgewise moment	R^3
P_{rot}	Rotor power	R^2
T_{rot}	Rotor torque	R^3
$A_{bld}(x)$	Blade sectional area	R^2
$I_{are}(x)$	Area moment of inertia	R^4
$I_{mas}(x)$	Mass moment of inertia	R^5
M_{bld}	Blade mass	R^3

R: Linear dependency, I: Size independency

2.3. Approach-II: Existing Scaling Trends

The most comprehensive work on wind turbine mass, power output and loads scale trends was made by Jamieson [16] by using the calculations in the UPWIND project. These data are shown in three parts. In the first part, the mass of turbine blade is shown as a function of rotor diameter. In the second and third parts, the loads data and the power output are presented, respectively.

The loads scaling trends [16] are presented in Figure 2.1 and Figure 2.2 in terms of diameter. The flapwise and the edgewise loads should scale with R^3 with respect to the linear scaling rules as shown in Table 2-1. However, from these two figures, it can be seen that the edgewise bending moment exponent is higher than the flapwise bending moment exponent of the scaling correlations with diameter.

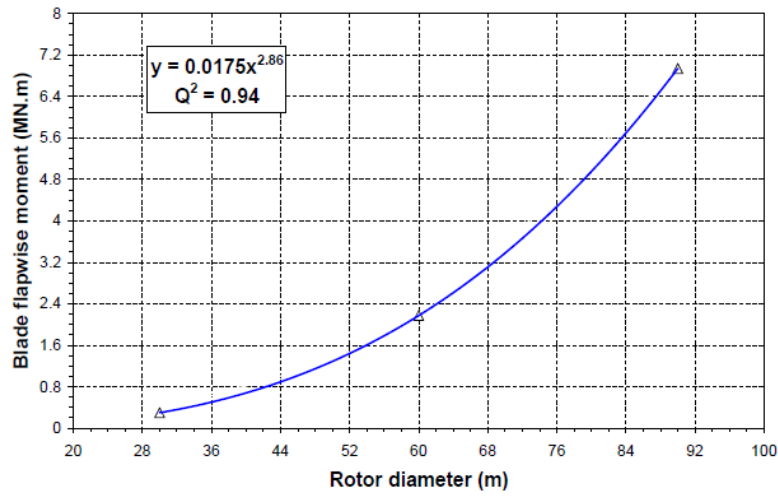


Figure 2.1. Flapwise Bending Moment [16]

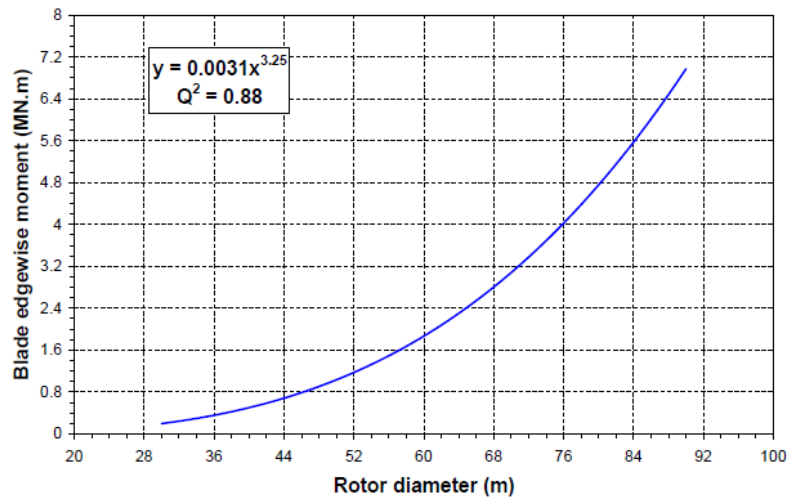


Figure 2.2. Edgewise Bending Moment [16]

The scaling behavior of the blade mass is one of the most important parameters for the blade design as stated in Ashuri's studies [15]. 52 data points which belong to 7 different manufacturers were used to obtain the blade-diameter-mass trend. As shown in Figure 2.3., by using curve-fitting to the existing data, a new mass-diameter relation was obtained as: $\text{Blade mass} = 0.6853R^{2.09}$ (where, the exponent is less than the linear scaling rules.) As shown in Figure 2.4., there is an almost square relation with the diameter for power output by using the curve fitting to the data points.

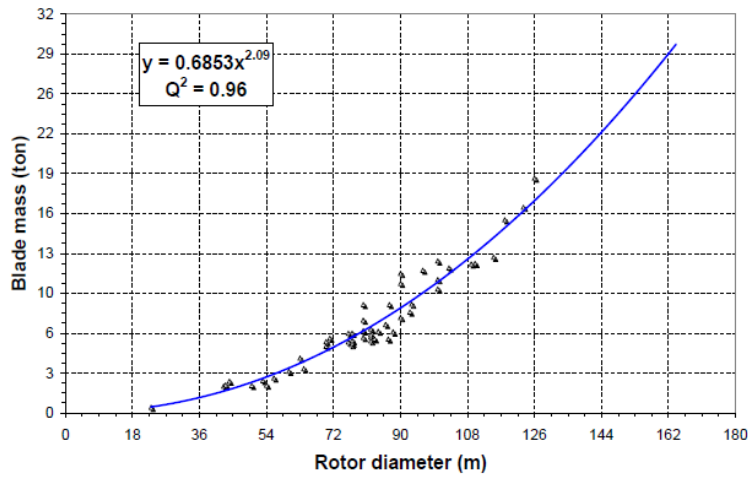


Figure 2.3. Mass – Diameter trends from existing data[15]

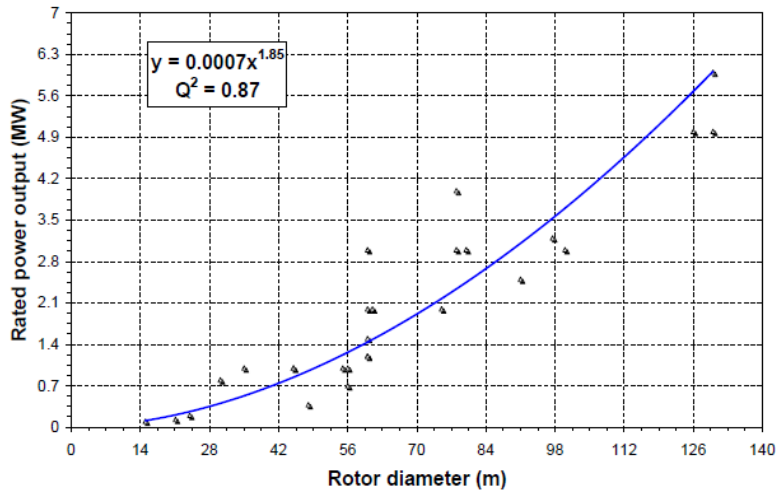


Figure 2.4. Power output vs rotor diameter [15]

2.4. Comparison of Scaling Approaches

Although the linear scaling laws are easiest way of scaling a wind turbine to another size, it is not accurate when compared with the existing data scaling trends. This is expected due to complexity of a wind turbine system as a whole in terms of several interdisciplinary areas such as aerodynamics, structure, control and complex wind conditions.

As shown in Figure 2.1. and Figure 2.2. for the existing data relations, the flapwise and edgewise bending moments have relations with the radius as $R^{2.86}$ and $R^{3.25}$, respectively. Therefore, there is a fair match between the existing data trends and the linear scaling rules which are as R^3 for both bending moments.

As shown in Figure 2.3., for mass predictions, by using the extrapolation of existing data, there is a $R^{2.29}$ relation with radius. This value is too below the linear scaling rule which is R^3 . The linear scaling rule of mass blade (R^3) could be still a valid law if the blade would be made from metal. However, the data points of the figure are taken from the composite blades.

However, for the total energy production, when comparing the linear scaling laws with the existing data trends, there is a near match between these scaling methods. In the linear scaling rule, the energy production has R^2 relation with the radius (diameter). As shown in Figure 2.4., for the existing data trends, this relation is $R^{1.85}$, which is quite near the linear scaling rule. It means that the energy production of wind turbines is compatible with the rule of the linear scaling.

The classical upscaling methods are not suitable for certain parameters for larger scale wind turbines. Therefore, there is a need for new and reliable scaling trends which are based on aerodynamic and structural theories in order to obtain accurate scaling rules.

The linear scaling rule formulation is more suitable during the conceptual design of wind turbines and using only this method is not feasible and reliable for larger scale wind turbines with good aerodynamic and structural performances.

On the other hand, the technical data from manufacturers are not available at larger scales. For this reason, the extrapolation of the existing data trends can result in uncertainties in the design.

CHAPTER 3

INVESTIGATION OF LINEAR UPSCALING EFFECTS ON WIND TURBINE BLADE DESIGN

3.1. Introduction

Looking at the market analysis of the use of large-scale wind turbines, there are many difficulties with regard to technical applicability. The increase in blade size also means an increase in blade mass and other components of the turbine. Although aerodynamic forces play an important role in the design of past and present commercial blades, it still plays an important role in the design of large diameter wind turbine blades, and in addition to aerodynamic effects, structural effects become important as well with increasing wind turbine diameter. This chapter examines the aerodynamic behavior and the structural behavior of very large-scale wind turbine rotors. In this chapter, NREL 5 MW turbine blade is taken as reference, as the baseline rotor, and three different turbine blades are obtained for 10 MW, 15 MW and 20 MW rotors by using the classical upscaling rules. The aerodynamic and structural behavior of turbine blades are examined and compared with each other by using the FAST [14] software of NREL for four different wind turbine blades, including the reference turbine blade.

3.1.1. Linear Upscaling with NREL 5 MW Reference Turbine Blade

Scaling laws can be used to estimate the properties of a larger diameter turbine blade and the effect of blade length on torque and forces, using the properties of the reference turbine blade. The classical scaling of the turbine blade is performed by a dimensional analysis where the variables are scaled according to the corresponding scale factors. By using the scaling laws based on this dimensional analysis, the turbine power, blade mass, stiffness properties and root moments can be obtained for a larger diameter

blade. In these classical scaling laws, the material similarity and the constant tip ratio are assumed.

First, we define the scale factor α as the ratio of the scaled rotor length (L_U) to the nominal rotor length (L_B):

$$\alpha = \frac{\text{Scaled Rotor Length}}{\text{Nominal Rotor Length}} = \frac{L_u}{L_b} \quad (3.1)$$

where, "U" represents the scaled blade and "B" represents the nominal blade. The scale factor can also be obtained as the ratio of the scaled blade rotor radius to the nominal rotor radius.

The blade mass can be expressed as;

$$m_u = \alpha^3 m_b \quad (3.2)$$

and, the rotor power can be expressed as:

$$P_u = \alpha^2 P_B \quad (3.3)$$

It is seen from the equations that as the rotor blade length increases, the rotor mass (α^3) grows faster than the rotor power (α^2). New designs can be made to reduce the mass growth due to the scale factor. Equation 3.2 is a volume-dependent scale because the material density is constant due to the assumption of material similarity. Since the rotor power depends on the area swept by the rotor, there is a square relationship in Equation 3.3.

The scaling laws can also be used to see the loads distributions on the rotors. For example, for the root bending moments, the relationships due to the aerodynamic forces or gravity loads are given below.

The aerodynamic lift and drag forces are expressed as:

$$F_L = \frac{1}{2} \rho A C_l V^2 \quad (3.4)$$

$$F_D = \frac{1}{2} \rho A C_d V^2 \quad (3.5)$$

where, V is velocity, ρ is air density, A is area, and C_l and C_d are aerodynamic coefficients. Both expressions for the aerodynamic forces are in the same mathematical form. The tip speed ratio depends on the wind speed and the rotational speed of the rotor. Since the scaling laws assume a constant tip speed ratio, to maintain the constant tip speed ratio for longer blades at the same wind speed, the rotational speed of the rotor is reduced linearly. Therefore, the area is the only parameter that depends on the scale in these equations. Therefore, the aerodynamic forces, such as both lift and drag, are scaled by the square of the scale factor.

For the bending moments due to the aerodynamic loads, α^2 dependence as the product of the force on the blade elements and α^1 dependence due to the position of the applied load on the blade occur. Thus, the moments resulting from the aerodynamic loads are scaled with the following cubic relationship:

$$M_U^{aero} = \alpha^3 M_L^{aero} \quad (3.6)$$

For the root bending moments due to gravity loads, these moments occur depending on the blade mass and the position where the load is applied. For the classical scaling, the blade mass grows with the cube of the scale factor (Equation 3.2) and the position is scaled linearly. Therefore, the gravitational moments increase with the fourth power of the scale factor:

$$M_U^{grav} = \alpha^4 M_L^{grav} \quad (3.7)$$

Thus, it is seen from Equations 3.6 and 3.7 that the moments due to gravity loads are scaled at a faster rate than the moments due to aerodynamic loads. The aerodynamic loads for blades are typically greater than the gravity loads. Thus, the root bending moments caused by the aerodynamic loads have been the main design factor, especially in the spanwise direction of the blade. However, it is clear that as the blade length increases, the root bending moments due to gravity loads increase by exceeding the moments caused by the aerodynamic loads. The gravitational loads basically resist the forward-reverse (chordwise) direction. Larger gravity loading requires additional reinforcement and design adjustments in the lead-lag direction.

The root bending moment relationships can also be rewritten in terms of stress. The stress due to the aerodynamic loads is completely independent of the scale factor (α^0). However, the stress due to gravity loads grows linearly with the scale factor (α^1). These relationships is important for strength and fatigue calculations in structural analyses.

Table 2-1 shows the relationships between the design parameters and the scale factor based on the classical linear scaling rules.

3.2. Reference Rotor Model and Rotor Modeling

In this study, NREL 5 MW rotor with a blade length of 61.5 meters is taken as the reference rotor (baseline rotor). Using this reference model, new rotors of 10 MW, 15 MW and 20 MW wind turbines are obtained by using the classical scaling laws specified in the previous section.

3.2.1. NREL 5 MW Reference Turbine Model

An aeroelastic model has been developed for the 5 MW turbine by examining the existing conceptual designs and similar designs in NREL. The baseline wind turbine blade model is analyzed by using the FAST aero-elastic code. This baseline wind turbine model, the NREL 5 MW rotor, has been widely used by wind energy researchers. The turbine model includes the distributed features for the blades and the tower. For the NREL 5 MW turbine model, the structural and aerodynamic properties of the DOWEC [2] reference turbine are used, but the blade length is changed from 64.5 m to 61.5 m. Table 3-1 presents the general characteristics of the NREL 5 MW reference turbine. The chord and twist angle distributions, and the airfoil distribution of the NREL 5 MW reference turbine are presented in Table 3-2 and Table 3-3

Table 3-1 General characteristics of the NREL 5 MW reference turbine [15]

Design Specification	Value (Unit)
Rated Power	5 (MW)
Rotor, Hub diameter	126.3 (m)
Rotor orientation, configuration	Upwind, 3 bladed
Hub height	90.5 (m)
Cut-in, rated, Cut-out wind speed	3, 11.4, 25 (m/s)
Cut-in and rated rotor speed	6.9 and 12.1 (RPM)
Rated tip-speed	80 (m/s)
Shaft tilt, precone	5, 2.5 (deg)
Rotor, nacelle, tower mass	110, 240, 347.46 (ton)
Control strategy	Variable-speed, collective pitch
Peak power coefficient	0.482
Blade-pitch angle at peak power	0.0 (deg)
Rated mechanical power	5.297 (MW)
Rated generator torque	43093 (kN.m)
Generator slip in transition region	10 (%)
Maximum blade pitch rate	8 (deg/s)

Table 3-2 The chord length, twist angle distribution and airfoil distribution of the aerodynamic performance of the NREL 5 MW [5]

Node (-)	RNodes (m)	AeroTwst (°)	DRNodes (m)	Chord (m)	Airfoil Table (-)
1	2.8667	13.308	2.7333	3.542	Cylinder1.dat
2	5.6000	13.308	2.7333	3.854	Cylinder1.dat
3	8.3333	13.308	2.7333	4.167	Cylinder2.dat
4	11.7500	13.308	4.1000	4.557	DU40_A17.dat
5	15.8500	11.480	4.1000	4.652	DU35_A17.dat
6	19.9500	10.162	4.1000	4.458	DU35_A17.dat
7	24.0500	9.011	4.1000	4.249	DU30_A17.dat
8	28.1500	7.795	4.1000	4.007	DU25_A17.dat
9	32.2500	6.544	4.1000	3.748	DU25_A17.dat
10	36.3500	5.361	4.1000	3.502	DU21_A17.dat
11	40.4500	4.188	4.1000	3.256	DU21_A17.dat
12	44.5500	3.125	4.1000	3.010	NACA64_A17.dat
13	48.6500	2.319	4.1000	2.764	NACA64_A17.dat
14	52.7500	1.526	4.1000	2.518	NACA64_A17.dat
15	56.1667	0.863	2.7333	2.313	NACA64_A17.dat
16	58.9000	0.370	2.7333	2.086	NACA64_A17.dat
17	61.6333	0.106	2.7333	1.419	NACA64_A17.dat

Table 3-3 The thicknesses of the airfoil sections used in NREL 5MW Reference Turbine

Airfoil Type	Thickness (t/c)
Cylinder1	100%
Cylinder2	100%
DU40_A17	40.5%
DU35_A17	35.09%
DU30_A17	30%
DU25_A17	25%
DU21_A17	21%
NA64_A17	18%

3.2.2. Scaled Turbine Models

In this section, NREL 5 MW rotor is taken as the reference and new rotors of 10 MW, 15 MW and 20 MW have been obtained by using the classical scaling rules. The blade data from the DOWEC [4] report includes the detailed structural properties as mass per unit length, bending stiffness for each direction, and axial and torsional stiffness. The classical scaling laws assume the material similarity, therefore, the elasticity module and its density are constant. Therefore, the scaling of the cross-sectional stiffness properties depends entirely on the geometry. The bending and torsional stiffness values are scaled by the fourth power of the scale factor, while the axial stiffness values are scaled by the second power of the scale factor.

The mass and stiffness distributions for the 5 MW reference model and the scaled models of 10, 15 and 20 MW are given in Figure 3.1, Figure 3.2 and Figure 3.3. The blade mass per unit length was scaled by the square of the scaling factor. For the tower, the mass and stiffness properties are increased in the same way as the blade characteristics.

Similarly, the chord length was scaled linearly with the scaling factor and is presented in Figure 3.4. Since the twist angle distribution is independent of the scaling factor, it is used as the same for all.

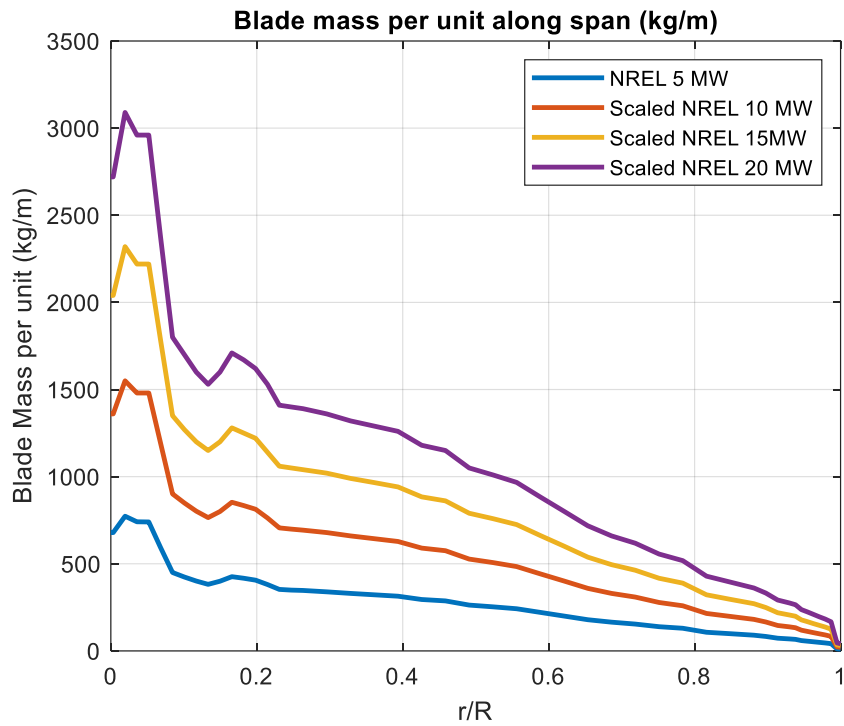


Figure 3.1 Mass Distribution per Length for Scaled Models

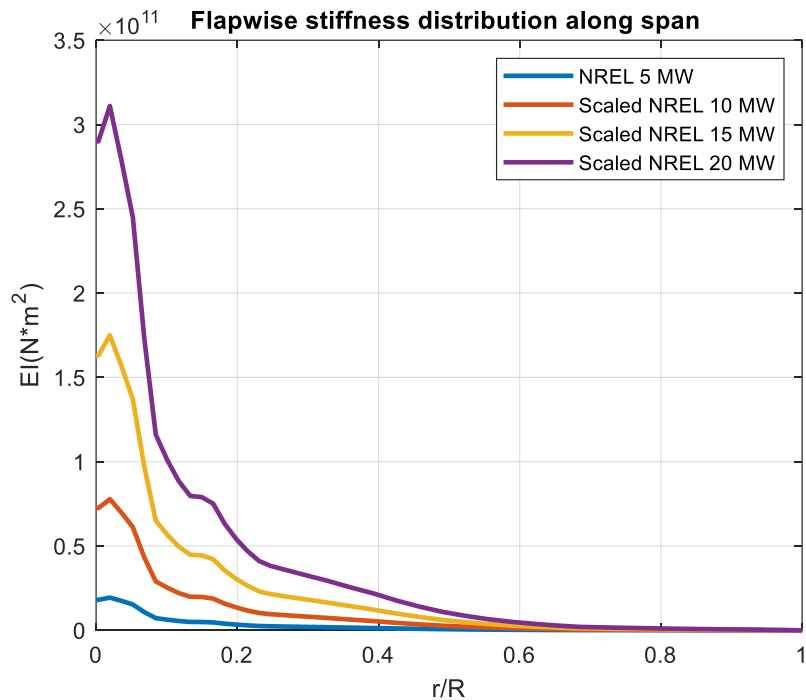


Figure 3.2 Stiffness Distribution in Flap-wise Direction for Scaled Models

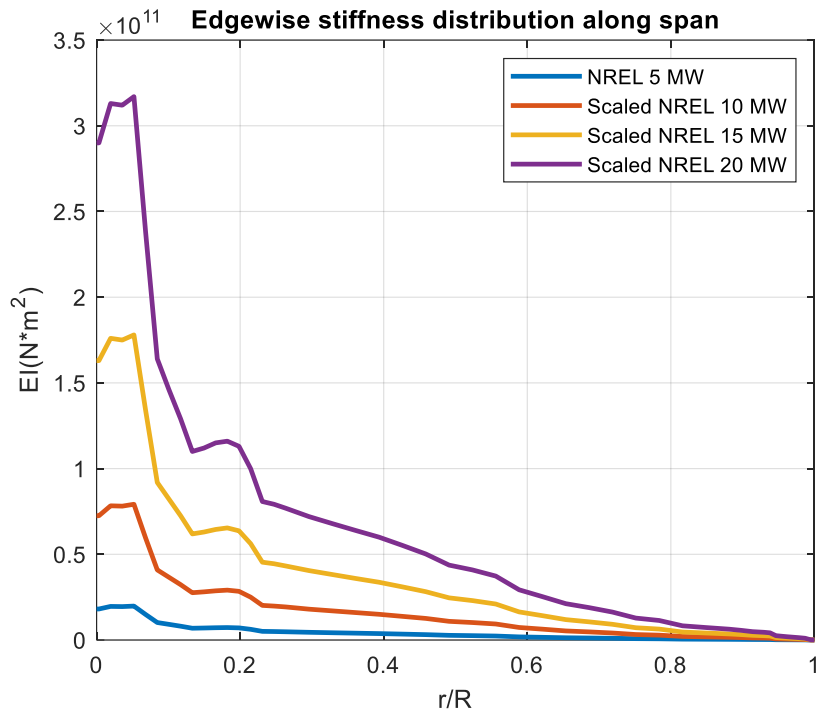


Figure 3.3 Stiffness Distribution in Edge-wise Direction for Scaled Models

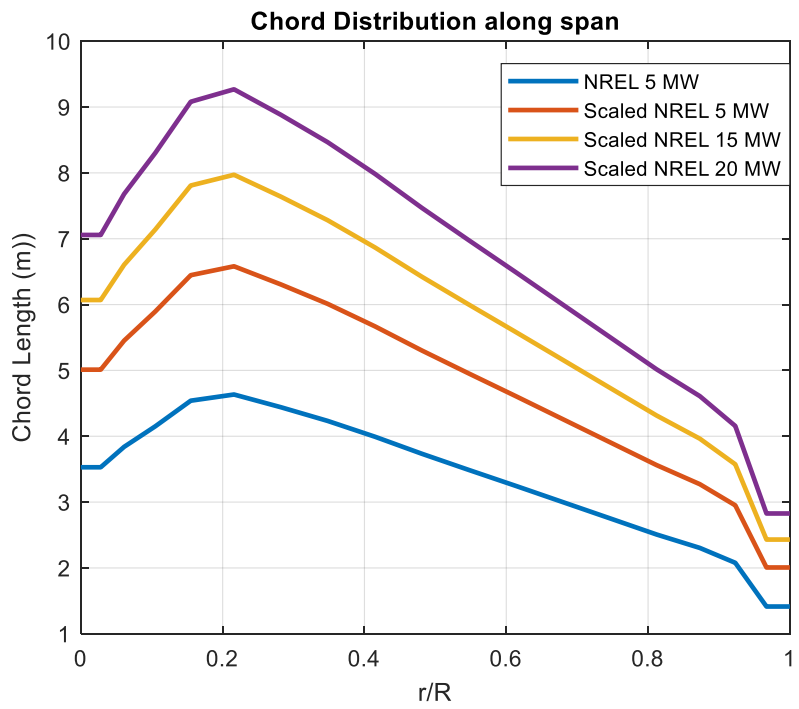


Figure 3.4 Chord Length Distribution for Scaled Models

Table 3-4 presents the blade parameters for the scaled models. The mass is scaled by the scaling factor cubic power as indicated previously, and the mass inertial moments are scaled by the fourth power. The chord length is obtained by linear correlation. The rotor speed is obtained inversely proportional to the scaling factor to obtain the same blade tip speed.

Table 3-4 *The blade parameters for the scaled models*

Power (MW)	Diameter(m)	Length (m)	Mass (kg)	Rotational Speed (RPM)
5	126	61.5	17740	12.1
10	178	87.0	50184	8.56
15	213	106.5	91528	7.44
20	246	123	137562	6.99

3.2.3. Performance Analysis of Scaled Wind Turbines

The scaled models obtained are examined in terms of aeroelastic analysis by using the FAST software. One of the analyses capabilities of FAST [1] is to simulate the nonlinear motion equations based on time. During this simulation, the time-dependent results are obtained by adding both structural and aerodynamic effects to the turbine rotor under certain wind conditions. The time-varying changes in the aerodynamic loads and performances can be analyzed by also taking structural effects into consideration. In these analyses, the specific wind conditions are also considered as a constant wind speed of 12 m/s.

3.2.3.1. Results of Aerodynamic Analysis

For the rotor power production, as can be seen in Figure 3.5, the performances of the rotors obtained by traditional scaling laws decrease sharply. Although the NREL 5 MW reference turbine may fluctuate for a short time, it has stabilized after a certain time. For the 10 MW rotor, the fluctuations in power became stable after a certain period of time, which is slightly longer than the 5 MW rotor, however, the performance coefficient decreased by half after it became stable. For the 15 MW rotor,

the fluctuations took much longer period than for the 10 MW rotor, and the performance is reduced by half as in the 10 MW rotor. For the 20 MW rotor, the performance power coefficient has never been reaching a steady-state value, and has remained fluctuating.

The thrust coefficients are presented in Figure 3.6 for the scaled rotors. For the 5 MW, 10 MW and 15 MW wind turbines, the thrust coefficient value is about 0.73. For the 20 MW rotor, the thrust coefficient has never been constant and has remained fluctuating like the power coefficient.

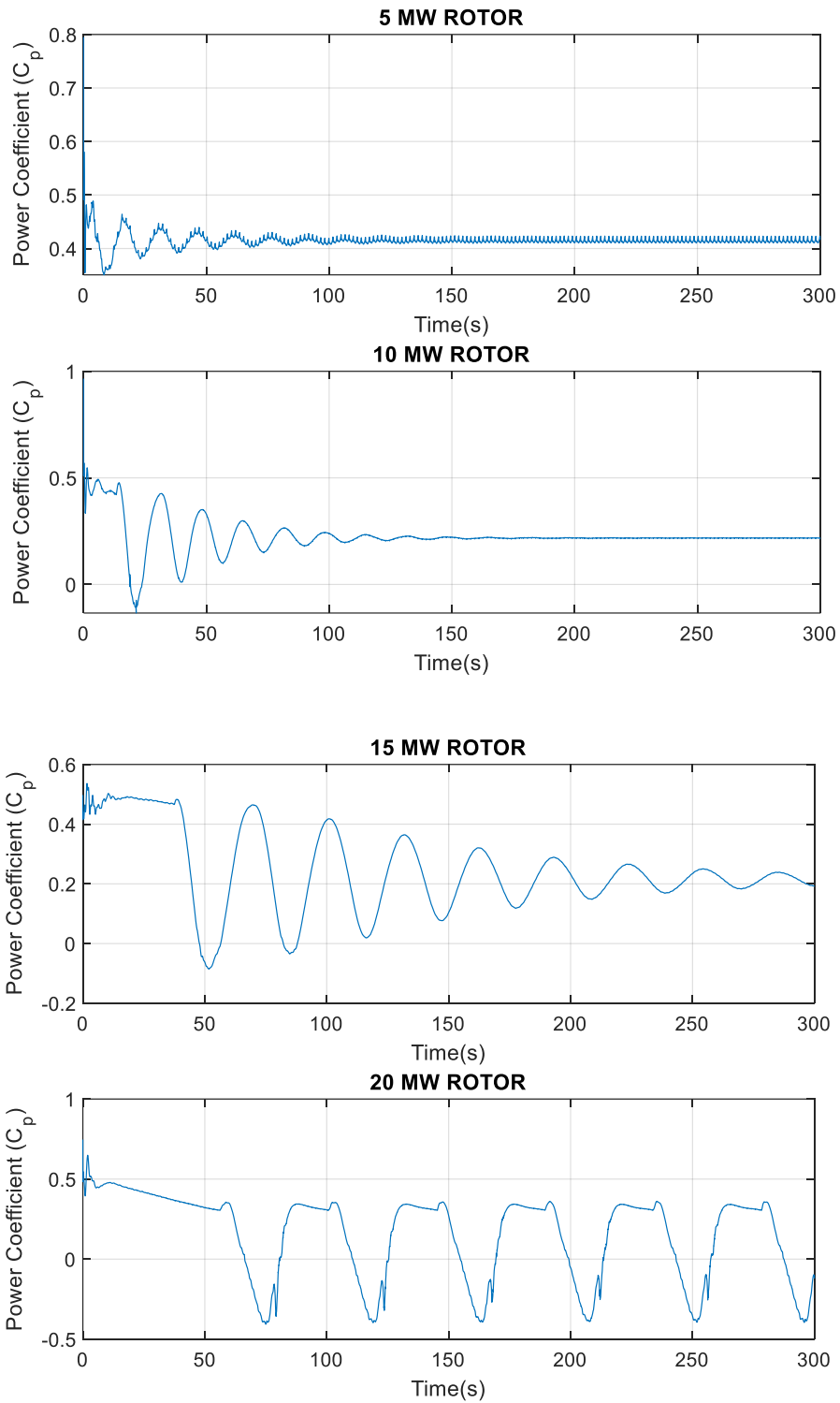


Figure 3.5 Time-dependent Power Coefficient (C_p) for Scaled Models

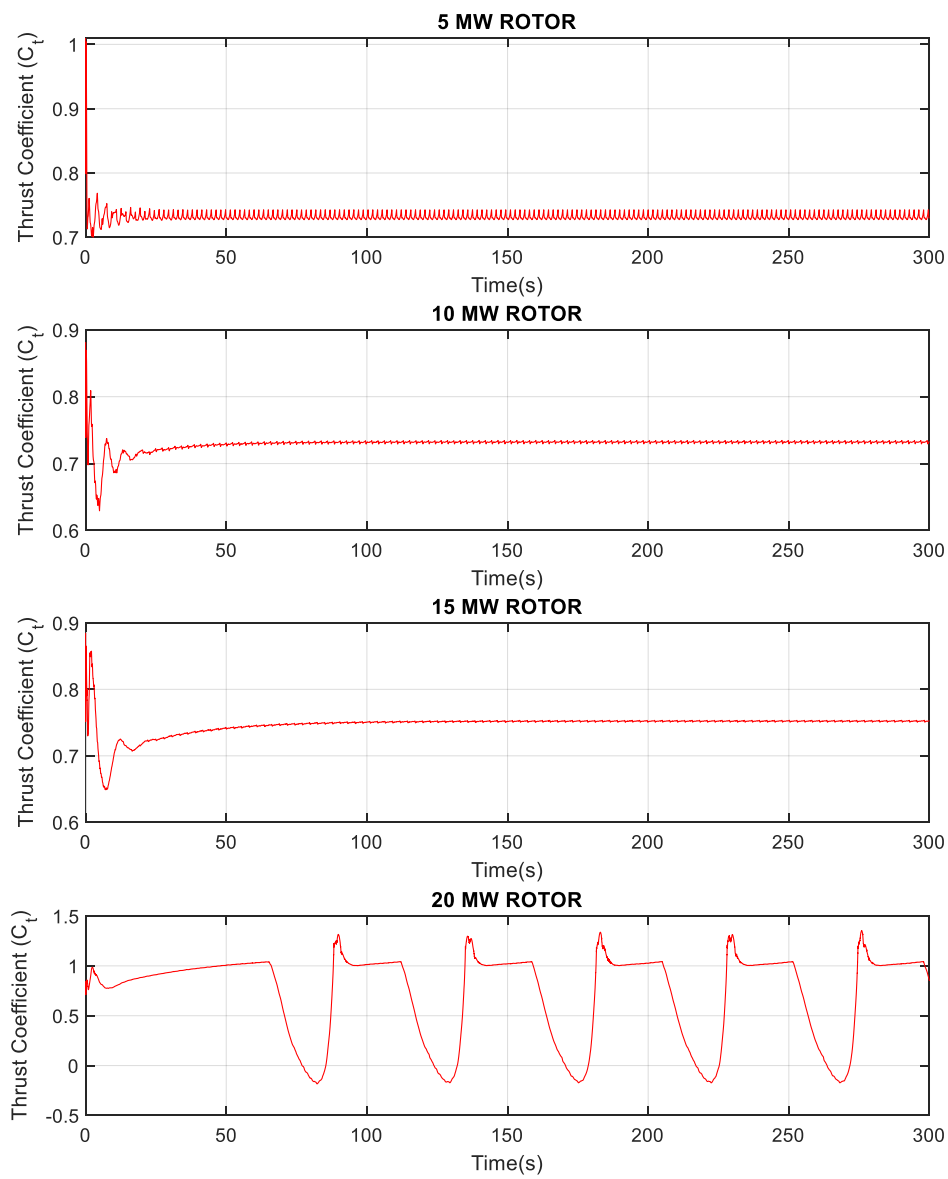


Figure 3.6 Time-dependent Thrust Coefficient (C_t) for Scaled Models

3.2.3.2. Results of Structural Analysis

This subsection presents the diameter-loads trends of the scaled blades. In Figure 3.7 and Figure 3.8, the relationships of the bending moments in flapwise and edgewise directions with the rotor diameter are presented. As it can be seen, the bending moments are scaled with $R^{4.338}$ and $R^{4.894}$ for the flapwise and edgewise directions, respectively. This means that the moment in the edgewise direction, which is mainly driven by gravity loads, is increased by the scale factor greater than the moment in the flapwise direction which is driven by the aerodynamic loads. This is the same as the the law of linear scaling which presents for the gravity-induced loads to be scaled faster than the aerodynamically driven loads. However, the predicted value for the scale factor is different than the expected.

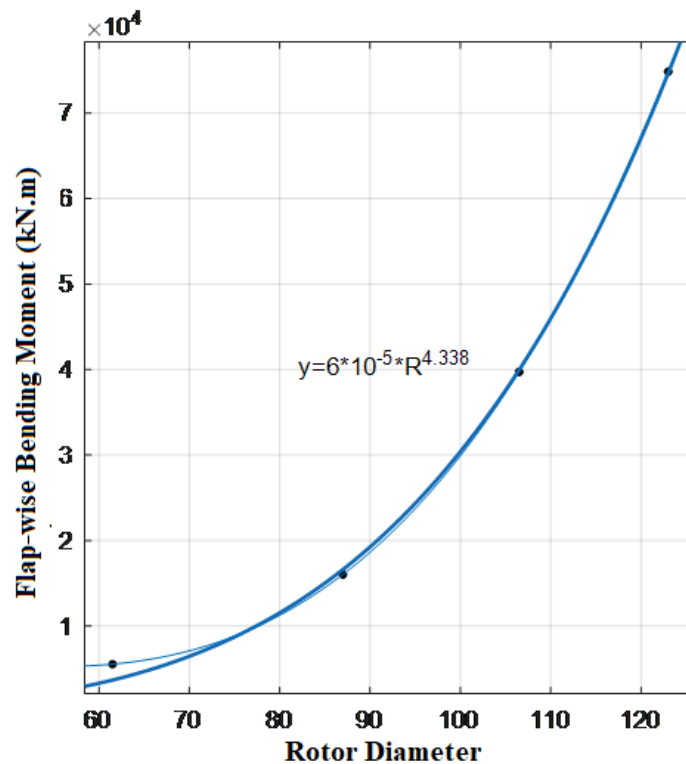


Figure 3.7 Bending Moment-Rotor Diameter Relationship in Flap-wise Direction

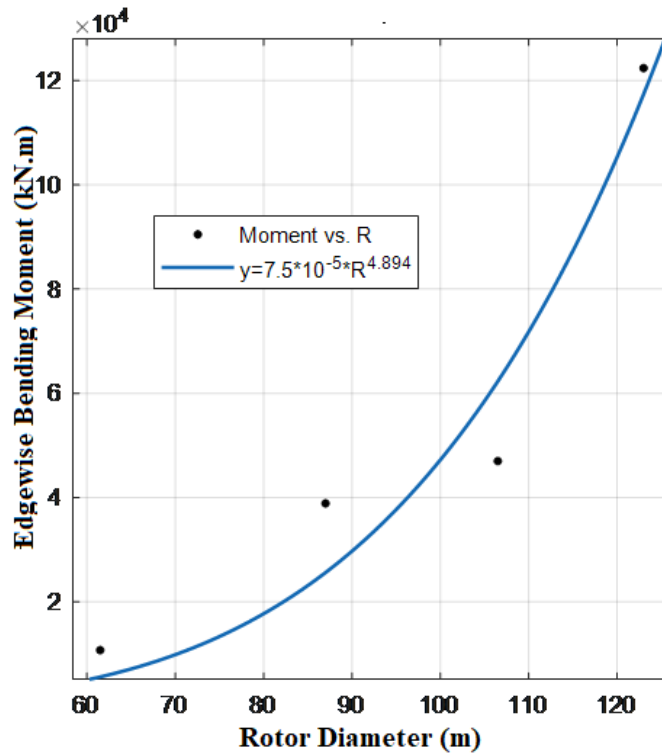


Figure 3.8 Bending Moment-Rotor Diameter Relationship in Edge-wise Direction

In Figure 3.9 and Figure 3.10, the time-dependent variations of the flapwise and edgewise bending moments for different scaled rotors are presented. As the size of the rotors increase, the amplitude of the fluctuations in the bending moments increase, and especially for the 20 MW rotor, the fluctuations don't get smaller with time, causing high and periodic changes in the loads. This sudden dynamic load change is critical for fatigue strength. As seen in Figure 3.10, the bending moments in the flapwise direction show more stable behavior than the moments in the edgewise direction. Therefore, the loads and moments in the edgewise direction become more critical for fatigue strength.

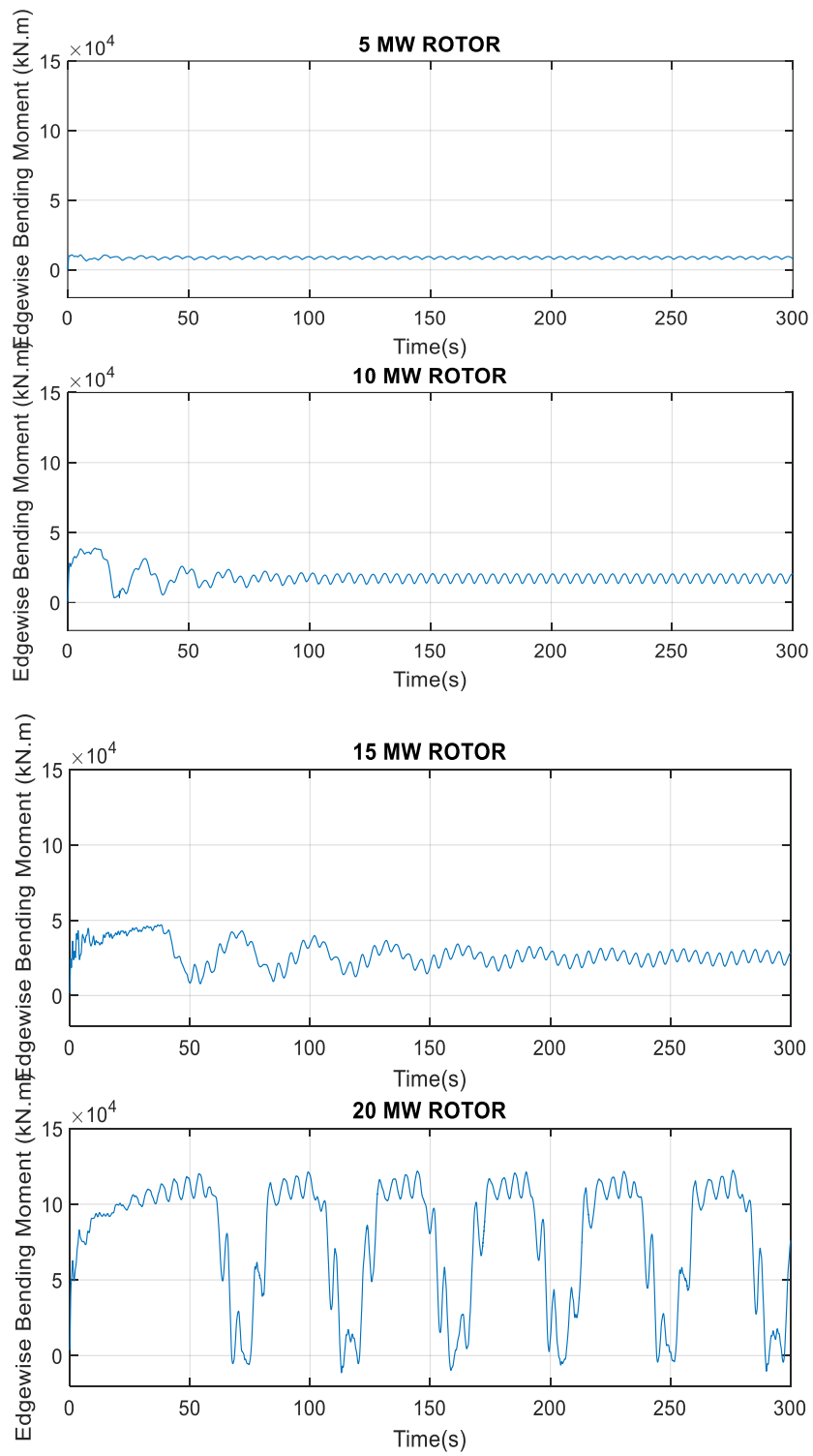


Figure 3.9 Bending Moments in Edgewise Direction for Scaled Models

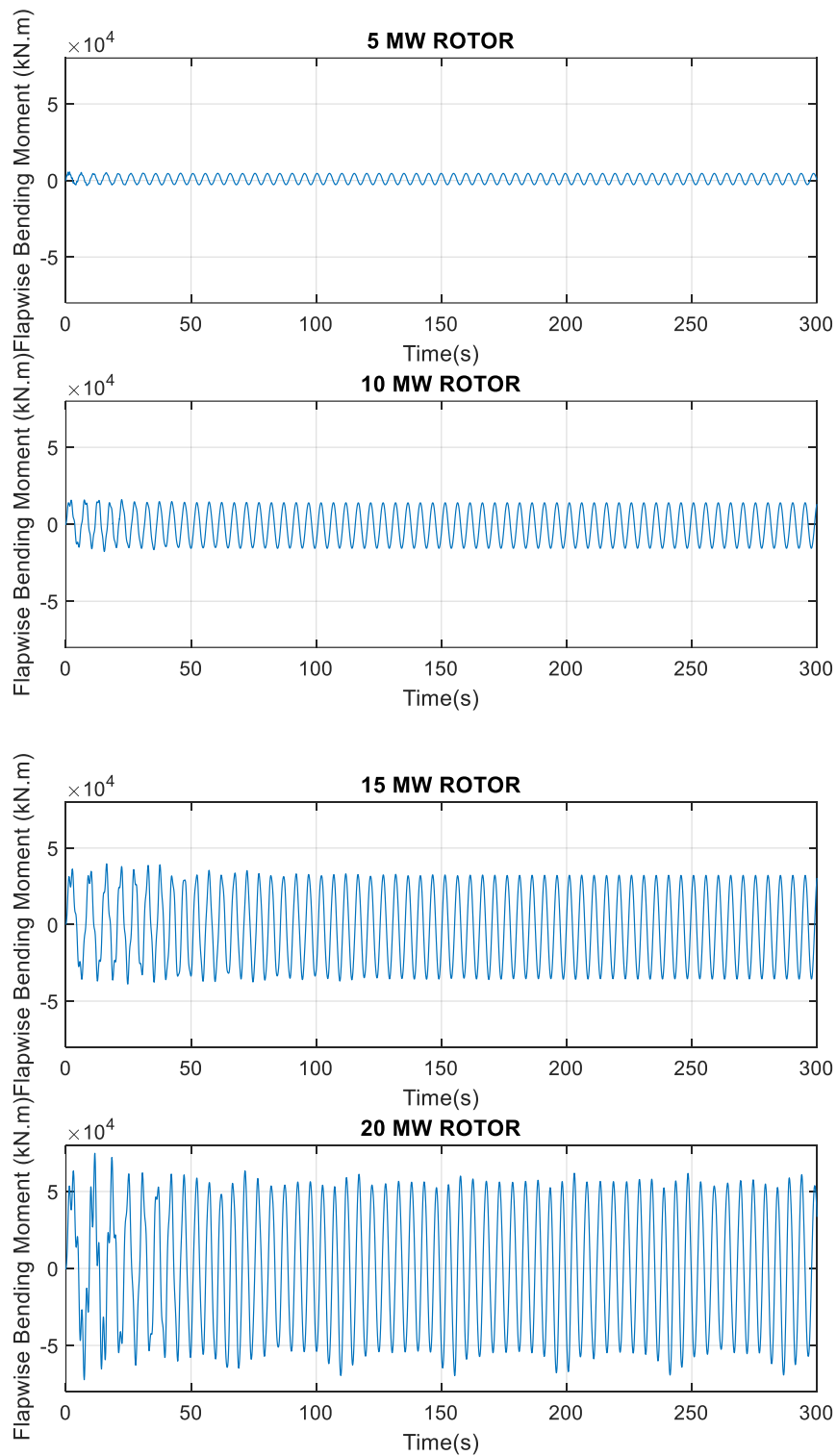


Figure 3.10 Bending Moments in Flap-wise Direction for Scaled Models

3.3. Optimum Wind Speed for 20 MW Rotor

For the 20 MW scaled rotor, obtained by the classical scaling, the performance results for a constant wind speed of 12 m/s are investigated. According to these results, both the aerodynamic and structural parameters such as power coefficient, thrust coefficient and bending moments are highly fluctuating and unstable. Therefore, the optimum wind speed is determined to operate at steady state with maximum performance.

Figure 3.11 shows the power coefficient variation for the 20 MW scaled rotor with respect to the changing wind speed. As it can be observed, a maximum power coefficient of 0.45 is obtained for a wind speed of 5 m/s. The performance decreases towards high speeds and the rotor operates unstable after 10 m/s wind speed.

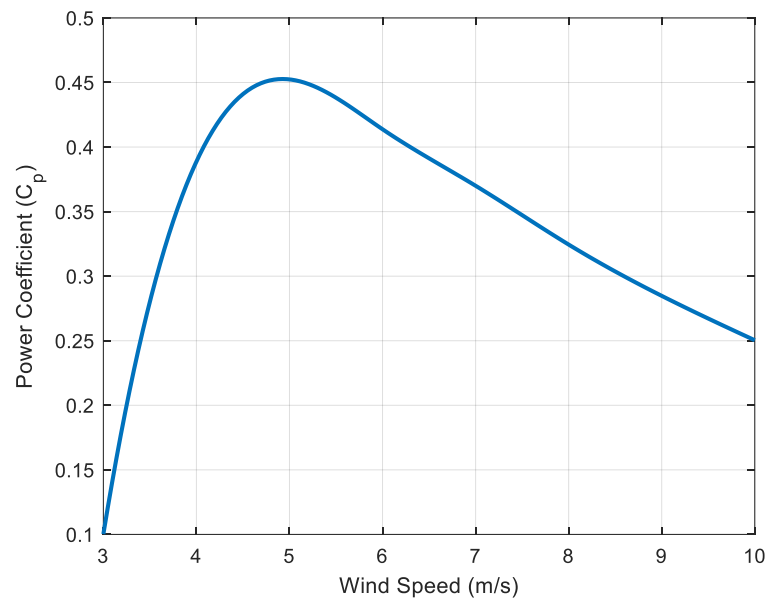


Figure 3.11 Power Coefficient Variation for Wind Speed for 20 MW rotor

According to these results, the aerodynamic and structural analyses are performed again by using the FAST code for a wind speed of 5 m/s. As shown in Figure 3.12, the oscillations are not observed in the edgewise bending moments due to the aerodynamic loads. The flapwise bending moment results due to gravity loads remain

similar with the 12 m/s case results because there is no change in the rotor mass and rigidity.

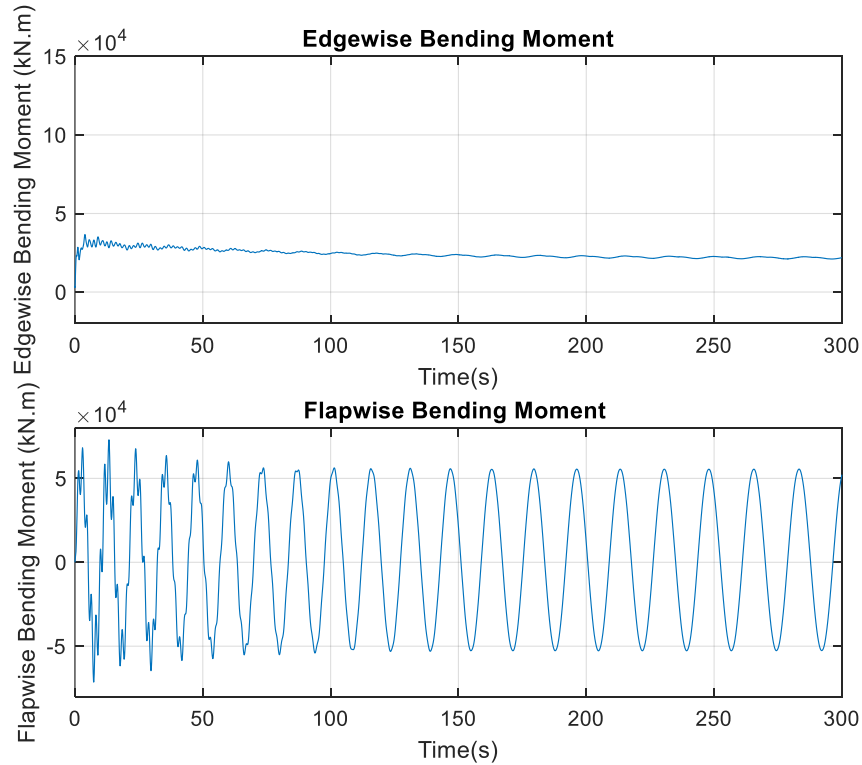


Figure 3.12 Flapwise and Edgewise Bending Moment for 20 MW at 5 m/s

As shown in Figure 3.12 and Figure 3.13 the aerodynamic performance results are quite stable and oscillation results are not observed at wind speed of 5 m/s. The power coefficient value is around 0.45 and the power of the rotor becomes constant around 15 MW. Thrust coefficient value is around 0.8.

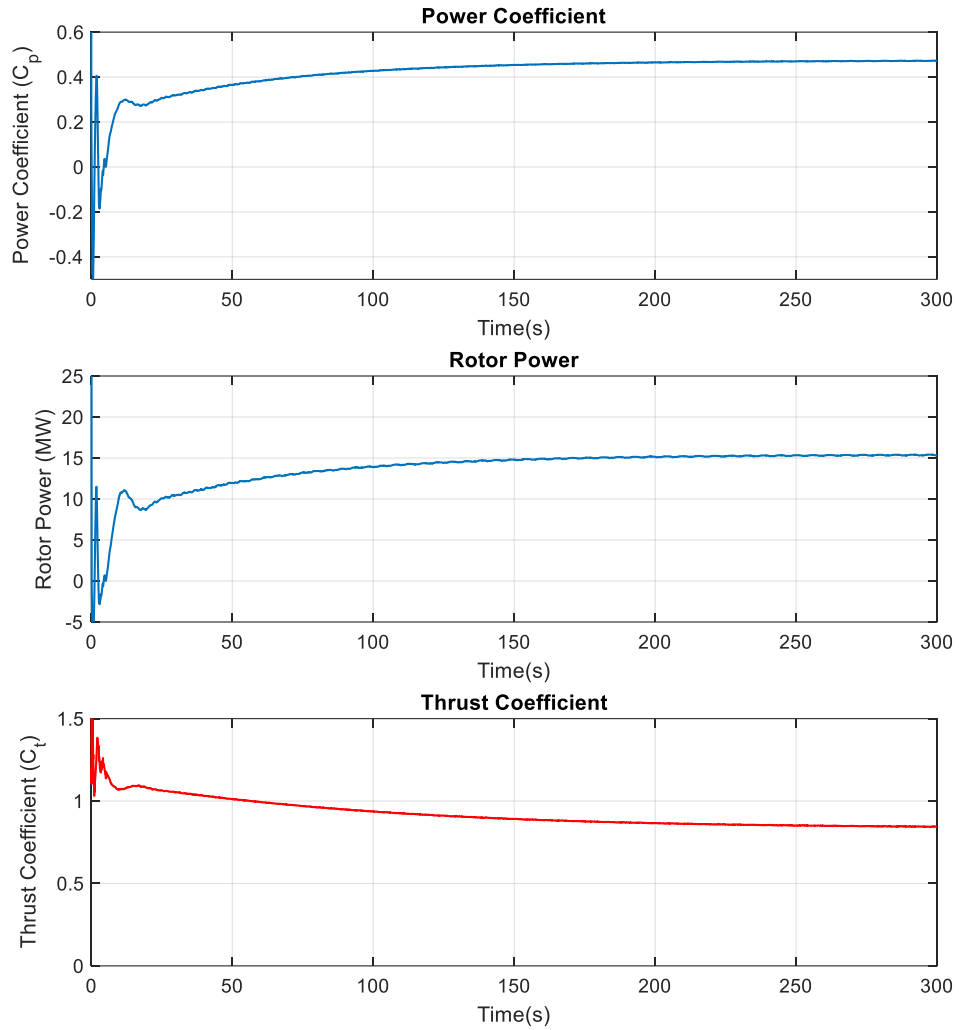


Figure 3.13 Power Coefficient, Rotor Power and Thrust Coefficient for 20 MW at 5 m/s

3.4. Summary

According to the results for the scaled rotors, both aerodynamic and structural performance losses have been observed for the wind turbine rotors modeled by the classical scaling laws, especially for very large rotors. It is concluded that in order to continue with the larger turbine design with better performances, the blade geometry must be redesigned and structurally more rigid and lighter materials should be used.

Hence, in the next part of the thesis, 5 MW, 10 MW, 15 MW and 20 MW wind turbines are optimized both structurally and aerodynamically and the results are compared.

CHAPTER 4

OPTIMIZATION AND DESIGN OF LARGE SCALE WIND TURBINES

4.1. Introduction

In this section, the aerodynamic blade shape and the blade mass of the 5 MW, 10 MW, 15MW and 20 MW wind turbine rotors have been optimized by using a multipurpose Genetic Algorithm (GA) and Blade Element Momentum (BEM) theory, with reference to the NREL 5 MW wind turbine rotor model. The optimization studies have been conducted to maximize the power generation and to minimize the blade mass.

4.2. Optimization Methodology

The design variables for the blade shape are the twist angle, chord length, percentage thickness, and shell thickness of the blade cross sections. In the optimization process, the wind speed range, rotor rpm range, maximum power value and maximum stress values are entered as constants of the optimization process.

In the aerodynamic analysis based on the Blade Element Momentum theory, the rotor blade is divided into several blade element sections. The structural and aerodynamic optimization studies are performed by taking the structural stresses, the bending moments and the mass per unit blade length into consideration for each of these blade elements.

The ideal rotor designs for 10 MW 15 MW and 20 MW turbines are also done by simplified analytical calculations for comparisons with the scaled and optimized rotor designs.

A multi-purpose design optimization is performed by using the Horizontal Axis Rotor Performance Optimization (HARP_Opt) code [16] developed by NREL. The HARP

code was developed by using the MATLAB Genetic Algorithm Optimization Toolbox and Statistics Toolbox. In this code, the Blade Element Momentum (BEM) theory is used to design horizontal axis turbine rotors. The objective of the optimization method is to maximize the turbine's annual power generation by minimizing the rotor mass. The Annual Energy Production (AEP) is calculated by using the Weibull wind speed distribution as [17]:

$$AEP = \sum_{i=1}^{N-1} 1/2(P(V_{i+1}) + (P(V_i)))x f(V_i < V_0 < V_{i+1})x 8760 \quad (4.1)$$

The powers at cut-out and cut-in speeds are indicated by $P(V_{i+1})$ and $P(V_i)$, 8760 represents the total hour in a year, and the wind speed probability density function using the Weibull distribution is represented by $f(V_i < V_0 < V_{i+1})$ as:

$$f(V_i < V_0 < V_{i+1}) = \exp\left(-\left(\frac{V_i}{c}\right)^k\right) - \exp\left(-\left(\frac{V_{i+1}}{c}\right)^k\right) \quad (4.2)$$

where, c is the scale parameter, k is the shape parameter and V is the wind speed.

While maximizing the energy production, minimizing the blade mass is a challenging objective. In this study, the blade mass has been reduced based on some structural constraints such as strain and moments. In order to achieve this goal, the optimal blade shape (with pre-bending, chord length, percentage thickness, and shell thickness distributions along the span) is calculated by using HARP_Opt code.

The algorithm of the HARP Optimization code is as shown in the Figure 4.1. Both aerodynamic and structural design parameters for an optimum turbine are calculated by using the multi-purpose optimization algorithm with the specific targets and constraints.

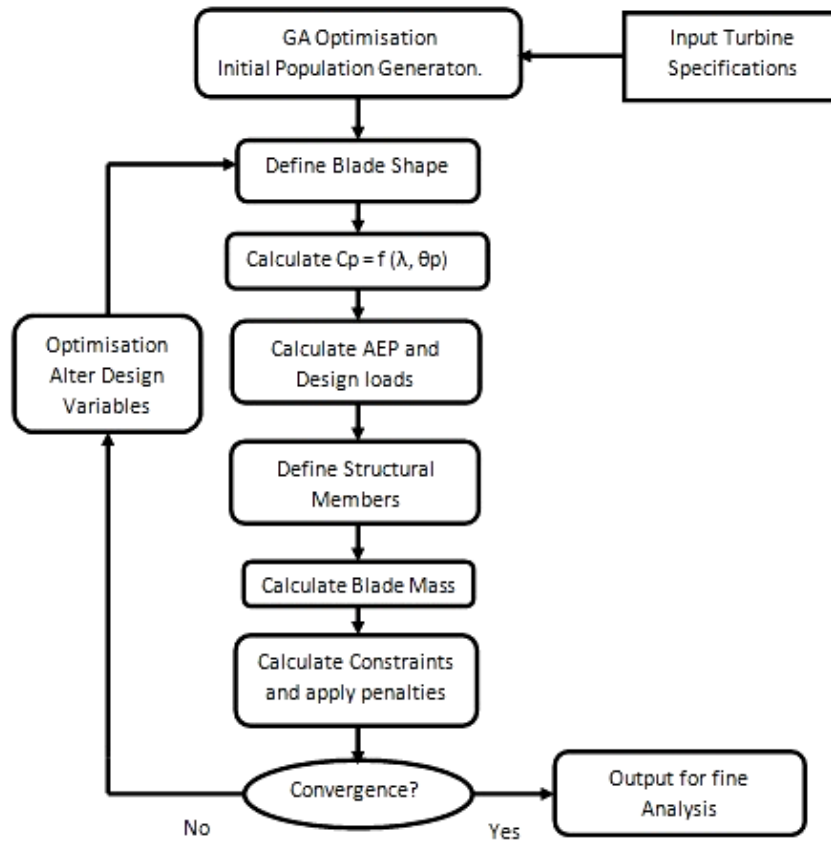


Figure 4.1 HARP Optimization Multi-objective design algorithm.

The structural analyses are performed by using the Euler - Bernoulli Beam Theory with the objective of minimizing the blade mass. In the Euler - Bernoulli Beam theory, the wind turbine blade is assumed to be a thin - shell cantilever beam with isotropic material properties. In order to analyze the structural stability, the design load is released from the maximum root moment under all operating conditions, together with the applied safety factor. This structural optimization is only achieved by taking into account the maximum permissible bending stress.

In structural optimization, the rotor blade with isotropic material properties is modeled as a simple beam model. The rotor blade section is modeled as a thin shell. Strain is calculated using Equation 4.3 below, with four strain gauges placed as shown in Figure 4.2.

$$\text{Bending Strain } \varepsilon_r = SF * \frac{M_r C_r}{EI_r} \quad (4.3)$$

where, M is the bending moment, C is the distance from the neutral axis, E is the modulus of elasticity, I is the moment of inertia, and the subscript r denotes the local radial position value.

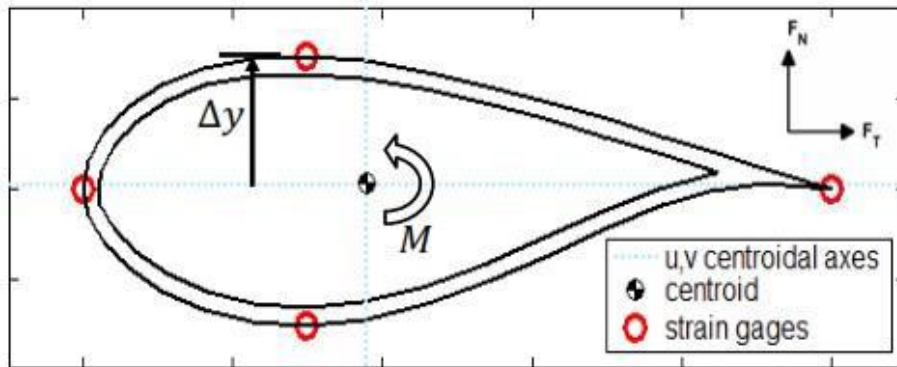


Figure 4.2 Wind turbine blade cross section showing centroidal axes, centroid and locations of strain gauges. [17]

4.3. Blade Element Momentum Theory (BEM)

In the Blade Element Momentum (BEM) theory, the Blade Element theory and the Momentum theory are combined. The Momentum theory represents a control volume analysis of the forces acting on the rotor disk based on the conservation of linear and angular momentum. The Blade Element theory represents an analysis of forces at a blade section as a function of blade geometry.

4.3.1. Momentum Theory (Actuator Disk Model)

The Momentum theory is based on the assumptions which are:

- no frictional drag,
- flow is homogeneous,
- incompressible,
- steady state,
- constant pressure increment with continuous velocity through the disc.

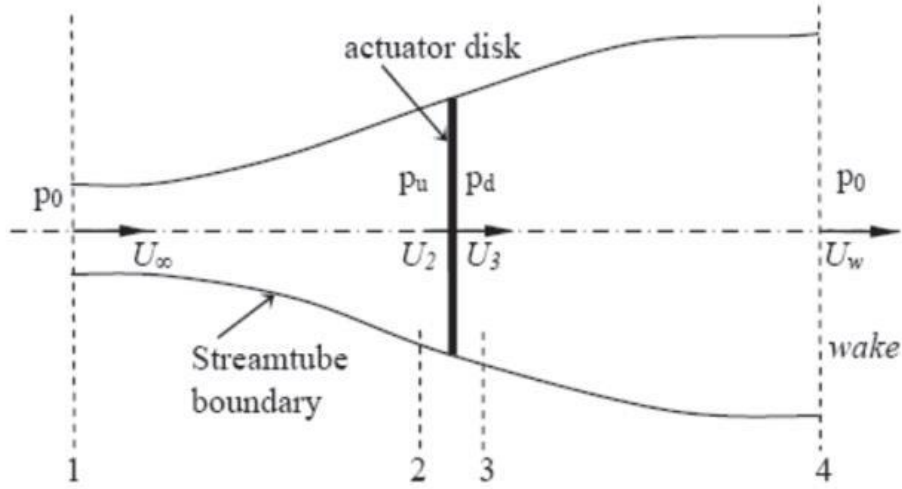


Figure 4.3. The Actuator Disc Model [18]

As shown in Figure 4.3, the first region is the free-stream region; the second, just before the blades; the third region, just after the blades; and the last one, the far wake region. The mass flow rate remains the same through the stream tube. According to the continuity equation, the equation along the stream tube can be expressed as:

$$\rho U_1 A_1 = \rho U_2 A_2 = \rho U_4 A_4 \quad (4.4)$$

The difference between U_1 and U_2 is called the axial induced velocity. This velocity is represented in terms of freestream velocity and it is nondimensionalized with the freestream velocity:

$$(U_1 - U_2)/U_1 = a \quad (4.5)$$

The velocity component, U_2 , can be expressed as:

$$U_2 = U_1(1 - a) \quad (4.6)$$

From conservation of momentum across the actuator disk;

$$(p_2 - p_3)A_2 = (U_1 - U_4)\rho A_2 U_1(1 - a) \quad (4.7)$$

By using Bernoulli's equation, pressure values are expressed in terms of velocities, the following relation is obtained as:

$$U_4 = U_1(1 - 2a) \quad (4.8)$$

The thrust can also be expressed as the net sum of the forces on each side of the actuator disc::

$$T = \frac{1}{2}\rho A_2(U_1^2 - U_4^2) \quad (4.9)$$

From Equations (3.3), (3.5) and (3.6), the axial thrust on the disc is:

$$T = \frac{1}{2}\rho AU^2[4a(1 - a)]$$

The power output of the rotor, P, is equal to the thrust times the velocity at the disc:

$$P = 2\rho A_2 U_1^3 a(1 - a) \quad (4.10)$$

The power coefficient is defined as the ratio of power extracted to the available power:

$$C_p = \frac{2\rho A_2 U_1^3 a(1 - a)}{\frac{1}{2}\rho U_1^3 A_2} = 4a(1 - a)^2$$

which shows an equation of power coefficient with respect to the induction factor. The maximum power coefficient can be found as:

$$\frac{dC_p}{da} = 0 \quad \text{and so,} \quad C_{pmax} = 0.593$$

This is the maximum power coefficient limit for a wind turbine rotor which is known as the Betz Limit.

4.3.1.1. Angular Momentum Theory

By considering the conservation of angular momentum in an annular stream tube as shown in Figure 4.4, while the blades rotate with an angular velocity of Ω , the blade wake rotates with an angular velocity ω , and for the small annular element the corresponding torque is calculated as:

$$dQ = d\dot{m}\rho\omega r^2 = (\rho U_2 2\pi r dr)(\omega r)r \quad (4.11)$$

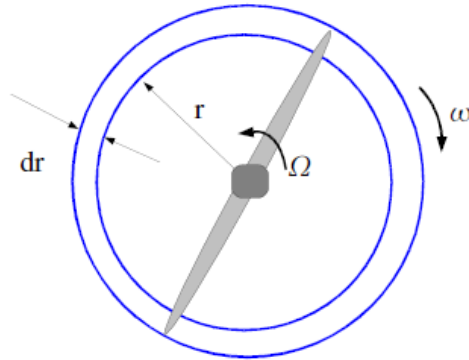


Figure 4.4. Rotating Annular Stream tube

The angular induction factor a' is defined as:

$$a' = \omega/2\Omega \quad (4.12)$$

and, the torque expression reduces to:

$$dQ = 4a'(1 - a)\frac{1}{2}\rho U\Omega r^2 2\pi r dr \quad (4.13)$$

The resulting thrust on an annular element, dT , is given by:

$$dT = 4a'(1 + a)\frac{1}{2}\rho U\Omega^2 r^2 2\pi r dr \quad (4.14)$$

4.3.1.2. Blade Element Theory

Blade element theory relies on two key assumptions:

- There are no aerodynamic interactions between different blade elements
- The forces on the blade elements are solely determined by the lift and drag coefficients.

The blade is divided up into N elements (usually between ten and twenty) as shown in Figure 4.5. Each of the blade elements have different pitch angle, chord length and twist angle as shown in Figure 4.6.

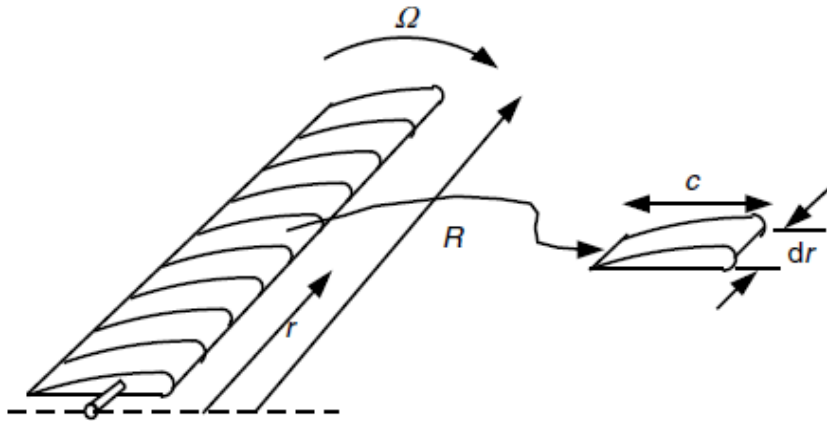


Figure 4.5. Schematic view of Blade Element Model [18]

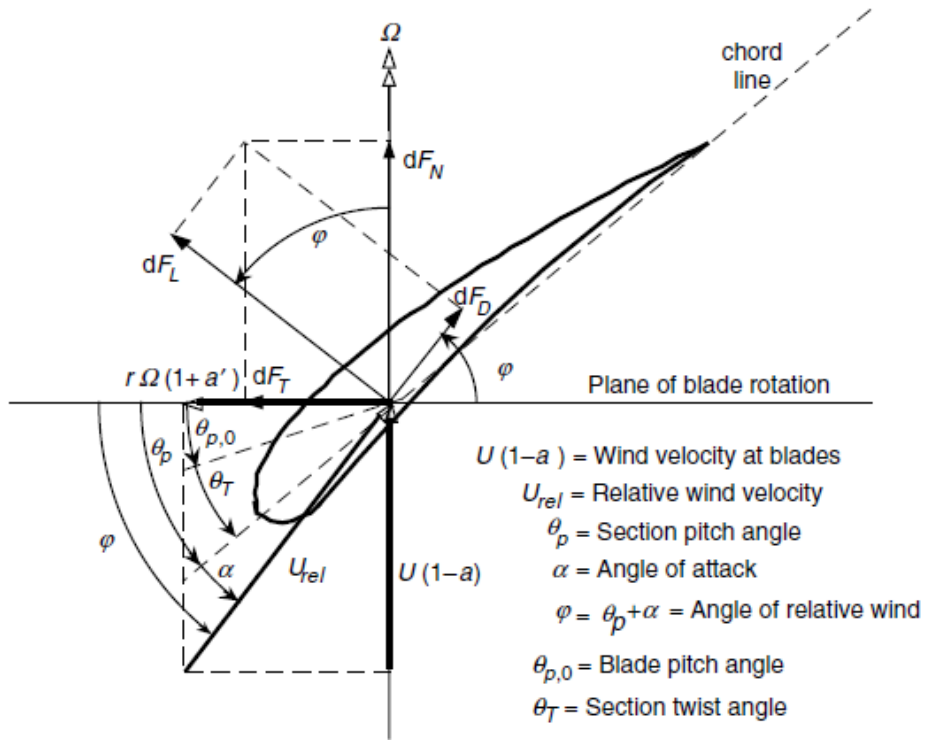


Figure 4.6. Blade geometry for analysis of a horizontal axis wind turbine [18]

From Figure 4.6, the following relationships can be determined;

$$\tan\varphi = \frac{U(1-a)}{\Omega r(1+a')} = \frac{1-a}{(1-a')\lambda_r} \quad (4.15)$$

$$U_{rel} = U(1 - a)/\sin\varphi \quad (4.16)$$

$$dF_L = C_l \frac{1}{2} \rho U_{rel}^2 c dr \quad (4.17)$$

$$dF_D = C_d \frac{1}{2} \rho U_{rel}^2 c dr \quad (4.18)$$

$$dF_N = dF_L \cos\varphi + dF_D \sin\varphi \quad (4.19)$$

$$dF_T = dF_L \sin\varphi - dF_D \cos\varphi \quad (4.20)$$

If the rotor has B blades, the total normal force (thrust) on the section at a distance, r , from the center is:

$$dF_N = B \frac{1}{2} \rho U_{rel}^2 (C_l \cos\varphi + C_d \sin\varphi) c dr \quad (4.21)$$

The differential torque due to the tangential force operating at a distance, r , from the center is given by:

$$dQ = B \frac{1}{2} \rho U_{rel}^2 (C_l \sin\varphi - C_d \cos\varphi) c dr \quad (4.22)$$

The relative velocity can be expressed as a function of the free stream wind using Equation 4.16. Thus, Equations 4.21 and 4.22 from Blade Element theory can be written as below as a function of the flow angles at the blade sections and airfoil characteristics:

$$dF_N = \sigma' \pi \rho U^2 (1 - a)^2 / \sin^2 \varphi (C_l \cos\varphi + C_d \sin\varphi) r dr \quad (4.23)$$

$$dF_T = \sigma' \pi \rho U^2 (1 - a)^2 / \sin^2 \varphi (C_l \sin\varphi - C_d \cos\varphi) r^2 dr \quad (4.24)$$

where, σ is the local solidity, defined by:

$$\sigma' = Bc/2\pi r \quad (4.25)$$

4.3.1.3. Tip Loss Correction

A correction factor is used in BEM theory in order to decrease effect of tip vortices which is occurred at the turbine blade tip. This correction factor, F , varies from 0 to 1 and characterizes the reduction in forces along the blade. According to this method, a correction factor, F , that must be introduced into the Equations 4.23 and 4.24, is defined as:

$$F = \left(\frac{2}{\pi}\right) \cos^{-1} \left[\exp \left(- \left\{ \frac{\left(\frac{B}{2}\right) \left[1 - \frac{r}{R}\right]}{\left(\frac{r}{R}\right) \sin \varphi} \right\} \right) \right] \quad (4.26)$$

4.3.1.4. Blade Element Momentum Theory

Thus, the thrust and torque equations in terms of flow parameters (Equations 4.13 and 4.14) from the Momentum theory, and the thrust and torque equations derived from the blade loads in terms of the lift and drag coefficients of the airfoil (Equations 4.23 and 4.24) are equated and the following relations are obtained for the induction factors:

$$C_l = 4F \sin \varphi \frac{(\cos \varphi - \lambda_r \sin \varphi)}{\sigma' (\sin \varphi + \lambda_r \cos \varphi)} \quad (4.27)$$

$$a = 1 / [1 + 4F \sin^2 \varphi / (\sigma' C_l \cos \varphi)] \quad (4.28)$$

$$a' = 1 / \left[\left(\frac{4F \cos \varphi}{\sigma' C_l} - 1 \right) \right] \quad (4.29)$$

Then, the power coefficient is calculated as:

$$C_p = \left(\frac{8}{\lambda^2}\right) \int_{\lambda_h}^{\lambda} F \sin^2 \varphi (\cos \varphi - \lambda_r \sin \varphi) (\sin \varphi + \lambda_r \cos \varphi) \left[1 - \left(\frac{C_d}{C_l}\right) \cot \varphi\right] \lambda_r^2 d\lambda_r \quad (4.30)$$

4.3.2. Design Optimization of 5 MW NREL Wind Turbine

In this section, the 5 MW NREL wind turbine is optimized by using the HARP optimization code. The aerodynamic and structural constraints and all the design inputs used in the optimization process are given in the Table 4-1. The Genetic Algorithm parameters [19] used in the optimizations are the population size (number of individuals per generation) as 25, the maximum number of generations for GA iterations as 25, the fraction of individuals created by crossover as 0.25, the number of elite individuals per generation as 1, and the error tolerance for the GA fitness value as 1.0x10-6.

Table 4-1 *Design inputs of the optimization of the 5 MW wind turbine*

Minimum flow speed = 2 m/s
Maximum flow speed = 26 m/s
Minimum allowable rotor speed = 4 rpm
Maximum allowable rotor speed = 25 rpm
Initial Weibull distribution long-term mean flow speed = 6.03 m/s
Weibull shape factor = 1.91
Weibull scale factor = 6.8
Shell thickness increment (mm) = 0.2
Minimum shell thickness (mm) = 1
Safety factor multiplied to bending moments = 1.2
Maximum allowable strain (micro-strain) = 3000
Density of bulk material (kgm³) = 1800
E (Modulus of elasticity of bulk material (GPa)) = 27.6

The airfoil profiles remain unchanged during the optimization process, while the chord, twist angle, nominal rotational speed and thickness are defined as the blade design variables to be optimized. The GA optimization for maximizing the Annual Energy Production (AEP) using the HARP optimization algorithm converged with 78 iterations as the number of stall generations exceeds the limiting value of 25 which have been defined already in the code.

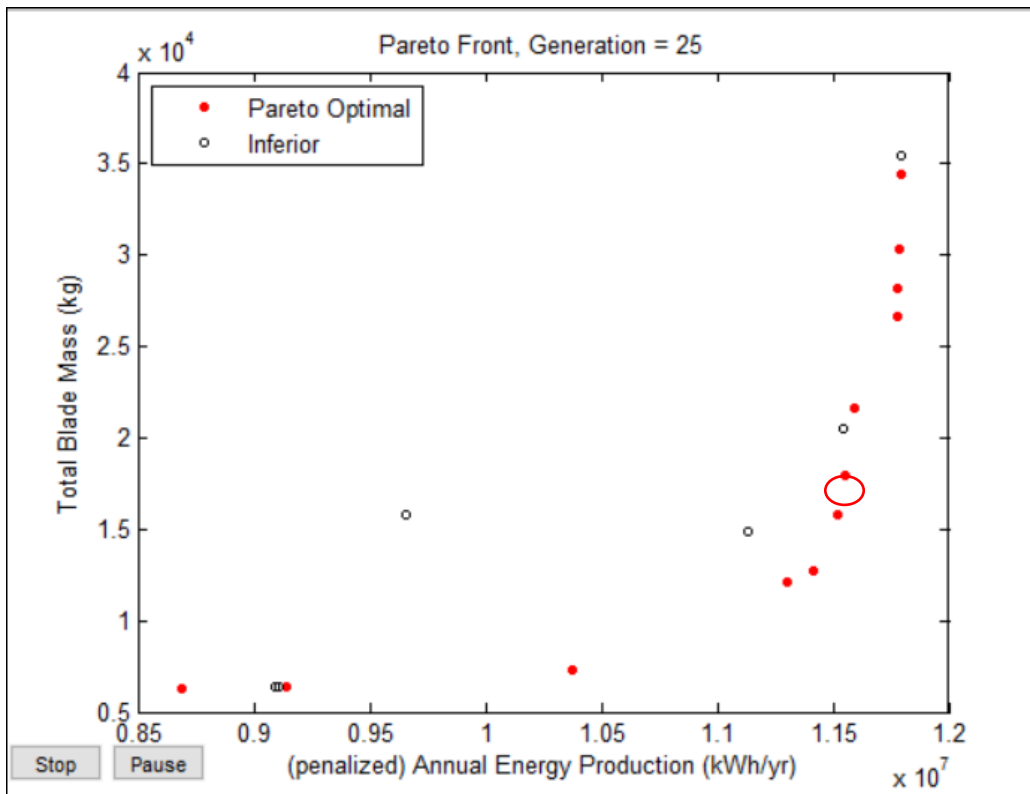


Figure 4.7 Annual Energy Production vs Blade Mass Relationship for 5 MW blade

In the Figure 4.7, the convergence of the optimization process according to the annual energy production and rotor mass are presented. As can be seen from the figure, the annual energy production has become stable after certain iterations. The optimal result is chosen as the blade mass close to the reference turbine. Optimized 5 MW turbine blade for the selected optimal result is obtained.

The optimized twist angle is obtained from 5 control points and based on the Bezier curve. The fifth-order Bezier curve is used to pass over these control points. The chord length is then optimized to reduce the total rotor mass which is the second target. The percentage thickness can be defined as the thickness per unit chord length. The dimensional thickness is calculated by combining the chord length and percentage thickness as $t = c * (t / c)$. As the optimization method is multi-purpose (multi-objective), the dimensional thickness is of greater importance in reducing the rotor

mass. However, the maximum strain value constraint, defined as 3000, prevents the rotor mass reduction.

4.3.3. Comparison of Original NREL 5 MW Blade with the Optimized NREL 5 MW Blade

In this comparison study, the original rotor parameters are compared with the optimized rotor parameters and the results are presented. By using comparison graphs, an idea is given about how different parameters such as twist angle, chord length, mass distribution, flapwise and edgewise stiffness values change from root to tip region. This is achieved by comparing the aerodynamic and structural parameters of the original rotor with the best values obtained from the optimization.

In Figure 4.8, the comparison of the chord length distribution for the original rotor blade and the optimized rotor blade is presented. Here, it is observed that the optimized blade chord length increases according to the original chord length up to 40 m rotor radius. However, a linear decrease is observed after 40 m. During optimization, no significant reduction in chord length is observed due to structural constraints.

In Figure 4.9 the twist angle comparison of the original blade and the optimized blade is shown. During optimization, an upper limit of 40 degrees and a lower limit of -10 degrees are defined for the twist angle. Therefore, twist angle values increase up to 48 m rotor blade radius. From 48 m of blade radius to tip, there is twist reduction.

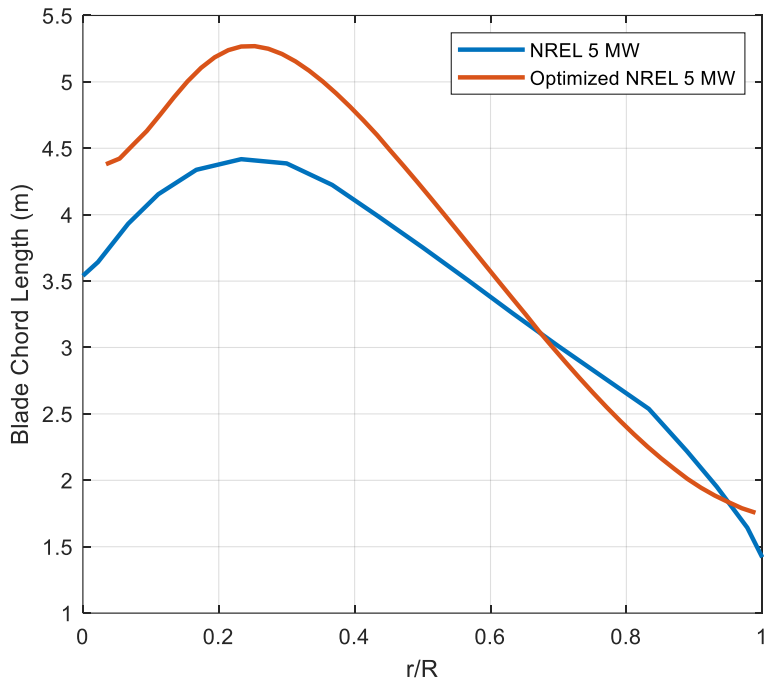


Figure 4.8 Comparison of Blade Chord length (m) of Original and Optimized blade.

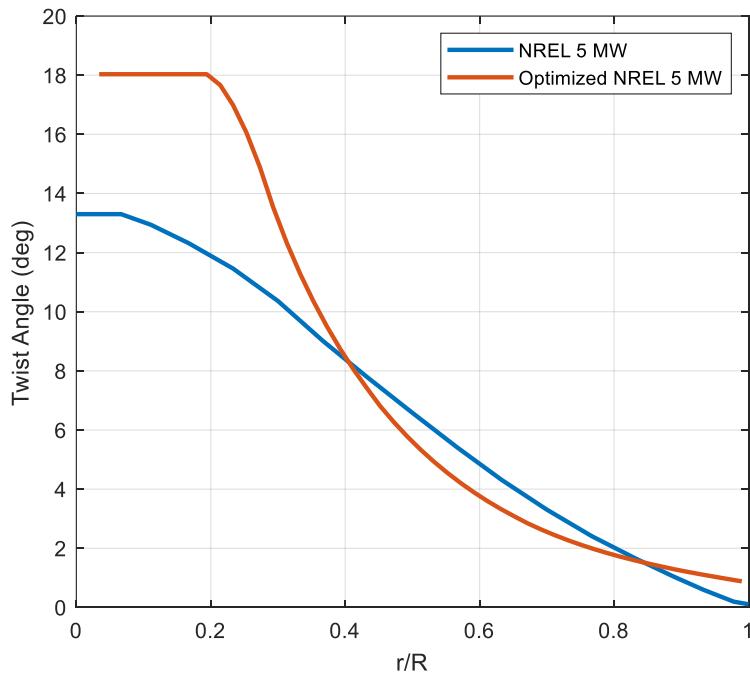


Figure 4.9 Comparison of Blade Twist of Original and Optimized Blade.

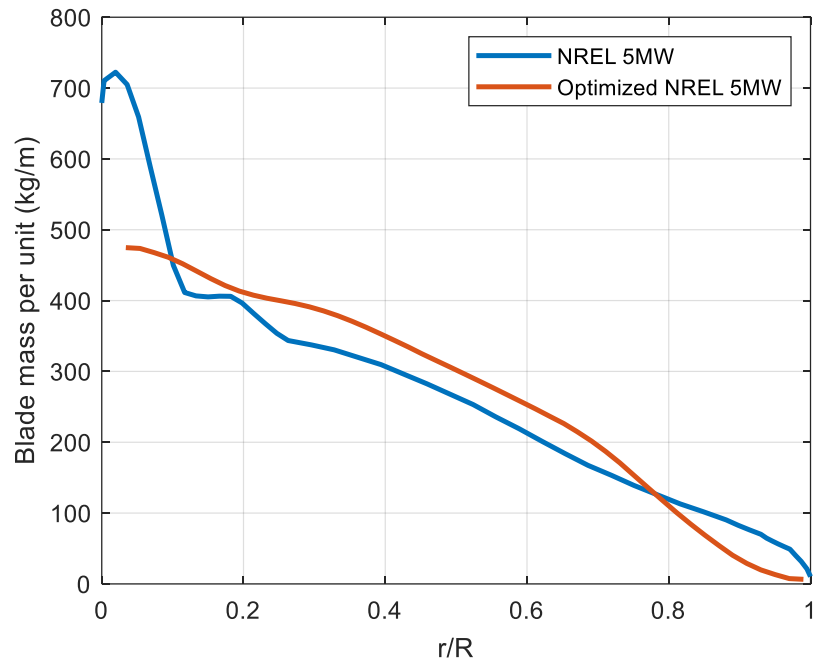


Figure 4.10 Mass per unit span (kg/m) distribution

In Figure 4.10 shows the blade mass per unit span having higher values in the root region and reducing into the tip region.

As shown in Figure 4.11, the flapwise stiffness is increased from root to 0.2 r/R, and from this station to the tip, the flapwise stiffness is remained the same. As shown Figure 4.12, the edgewise stiffness along span is increased from the root to near tip of the blade for the optimized NREL 5 MW blade.

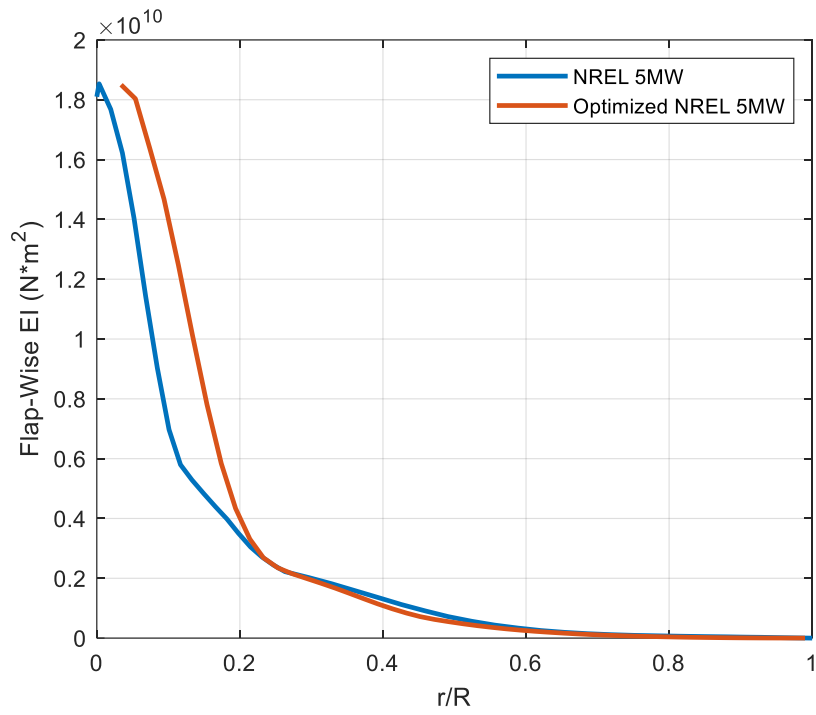


Figure 4.11 Flap-wise stiffness distribution along span

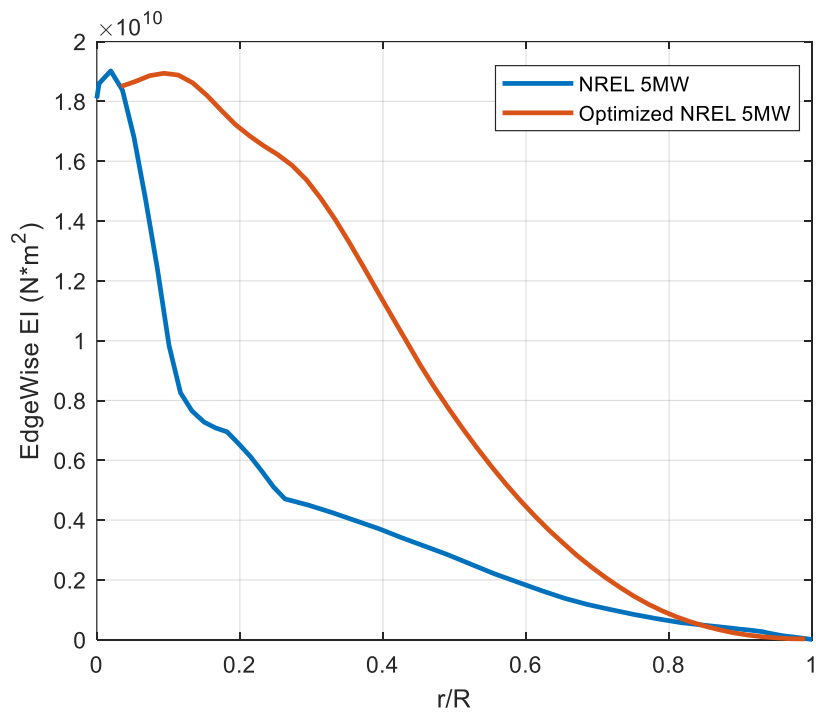


Figure 4.12 Edge-wise stiffness distribution along span

4.3.4. Performance Comparison of Original NREL 5 MW Rotor with the Optimized 5 MW Rotor.

The aerodynamic and structural performance analyses are done by using the FAST code for the baseline rotor and the optimized rotor for 5 MW power level and the performance results are compared with each other.

The performance power coefficient can be defined as the power generating capacity of a wind turbine. According to the analyses, it is observed that the power coefficient (C_p) value is increased for the optimized rotor as expected. For the original baseline 5 MW rotor, the power coefficient value is around 0.41, and for the optimized blade it is around 0.48 as shown in Figure 4.13.

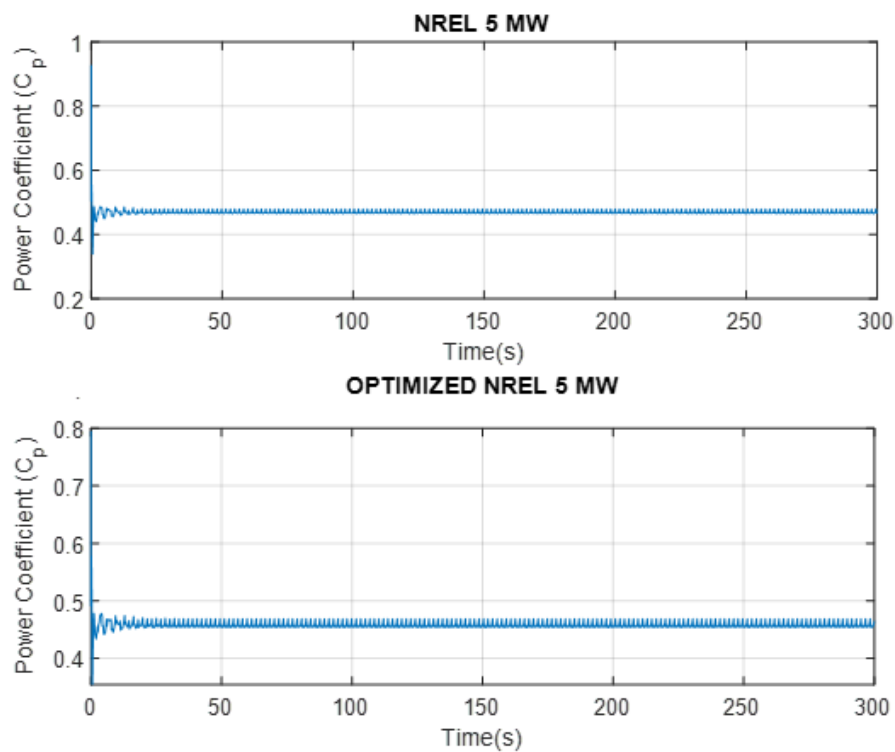


Figure 4.13 Comparison of Time-dependent Power Coefficient Value (C_p)

4.4. Multi-purpose Optimization of the 10, 15 and 20 MW Wind Turbines

In the previous section, the design optimization of the 5 MW wind turbine is presented in detail. In this section, 10, 15 and 20 MW wind turbines are designed using the same design methodology. This section presents all the design variables and design constraints as well as the characteristics of the resulting optimized wind turbines of 10, 15 and 20 MW. An aeroelastic design optimization methodology is used to achieve the optimum design for large wind turbines.

In this optimization study, the linear scaling laws are used to find the initial design variables. In other words, initial design variables of 10, 15 and 20 MW wind turbines are obtained without any conceptual change in their design by applying linear scaling laws to the original NREL 5 MW wind turbine.

As shown in Figure 4.14, Figure 4.16 and Figure 4.18, the optimization process for 10, 15 and 20 MW wind turbines are presented. In the convergence of the optimization process is presented according to the annual energy production and rotor mass. As can be seen from the figures, the annual energy production has become stable after certain iterations for all cases. The optimal results are marked on the figures. The optimal result is chosen as the blade mass being close to the reference turbine.

Also, upper and lower limits are presented for 10, 15 and 20 MW in Figure 4.15, Figure 4.17 and Figure 4.19, respectively. The upper and lower limits determined for 5 control points are determined as ± 1 neighborhood based on the chord length and the twist angle obtained by the classical scaling rules.

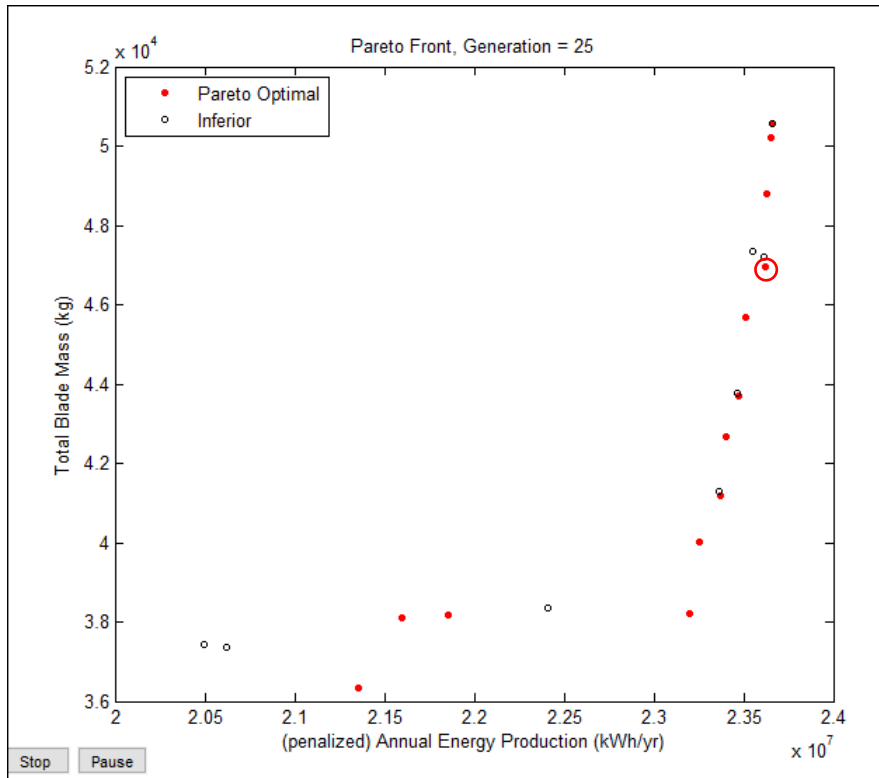


Figure 4.14 Annual Energy Production vs Blade Mass Relationship for 10 MW blade

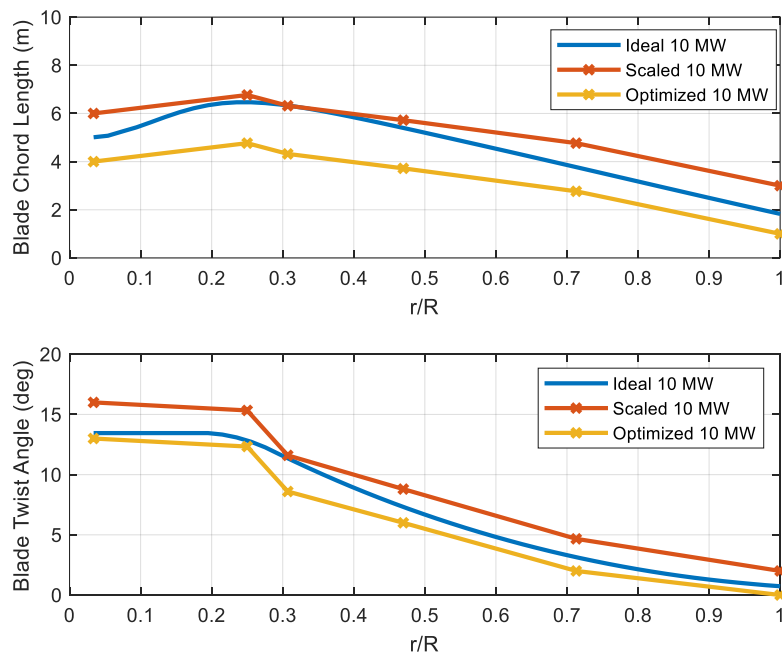


Figure 4.15 Upper and Lower Limits of chord and twist angle for 10MW

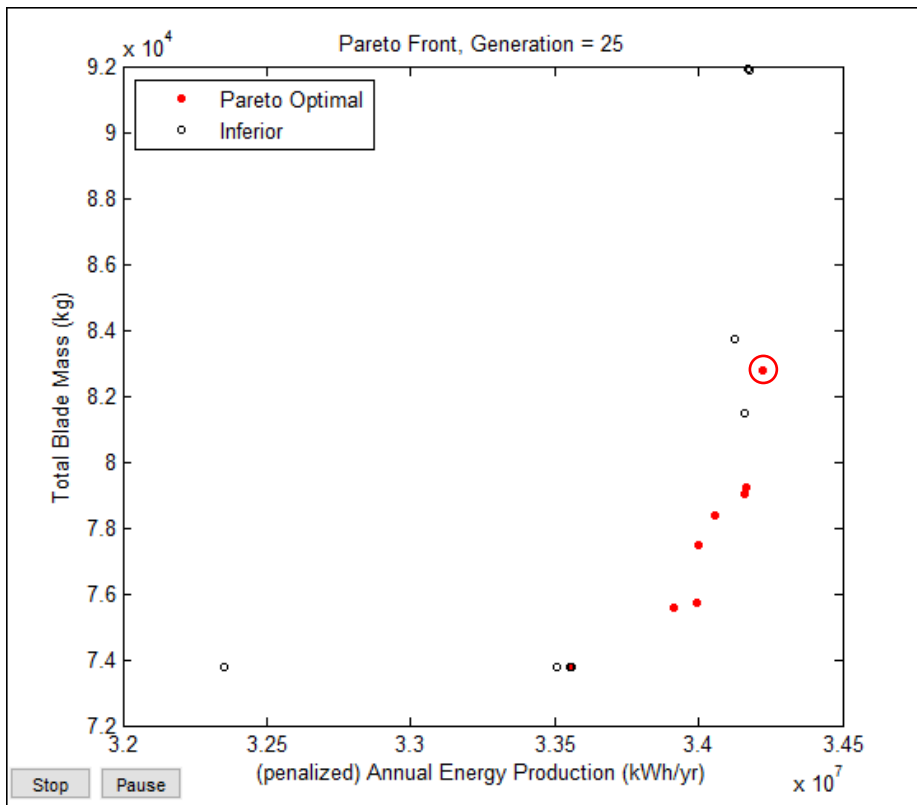


Figure 4.16 Annual Energy Production vs Blade Mass Relationship for 15 MW blade

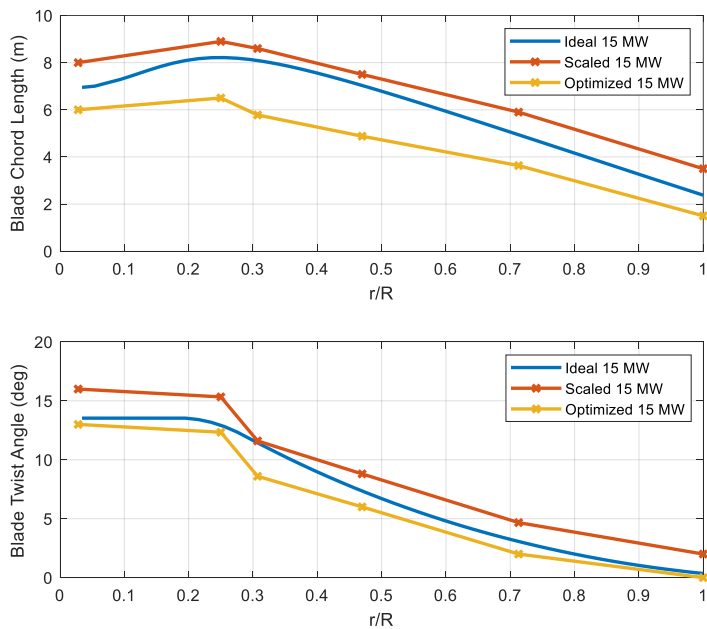


Figure 4.17 Upper and Lower Limits of chord and twist angle for 15 MW

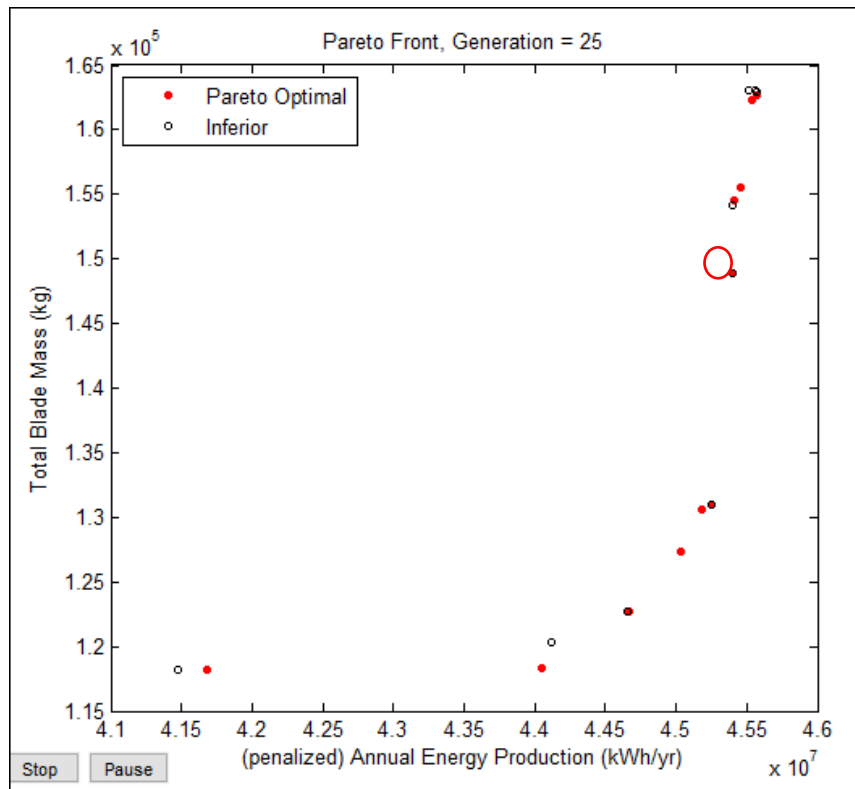


Figure 4.18 Annual Energy Production vs Blade Mass Relationship for 20 MW blade

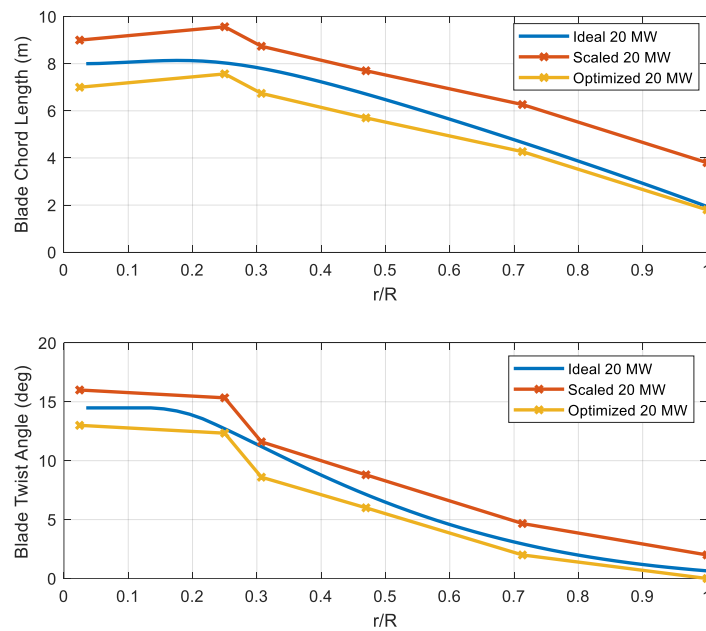


Figure 4.19 Upper and Lower Limits of chord and twist angle for 20 MW

4.4.1. Properties of the Optimized 10, 15 and 20 MW Wind Turbines

In this section, for the optimized 10, 15 and 20 MW rotors, the aerodynamic and structural properties are presented such as the chord length (Figure 4.20, Figure 4.21 and Figure 4.22), twist angle (Figure 4.23, Figure 4.24 and Figure 4.25), and the distributed blade section mass per unit length, the flapwise and edgewise stiffness (Figure 4.26, Figure 4.27 and Figure 4.28). To enable a detailed comparison, the distributions for the scaled wind turbine rotors are also presented for 10, 15 and 20 MW. Also, for the chord length and the twist angle, the ideal rotor properties, which are obtained from the in-house simplified BEM code, are presented for comparison. Table 4-2 summarizes the properties of the optimized 10, 15 and 20 MW wind turbines.

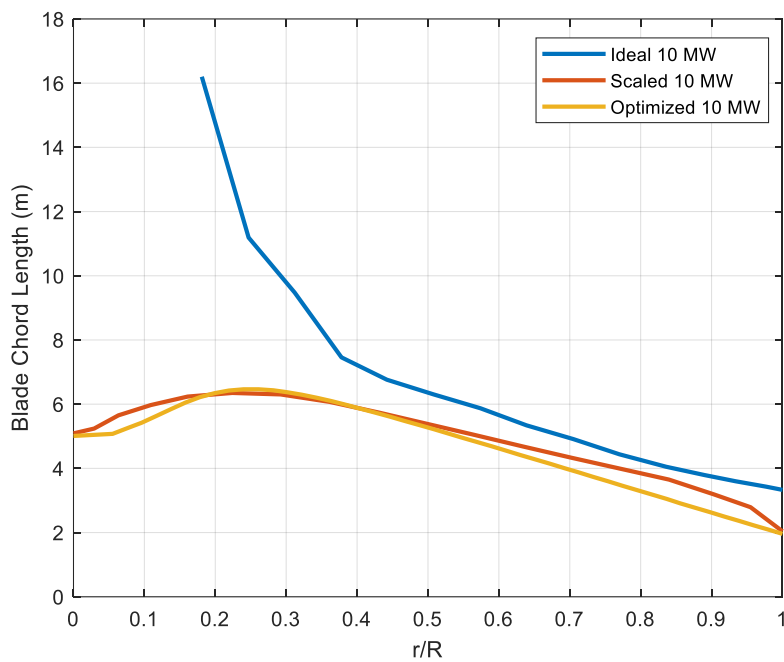


Figure 4.20 Chord Length Comparison for 10 MW Blade

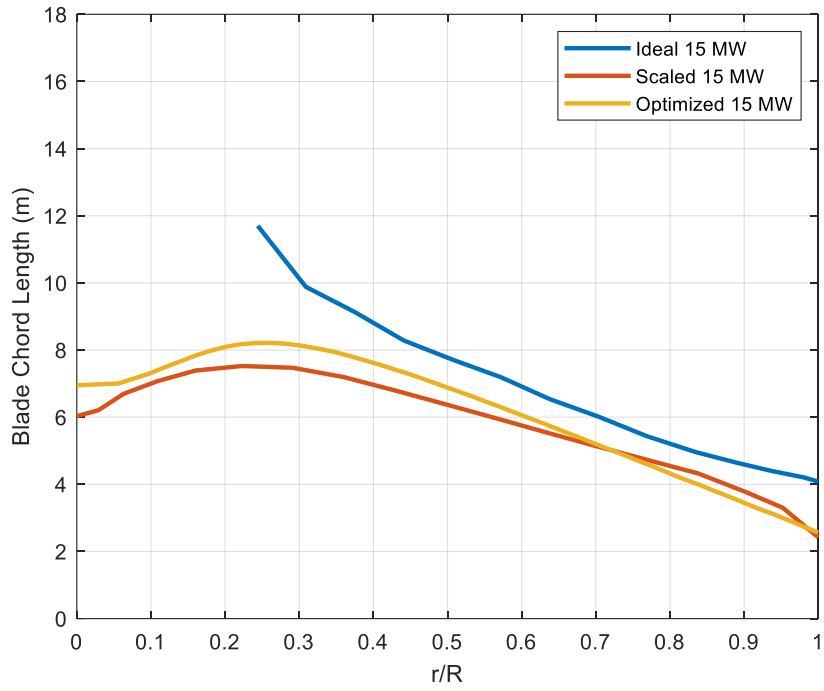


Figure 4.21 Chord Length Comparison for 15 MW Blade

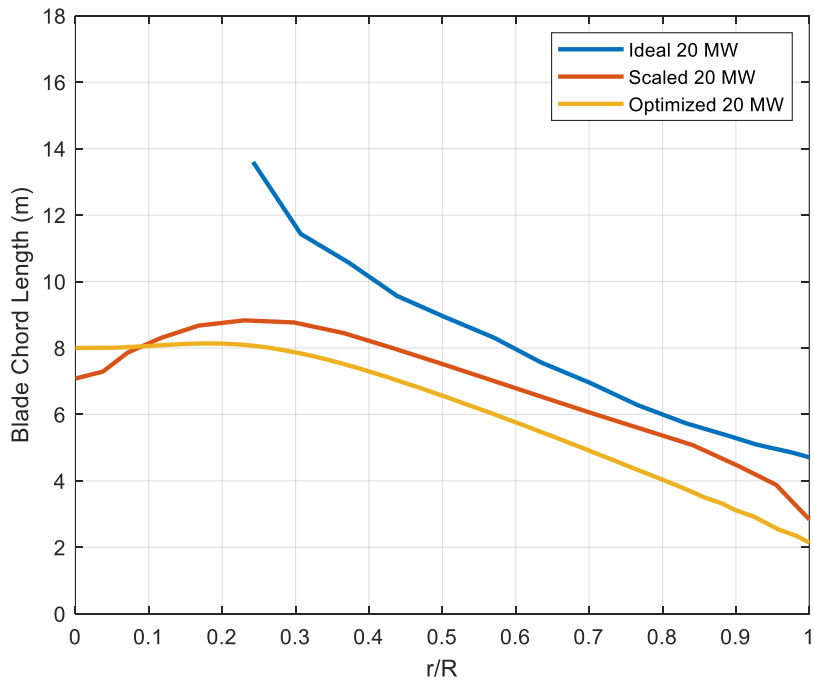


Figure 4.22 Chord Length Comparison for 20 MW Blade

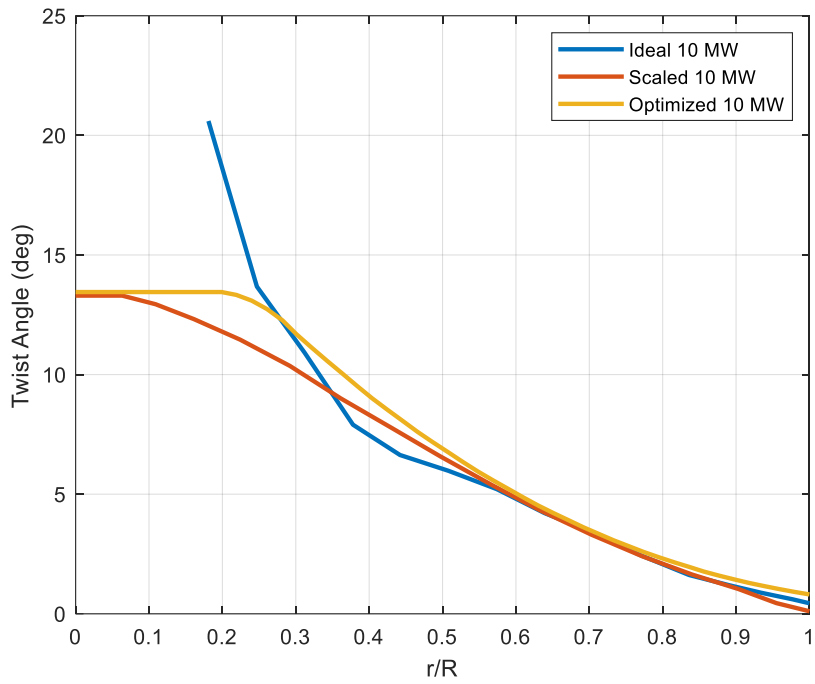


Figure 4.23 Twist Angle Comparison for 10 MW Blade

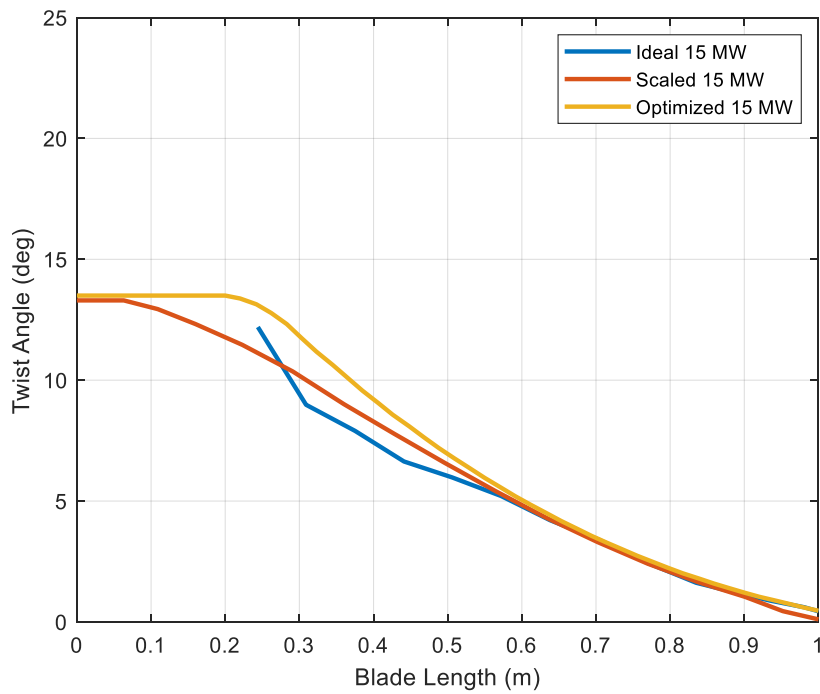


Figure 4.24 Twist Angle Comparison for 15 MW Blade

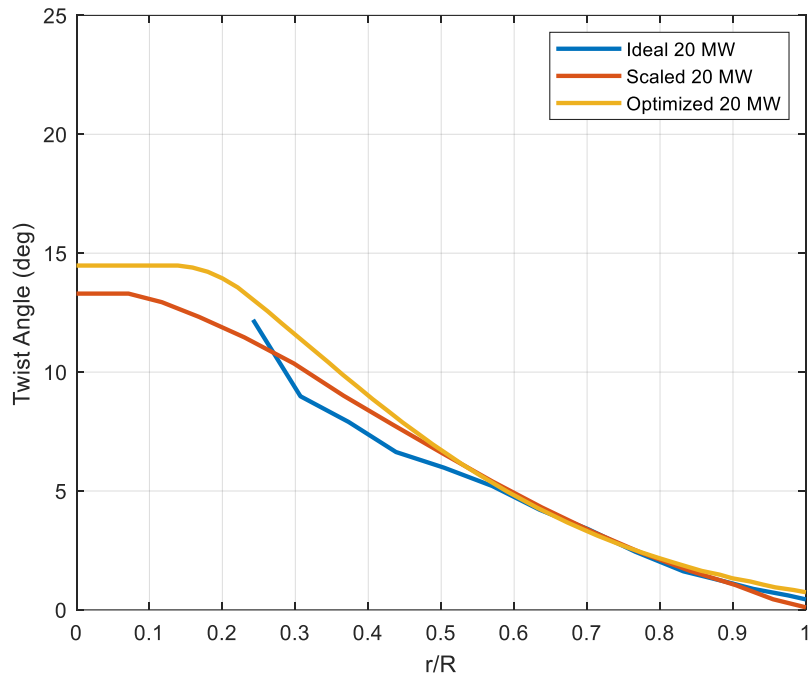


Figure 4.25 Twist Angle Comparison for 20 MW Blade

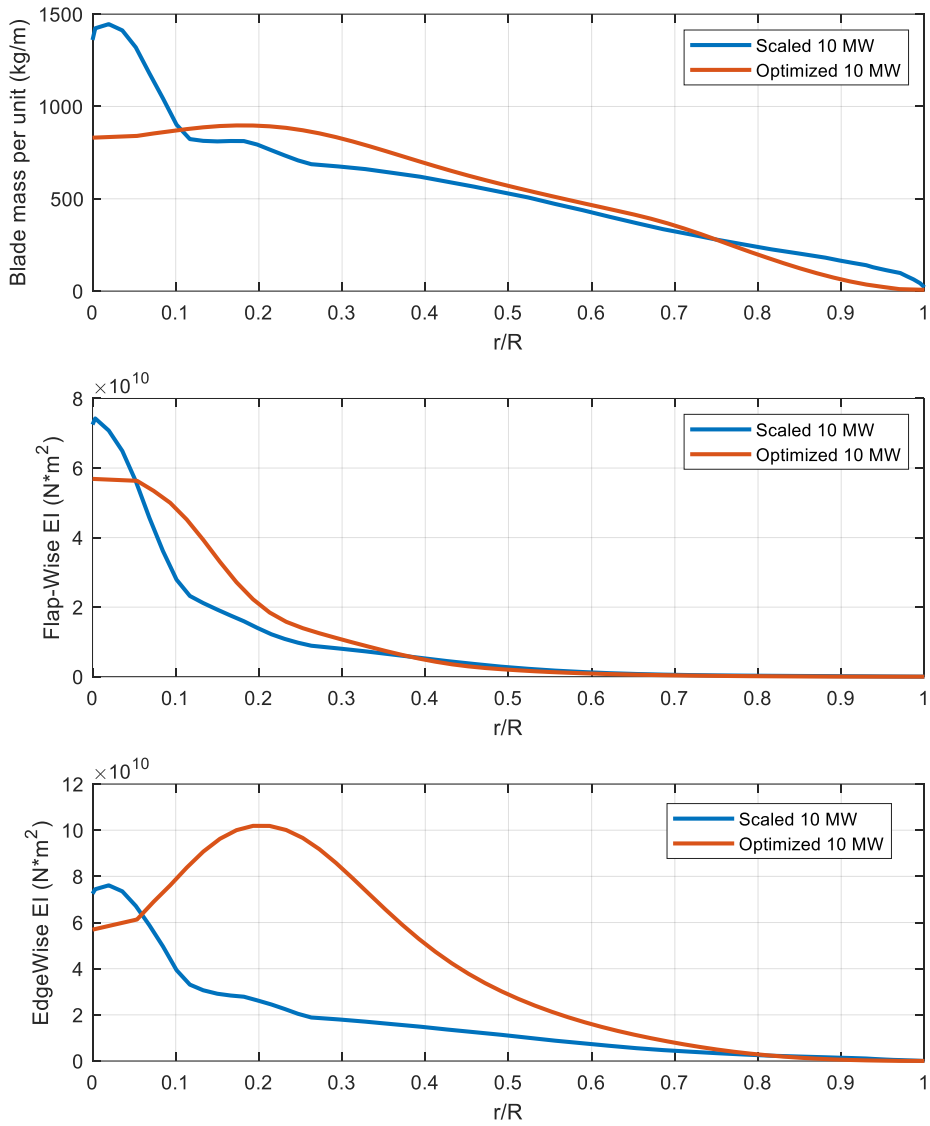


Figure 4.26 Structural Properties Comparison for 10 MW blade

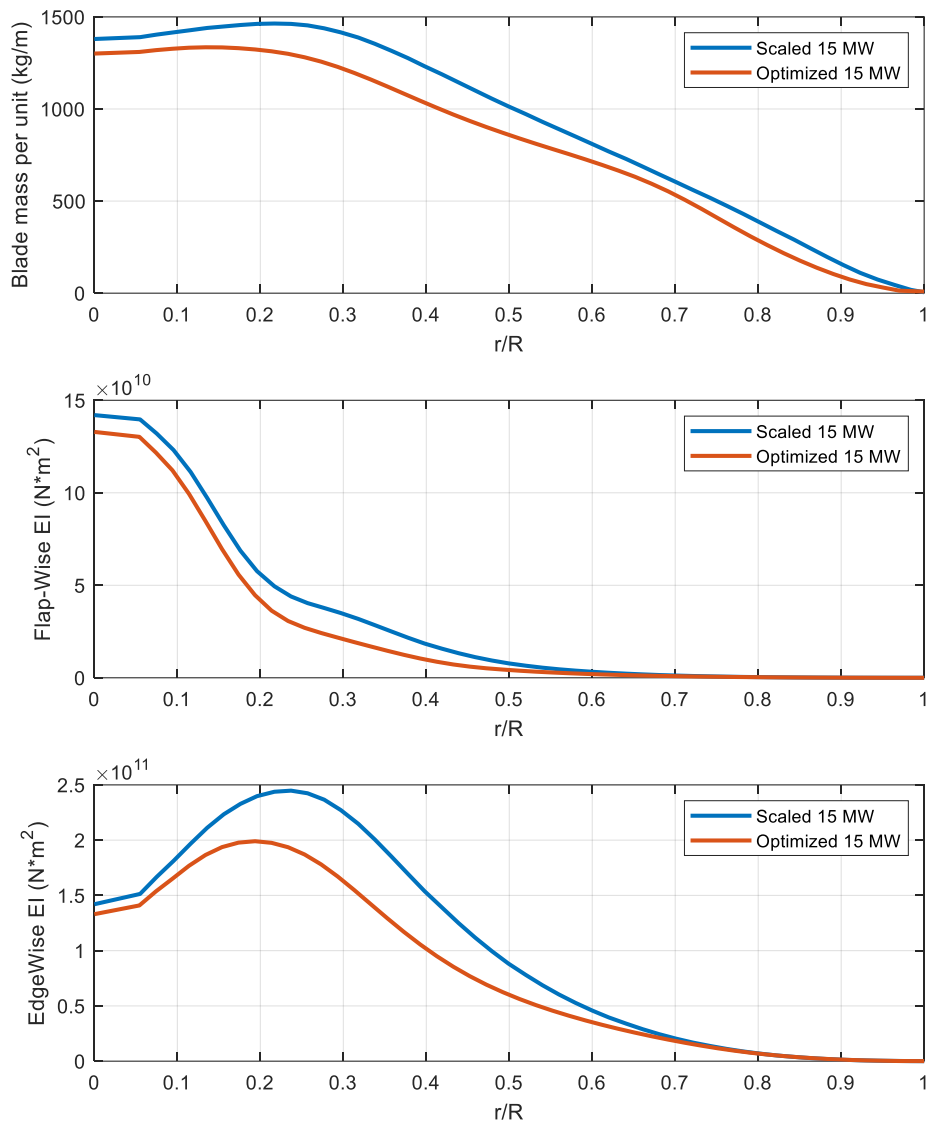


Figure 4.27 Structural Properties Comparison for 15 MW blade

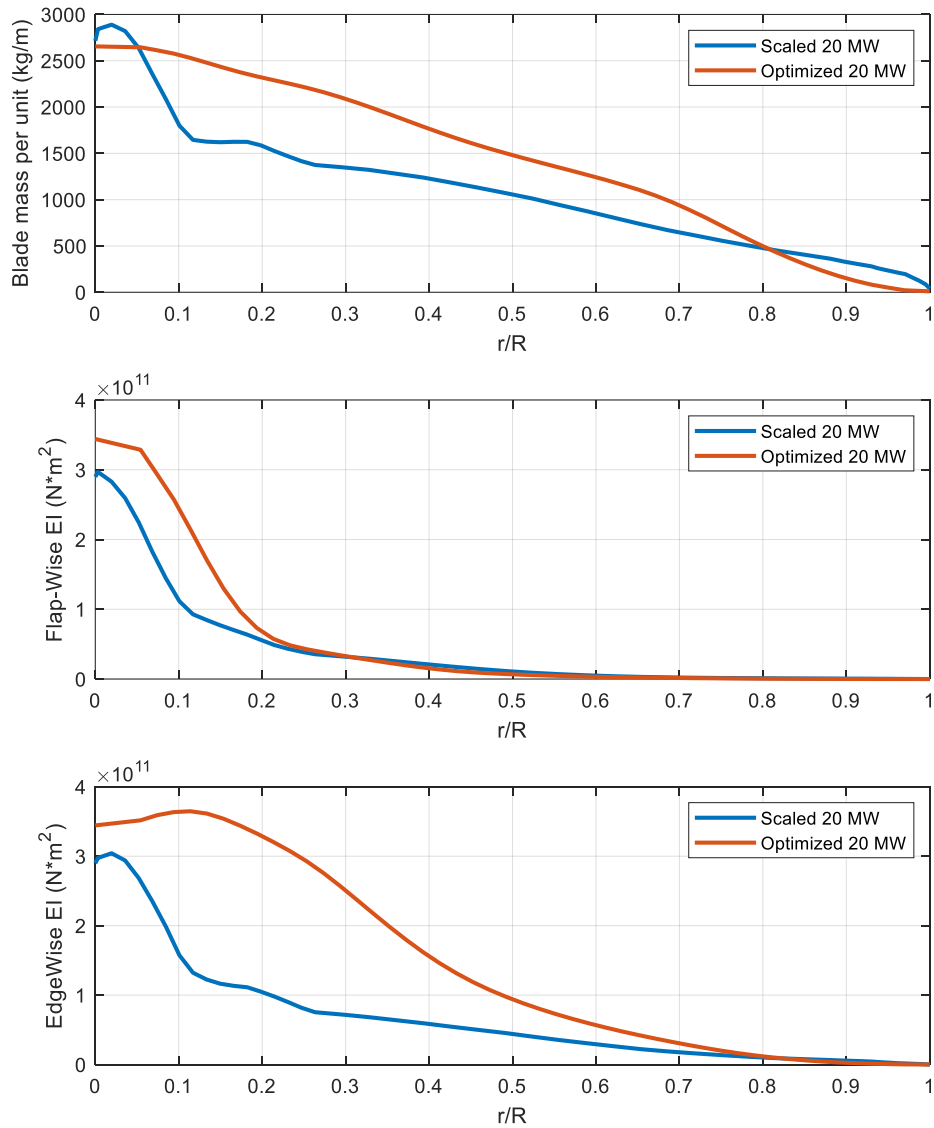


Figure 4.28 Structural Properties Comparison for 20 MW blade

Table 4-2 The gross properties of the optimized blade

Power (MW)	Diameter(m)	Length (m)	Mass (kg)	Rotational Speed (RPM)
10	178	87.0	46721	8.56
15	213	106.5	82303	7.44
20	246	123	162396	6.99

4.4.2. Performance Analysis of the Optimized 10, 15 and 20 MW Wind Turbines

Based on the blade design parameters obtained from the genetic algorithm optimization, the optimized 10, 15 and 20 MW wind turbine blades are then modelled and analyzed by using the FAST software, together with the original NREL 5 MW baseline model. The aerodynamic and structural performances are compared with each other.

As can be seen in Figure 4.29, the power coefficient value for all optimized wind turbine rotors is approximately 0.45. Compared to the results obtained with the classical scaling in Chapter 3, there is a performance increase of at least 2 times aerodynamically. In Figure 4.30, the rotor power is also presented for the optimized rotors showing power levels of 10, 15, and 20 MWs as expected.

The time-dependent thrust coefficient changes are presented in Figure 4.31 for the optimized rotors. For the optimized 10 MW wind turbine, the thrust coefficient is about 0.65. For the optimized 15 and 20 MW rotors, the thrust coefficient is about 0.6 and 0.75, respectively.

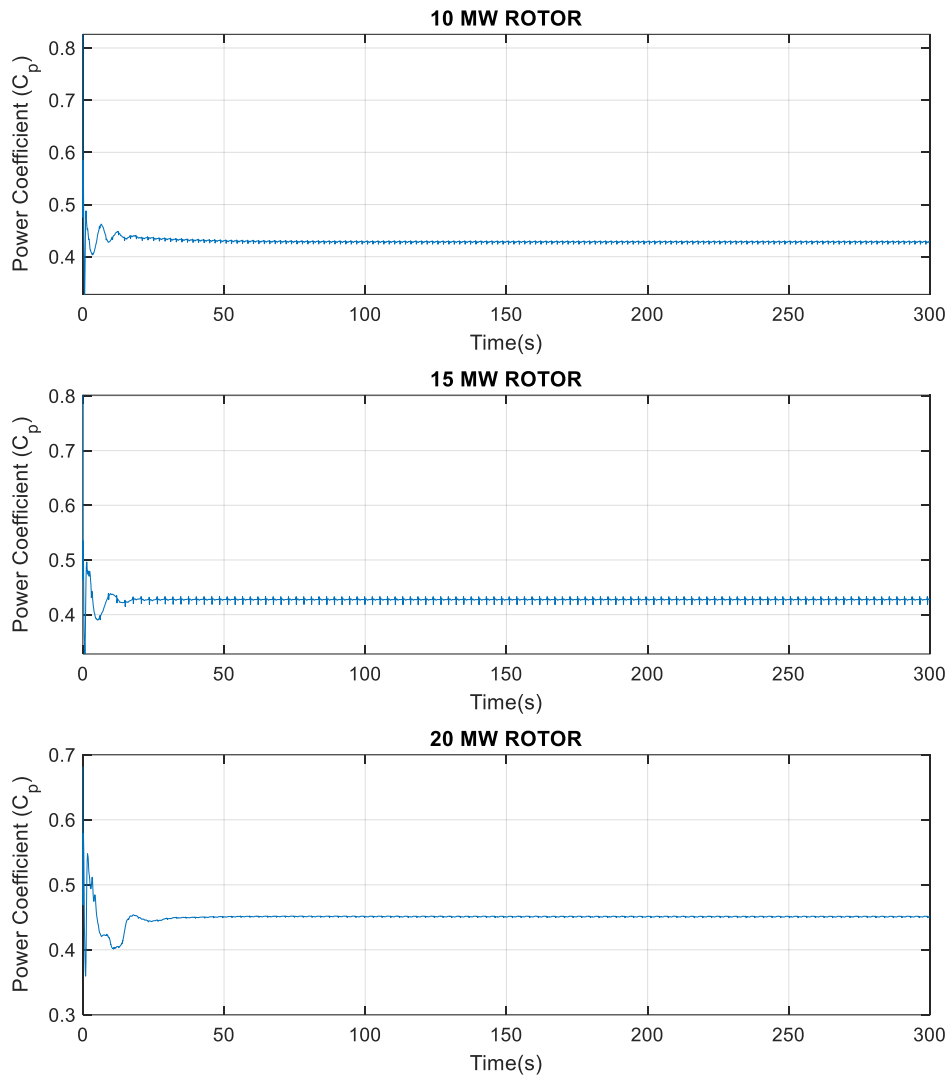


Figure 4.29 Time dependent power coefficient (C_p) for optimized wind turbine blade

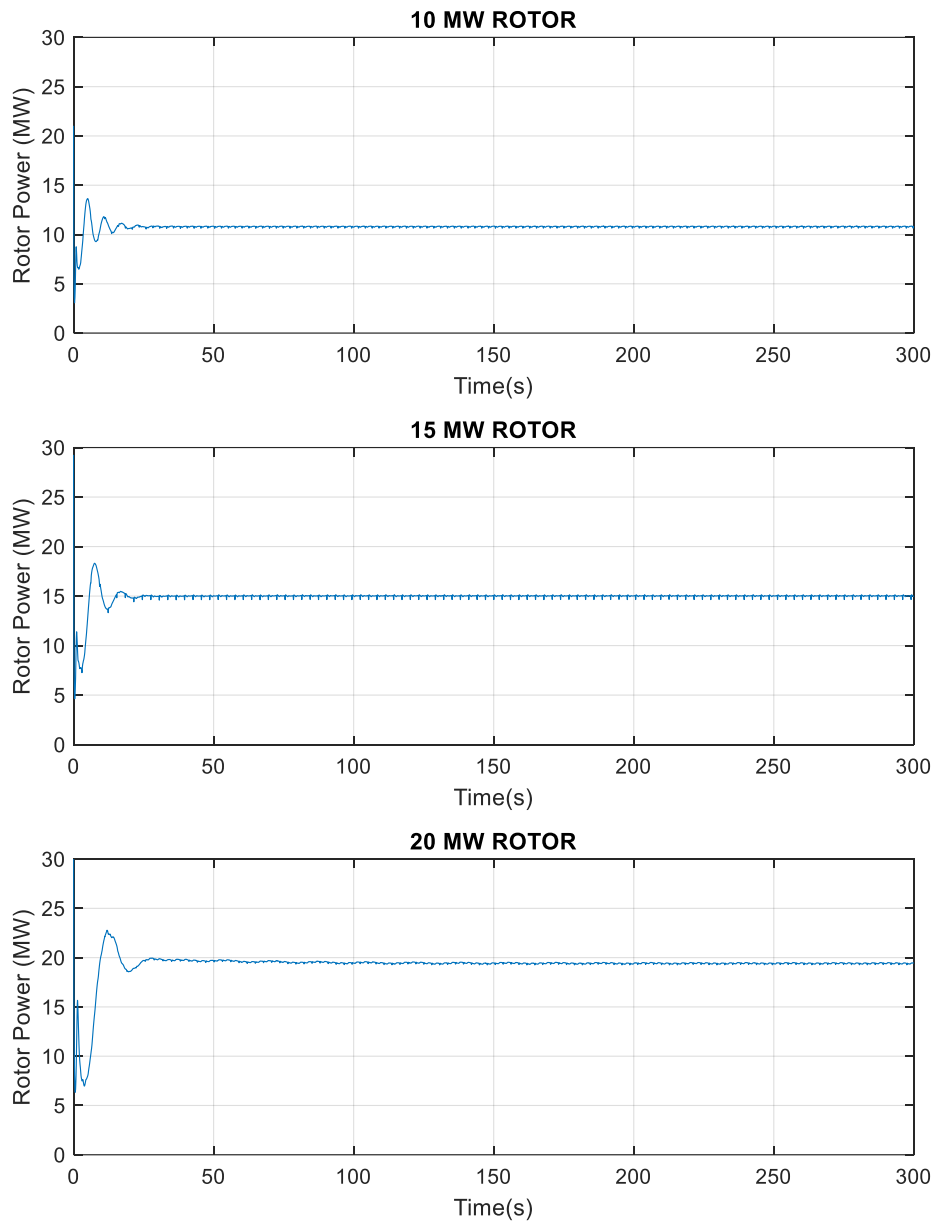


Figure 4.30 Time dependent Rotor Power for optimized wind turbine blade

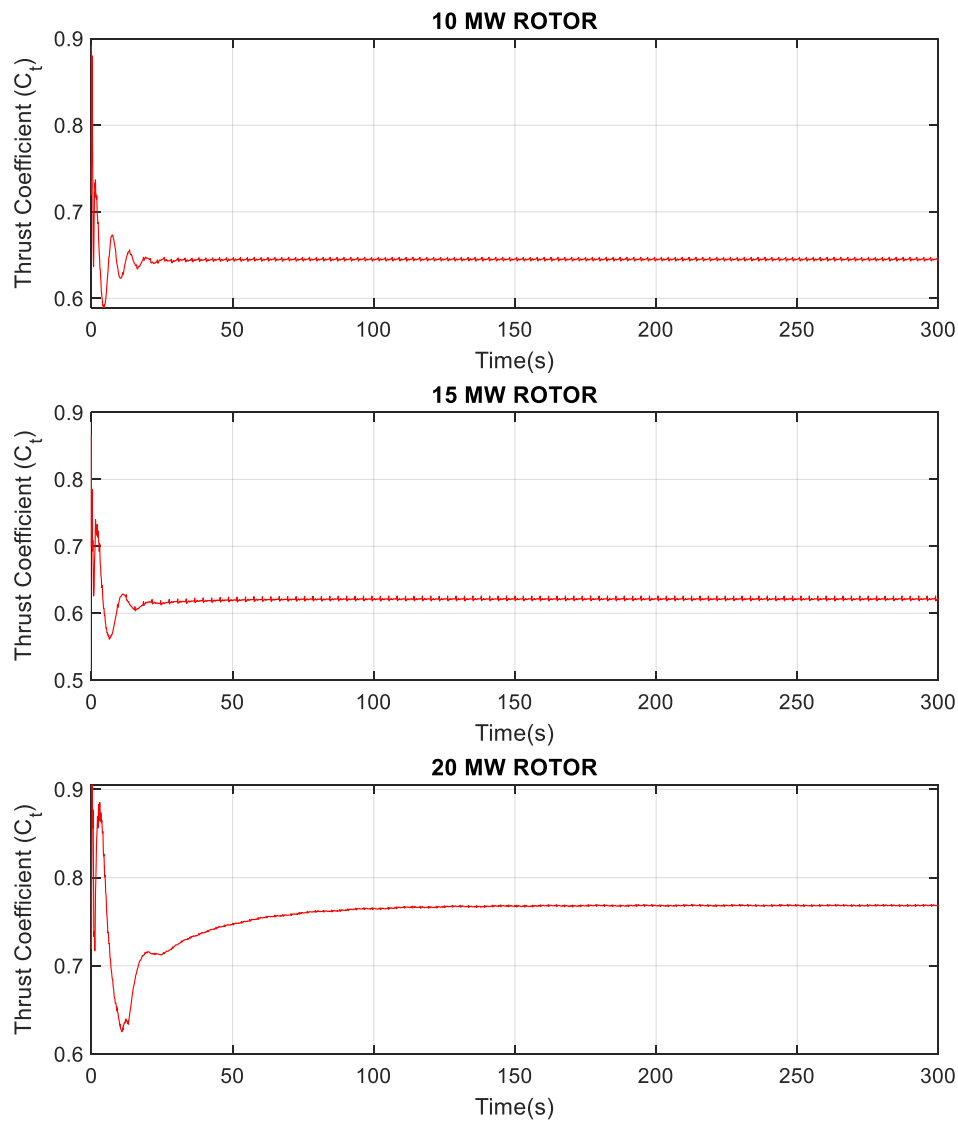


Figure 4.31 Time dependent thrust coefficient (C_t) for optimized wind turbine blade

According to the results obtained in Chapter 3, the bending moment changes in the edgewise direction shows a stable behavior for 5 MW rotor, however the moment changes show more fluctuations as the rotor size is increased. Especially, when the 20 MW model was examined, the sudden load and moment change over time was quite high and continue being unstable. However, the time-dependent moment variation in

the edgewise direction shows a very stable behavior for a fairly constant value for the optimized rotors. For optimized rotors, it is clearly observed that the structurally lighter and more rigid designs are achieved. The results for the bending momenta are shown in Figure 4.32 and Figure 4.33.

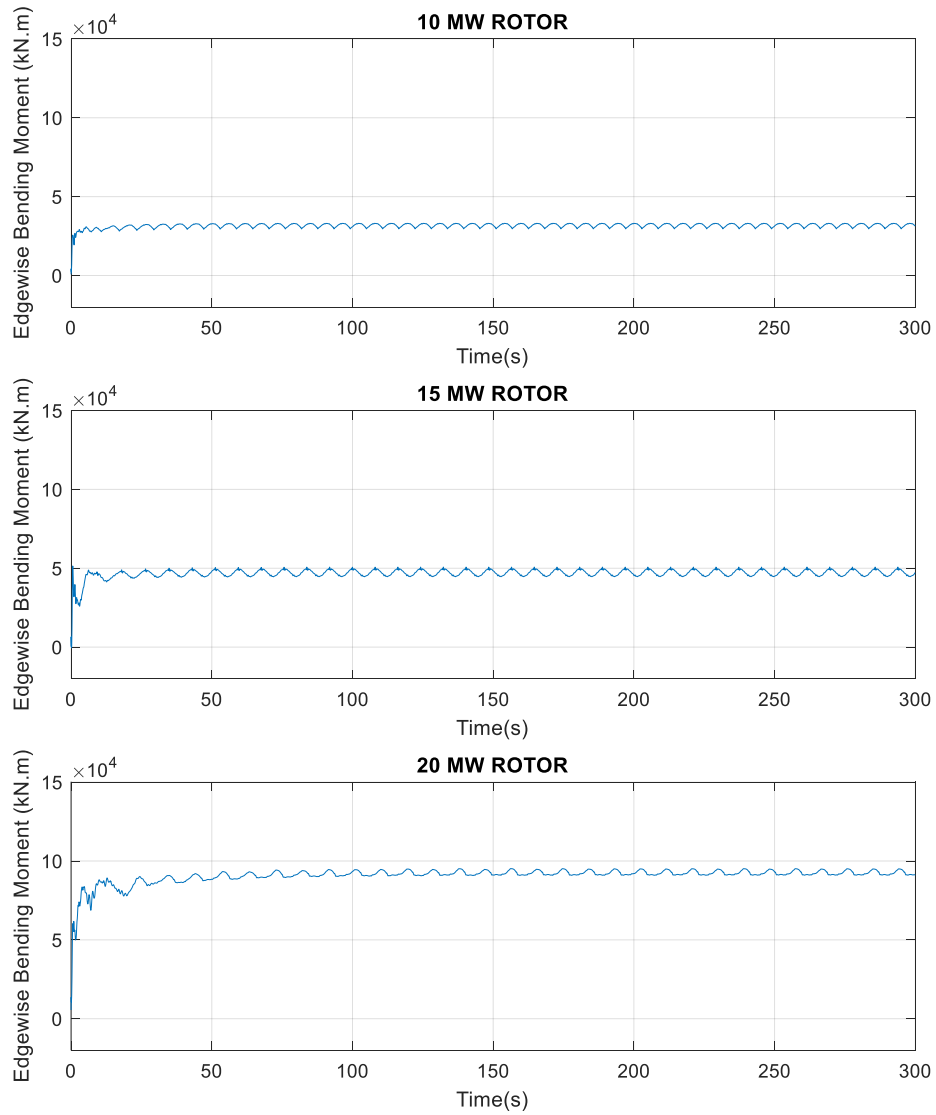


Figure 4.32 Edge-wise Bending Moment for Optimized Wind Turbine Blade

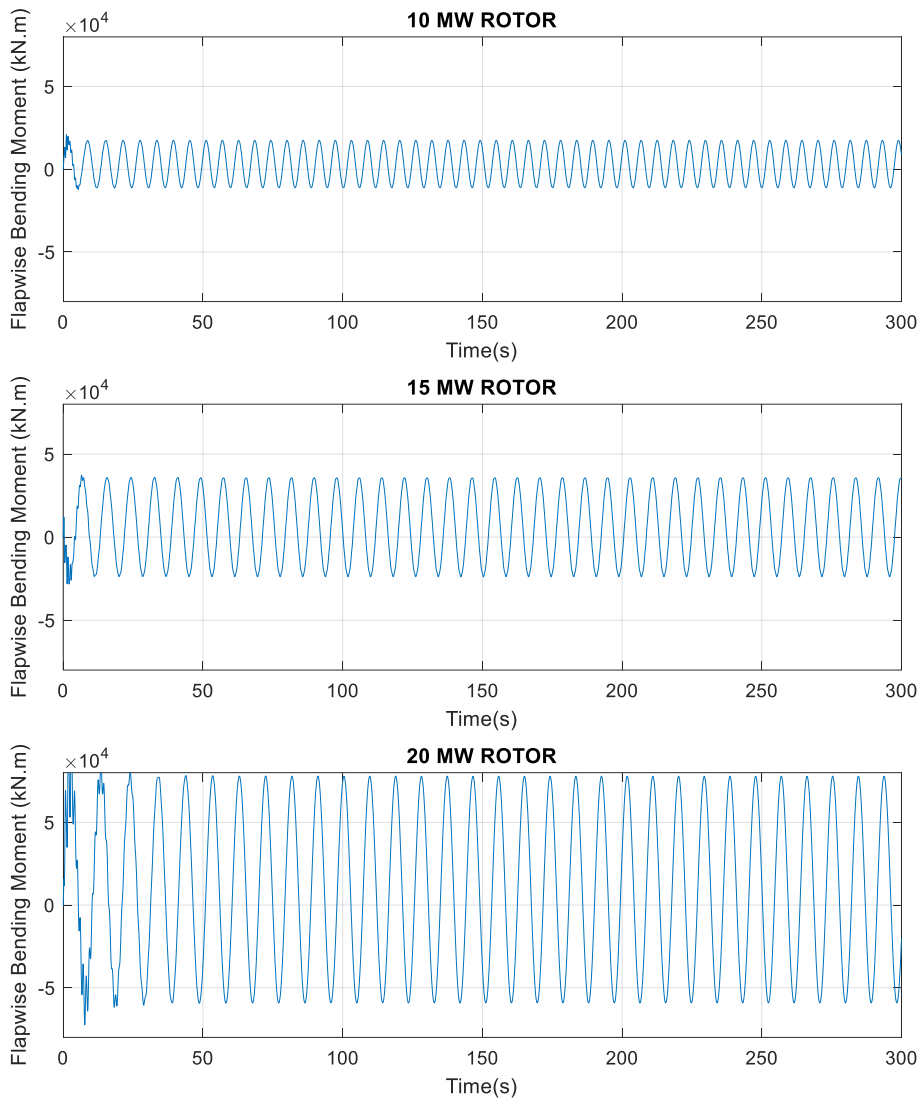


Figure 4.33 Flap-wise Bending Moment for Optimized Wind Turbine Blade

4.4.3. Scaling Trends

The design of optimized wind turbines for 10, 15 and 20 MW power levels are presented in the previous sections. Using the data obtained from these wind turbine designs, the new scaling trends are plotted to see the impact on future off-shore large-

scale wind turbine designs. The scaling trends are presented in detail in the following figures.

The total blade mass variation with diameter of the optimized wind turbines is presented in Figure 4.34. As shown in the figure, the diameter-dependent mass increase for the optimized rotor blades has an exponential value of 3.121. This value is higher than the value of 3 in the linear scaling law.

According to the linear scaling law, the exponential scale is $R^{4.654}$ for the moment-diameter relationship in the flapwise direction and $R^{4.121}$ for the edgewise direction. As can be seen in Figure 4.35 and Figure 4.36, showing more complex behavior, the bending moment scales with $R^{3.121}$ and $R^{3.695}$ for the edgewise and flapwise components, respectively.

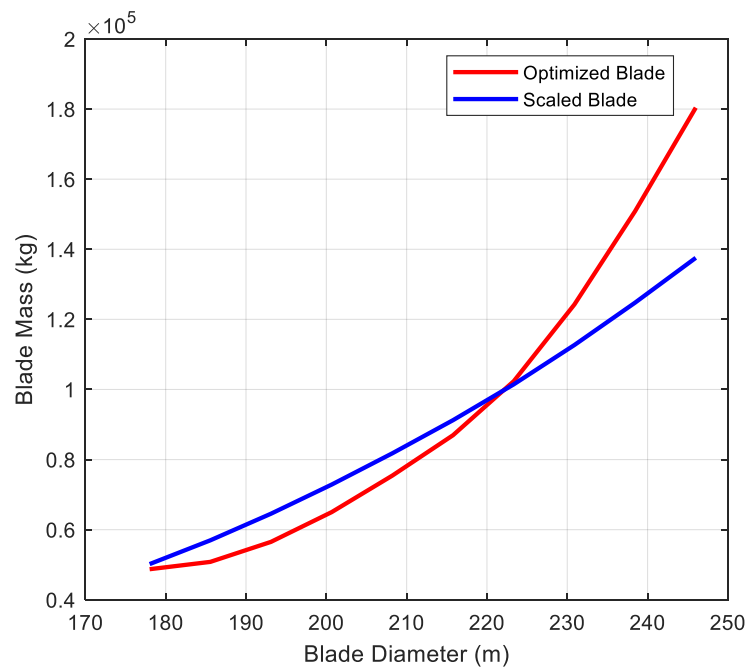


Figure 4.34 Curve fit graph for mass trend for the optimized blade and the scaled blade

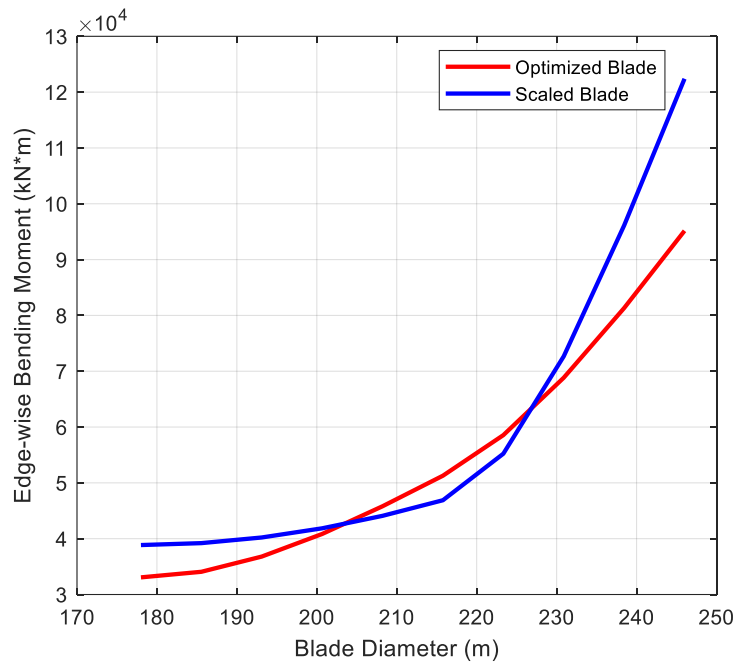


Figure 4.35 Curve fit graph for edge-wise bending moment trend for the optimized blade and the scaled blade

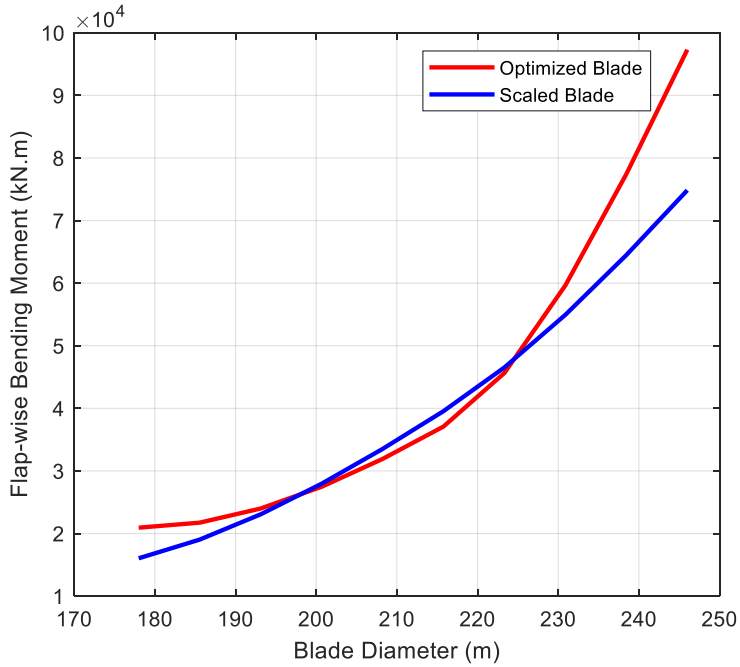


Figure 4.36 Curve fit graph for flapwise bending moment trend for the optimized blade and the scaled blade

4.5. Summary

The optimized rotor blades are analyzed both aerodynamically and structurally by using the FAST software. The optimized rotors are compared with the scaled rotors obtained in Chapter 3. Aerodynamically, a dramatic increase in power coefficient was observed for all optimized rotors compared to the scaled rotors. In addition, the structural performance results are also compared. The time-dependent changes in the bending moments analysis in the edgewise direction has become more stable for the optimized blades than the classical scaled blades. In addition, the diameter-dependent scaling trends are obtained for the scaled blades and the optimized blades. For the optimized blades, the mass increase is greater depending on the diameter. Despite this increase in the blade mass, however, the moment change with diameter is less than the blade obtained by classical scaling.

CHAPTER 5

CONCLUSION

In this thesis, the upscaling trends for designing larger-scale wind turbine rotors are investigated by an optimization methodology using the Blade Element Momentum theory and Genetic Algorithm and by comparisons of the aerodynamic and structural performances. Both the FAST software with aerodynamic and structural analyses and the HARP_Opt software with multi-purpose design optimization feature are used for the analyses and optimizations. NREL 5 MW turbine blade is taken as a reference blade and three different larger turbine blades are designed for 10 MW, 15 MW and 20 MW rotors. The aeroelastic behavior of the turbine blades are also examined and compared with each other.

First, the larger rotors are designed by using the classical upscaling rules. Both aerodynamic and structural performance losses are observed for the wind turbine rotors modeled by the classical upscaling rules, especially for very large rotors (15 and 20 MW). As a result, in order to improve the larger wind turbine rotor design, the optimization studies are performed to redesign the blade geometry. The optimum chord, twist and mass distributions of the blade geometry are obtained for better aerodynamic power performance and for structurally more rigid and lighter blades. The objective function for the blade design optimization is to maximize the annual energy production by reducing the blade mass.

In the optimization studies, the NREL 5 MW reference wind turbine rotor is first optimized as a validation case by using the BEM and GA with the HARP_Opt software. Then, the optimized NREL 5MW blade is analyzed using the FAST software and comparisons are made with the reference blade. The aerodynamic power increase of 15% is observed. By using the same design methodology, the upscaled 10 MW, 15 MW and 20 MW wind turbine rotors are optimized both aerodynamically and structurally and the comparisons are made. The blade geometry properties such as

twist angle, chord length, and the structural properties such as blade mass, flap-wise stiffness and edge-wise stiffness are compared for both the optimized and the upscaled rotor blades.

Furthermore, the optimized rotors are also analyzed both aerodynamically and structurally by using the FAST software and compared with the upscaled rotors. Aerodynamically, there is a dramatic increase in power coefficient for all optimized blades compared to the scaled blades. Structurally, the time-dependent moment change in the edge-wise direction becomes more stable for the larger-size optimized blades compared to the scaled blades.

In addition, instead of using the classical upscaling trends, from the analyses of the optimized large-scale wind turbine designs, new scaling trends that can be used during the design of such large-scale rotors are formulated. For the optimized blades, the mass increase with diameter is greater than for the scaled blades. Despite this increase, however, the moment change with diameter is much less than the classical upscaling rules.

5.1. Future Recommendations

The future works and recommendations can be summarized as;

- Instead of the aerodynamic analysis methods used, the optimization methodology can be improved by using aerodynamically more advanced methods such as Panel Methods or Computational Fluid Dynamics (CFD) analysis.
- Aerodynamic modeling can be improved by also optimizing the airfoil shapes.
- Instead of the structural analysis methods used, the optimization methodology can be improved by using structurally more advanced models such as classical lamination theory or Finite Element Analysis (FEA).
- Structural modeling can be improved by using composite blade models in which material properties and topology are more accurately modeled.

Composite layer analysis can be expanded to minimize blade mass for the optimization process.

- Instead of genetic algorithm optimization method, panel search optimization algorithm which is much faster and more determinative than genetic algorithm can be used.
- Tip Speed Ratio change with diameter can be considered during the optimization. Performance comparisons can be made for different wind speeds and pitching controls.

REFERENCES

- [1] P. Broøndsted and R. P. L. Nijssen, *Advances in wind turbine blade design and materials*. 2013.
- [2] C. Lindenburg, D. Winkelaar, and E. L. Van Der Hooft, “DOWEC 6 MW PRE-DESIGN Aero-elastic modelling of the DOWEC 6 MW pre-design in PHATAS,” *Distribution*, no. September, pp. 1–46, 2003.
- [3] C. Lindenburg, “Aeroelastic Modelling of the LMH64-5 Blade,” 2002.
- [4] J. Peeringa, R. Brood, O. Ceyhan, W. Engels, G. de Winkel, and G. De Winkel, “Upwind 20MW Wind Turbine Pre-Design: Blade design and control,” *ECN-E--11-017 December*, no. December, pp. 1–53, 2011.
- [5] J. Jonkman, S. Butterfield, W. Musial, and G. Scott, “Definition of a 5-MW Reference Wind Turbine for Offshore System Development,” 2009.
- [6] D. A. Griffin, “WindPACT Turbine Design Scaling Studies Technical Area 1 - Composite Blades for 80-to 120-Meter Rotor.,” *Natl. Renew. Energy Lab. NREL/SR-500-29492*, 2001.
- [7] D. J. Malcolm and A. C. Hansen, “WindPACT Turbine Rotor Design Study: June 2000--June 2002 (Revised),” no. April, 2006.
- [8] P. C. Capponi, T. Ashuri, G. J. W. Van Bussel, and B. Kallesoe, “A non-linear upscaling approach for wind turbines blades based on stresses,” *Eur. Wind Energy Conf. Exhib. 2011, EWEC 2011*, no. January, pp. 115–118, 2011.
- [9] R. P. L. Nijssen, M. B. Zaaijer, W. A. A. M. Bierbooms, G. A. M. van Kuik, D. R. V. van Delft, and T. van Holten, “The Application of Scaling Rules in Up-scaling and Marinisation of a Wind Turbine,” in *European Wind Energy Conference and Exhibition (EWEC)*, 2001.
- [10] G. Sieros, P. Chaviaropoulos, J. D. Sørensen, B. H. Bulder, and P. Jamieson, “Upscaling wind turbines: theoretical and practical aspects and their impact on the cost of energy,” *Wind Energy*, 2012.
- [11] T. Ashuri, M. B. Zaaijer, J. R. R. A. Martins, and J. Zhang, “Multidisciplinary design optimization of large wind turbines - Technical, economic, and design challenges,” *Energy Convers. Manag.*, vol. 123, pp. 56–70, 2016.
- [12] R. Kazacoks and P. Jamieson, “Influence of scaling effects on hub loads of a horizontal wind turbine,” *IET Conf. Publ.*, vol. 2014, no. CP651, pp. 1–6, 2014.

- [13] T. Ashuri and M. B. Zaaijer, "Size effect on wind turbine blade's design drivers," *Eur. Wind Energy Conf. Exhib. 2008*, vol. 6, pp. 3371–3376, 2008.
- [14] J. M. Jonkman and M. L. Buhl, "FAST Users Guide NREL/EL-500-29798," 2005.
- [15] T. Ashuri, *Beyond Classical Upscaling : Integrated Aeroservoelastic Design and Optimization of Large Offshore Wind Turbines*. 2012.
- [16] P. Jamieson, *Innovation in Wind Turbine Design*. 2011.
- [17] D. C. Sale, "HARP_Opt User's Guide," *NWTC Des. Codes, Available http://wind.nrel.gov/designcodes/simulators/HARP_Opt/Last Modif.*, 2010.
- [18] J. F. Manwell, J. G. McGowan, and A. L. Rogers, *Wind Energy Explained: Theory, Design and Application*. 2010.
- [19] A. James, "Turbine Blade using Genetic Algorithm," vol. 3, no. 12, pp. 875–882, 2014.

APPENDICES

A. Fast Inputs File For 10, 15 and 20 MW Optimized Rotor

```

1  ----- FAST v8.16.* INPUT FILE -----
2  FAST Certification Test #18: NREL 10.0 MW Optimized Wind Turbine (Onshore)
3  ----- SIMULATION CONTROL -----
4  false      Echo          - Echo input data to <RootName>.ech (flag)
5  "FATAL"    AbortLevel    - Error level when simulation should abort (string)
6  {"WARNING", "SEVERE", "FATAL"}
7  300      TMax          - Total run time (s)
8  0.00625  DT            - Recommended module time step (s)
9  2        InterpOrder    - Interpolation order for input/output time history
10 (-) {1=linear, 2=quadratic}
11 0        NumCrctn      - Number of correction iterations (-) {0=explicit
12 calculation, i.e., no corrections}
13 99999    DT_UJac        - Time between calls to get Jacobians (s)
14 1E+06    UJacSclFact    - Scaling factor used in Jacobians (-)
15 ----- FEATURE SWITCHES AND FLAGS -----
16 1        CompElast      - Compute structural dynamics (switch) {1=ElastoDyn;
17 2=ElastoDyn + BeamDyn for blades}
18 1        CompInflow     - Compute inflow wind velocities (switch) {0=still
19 air; 1=InflowWind; 2=external from OpenFOAM}
20 2        CompAero        - Compute aerodynamic loads (switch) {0=None;
21 1=AeroDyn v14; 2=AeroDyn v15}
22 1        CompServo      - Compute control and electrical-drive dynamics
23 (switch) {0=None; 1=ServoDyn}
24 0        CompHydro      - Compute hydrodynamic loads (switch) {0=None;
25 1=HydroDyn}
26 0        CompSub        - Compute sub-structural dynamics (switch) {0=None;
27 1=SubDyn}
28 0        CompMooring    - Compute mooring system (switch) {0=None; 1=MAP++;
29 2=FEAMooring; 3=MoorDyn; 4=OrcaFlex}
30 0        CompIce        - Compute ice loads (switch) {0=None; 1=IceFloe;
31 2=IceDyn}
32 ----- INPUT FILES -----
33 "5MW_Baseline/NRELOffshrbaseline10MWopt_Onshore_ElastoDyn.dat"  EDFile      -
34 Name of file containing ElastoDyn input parameters (quoted string)
35 "5MW_Baseline/NRELOffshrbaseline10MWopt_BeamDyn.dat"           BDBldFile(1) - Name of file
36 containing BeamDyn input parameters for blade 1 (quoted string)
37 "5MW_Baseline/NRELOffshrbaseline10MWopt_BeamDyn.dat"           BDBldFile(2) - Name of file
38 containing BeamDyn input parameters for blade 2 (quoted string)
39 "5MW_Baseline/NRELOffshrbaseline10MWopt_BeamDyn.dat"           BDBldFile(3) - Name of file
40 containing BeamDyn input parameters for blade 3 (quoted string)
41 "5MW_Baseline/NRELOffshrbaseline10MW_InflowWind_12mps.dat"     InflowFile   - Name
42 of file containing inflow wind input parameters (quoted string)
43 "5MW_Baseline/NRELOffshrbaseline10MWopt_Onshore_AeroDyn15.dat" AeroFile      -
44 Name of file containing aerodynamic input parameters (quoted string)
45 "5MW_Baseline/NRELOffshrbaseline5MW_Onshore_ServoDyn.dat"     ServoFile    - Name of
46 file containing control and electrical-drive input parameters (quoted string)
47 "unused"    HydroFile    - Name of file containing hydrodynamic input
48 parameters (quoted string)
49 "unused"    SubFile      - Name of file containing sub-structural input
50 parameters (quoted string)
51 "unused"    MooringFile  - Name of file containing mooring system input
52 parameters (quoted string)
53 "unused"    IceFile      - Name of file containing ice input parameters (quoted
54 string)
55 ----- OUTPUT -----
56 True      SumPrint      - Print summary data to "<RootName>.sum" (flag)
57 5         SttsTime      - Amount of time between screen status messages (s)
58 99999    ChkptTime      - Amount of time between creating checkpoint files for
59 potential restart (s)
60 "default" DT_Out        - Time step for tabular output (s) (or "default")
61 0         TStart        - Time to begin tabular output (s)
62 3         OutFileFmt     - Format for tabular (time-marching) output file
63 (switch) {1: text file [<RootName>.out], 2: binary file [<RootName>.outb],
64 3: both}
65 True      TabDelim      - Use tab delimiters in text tabular output file?
66 (flag) {uses spaces if false}
67 "E510.3E2" OutFmt       - Format used for text tabular output, excluding the
68 time channel. Resulting field should be 10 characters. (quoted string)
69 ----- LINEARIZATION -----

```

```

43 False      Linearize      - Linearization analysis (flag)
44      2  NLinTimes      - Number of times to linearize (-) [>=1] [unused if
      Linearize=False]
45      30,      60  LinTimes      - List of times at which to linearize (s)
      [1 to NLinTimes] [unused if Linearize=False]
46      1  LinInputs      - Inputs included in linearization (switch) {0=none;
      1=standard; 2=all module inputs (debug)} [unused if Linearize=False]
47      1  LinOutputs      - Outputs included in linearization (switch) {0=none;
      1=from OutList(s); 2=all module outputs (debug)} [unused if Linearize=False]
48 False      LinOutJac      - Include full Jacobians in linearization output (for
      debug) (flag) [unused if Linearize=False; used only if LinInputs=LinOutputs=2]
49 False      LinOutMod      - Write module-level linearization output files in
      addition to output for full system? (flag) [unused if Linearize=False]
50 ----- VISUALIZATION -----
51      0  WrVTK      - VTK visualization data output: (switch) {0=none;
      1=initialization data only; 2=animation}
52      1  VTK_type      - Type of VTK visualization data: (switch)
      {1=surfaces; 2=basic meshes (lines/points); 3=all meshes (debug)} [unused
      if WrVTK=0]
53 true      VTK_fields      - Write mesh fields to VTK data files? (flag)
      {true/false} [unused if WrVTK=0]
54      15  VTK_fps      - Frame rate for VTK output (frames per second){will
      use closest integer multiple of DT} [used only if WrVTK=2]
55

```

Figure A. 1 Fast Input File for optimized 10 MW rotor

```

1 ----- AERODYN v15.03.* INPUT FILE -----
2 NREL 10.0 MW offshore baseline aerodynamic input properties.
3 ===== General Options =====
4 False      Echo          - Echo the input to "<rootname>.AD.ech"? (flag)
5 "default"  DTAero         - Time interval for aerodynamic calculations (or
6 "default") (s)
7           1 WakeMod      - Type of wake/induction model (switch) {0=none,
           1=BEMT}
8           2 AFAeroMod    - Type of blade airfoil aerodynamics model (switch)
           {1=steady model, 2=Beddoes-Leishman unsteady model}
9           1 TwrPotent    - Type tower influence on wind based on potential
           flow around the tower (switch) {0=none, 1=baseline potential flow,
           2=potential flow with Bak correction}
10 False     TwrShadow     - Calculate tower influence on wind based on
downstream tower shadow? (flag)
11 True      TwrAero       - Calculate tower aerodynamic loads? (flag)
12 False     FrozenWake    - Assume frozen wake during linearization? (flag)
[used only when WakeMod=1 and when linearizing]
13 ===== Environmental Conditions =====
14 1.225     AirDens       - Air density (kg/m^3)
15 1.464E-05 KinVisc      - Kinematic air viscosity (m^2/s)
16 335       SpdSound     - Speed of sound (m/s)
17 ===== Blade-Element/Momentum Theory Options =====
18 2 SkewMod  - Type of skewed-wake correction model (switch)
           {1=uncoupled, 2=Pitt/Peters, 3=coupled} [used only when WakeMod=1]
19 True      TipLoss      - Use the Prandtl tip-loss model? (flag) [used only
when WakeMod=1]
20 True      HubLoss     - Use the Prandtl hub-loss model? (flag) [used only
when WakeMod=1]
21 true      TanInd      - Include tangential induction in BEMT
calculations? (flag) [used only when WakeMod=1]
22 true      AIDrag      - Include the drag term in the axial-induction
calculation? (flag) [used only when WakeMod=1]
23 true      TIDrag      - Include the drag term in the tangential-induction
calculation? (flag) [used only when WakeMod=1 and TanInd=TRUE]
24 "Default" IndToler    - Convergence tolerance for BEMT nonlinear solve
residual equation (or "default") (-) [used only when WakeMod=1]
25 100       MaxIter     - Maximum number of iteration steps (-) [used only
when WakeMod=1]
26 ===== Beddoes-Leishman Unsteady Airfoil Aerodynamics Options =====
           [used only when AFAeroMod=2]
27 3 UAMod   - Unsteady Aero Model Switch (switch) {1=Baseline
model (Original), 2=Gonzalez's variant (changes in Cn,Cc,Cm),
3=Minemima/Pierce variant (changes in Cc and Cm)} [used only when
AFAeroMod=2]
28 True      FLookup     - Flag to indicate whether a lookup for f' will be
calculated (TRUE) or whether best-fit exponential equations will be used (FALSE); if
FALSE S1-S4 must be provided in airfoil input files (flag) [used only when
AFAeroMod=2]
29 ===== Airfoil Information =====
30 1 InCol_Alfa - The column in the airfoil tables that contains
the angle of attack (-)
31 2 InCol_Cl  - The column in the airfoil tables that contains
the lift coefficient (-)
32 3 InCol_Cd  - The column in the airfoil tables that contains
the drag coefficient (-)
33 4 InCol_Cm  - The column in the airfoil tables that contains
the pitching-moment coefficient; use zero if there is no Cm column (-)
34 0 InCol_Cpmin - The column in the airfoil tables that contains
the Cpmin coefficient; use zero if there is no Cpmin column (-)
35 8 NumAFfiles - Number of airfoil files used (-)
36 "Airfoils/Cylinder1.dat" AFNames - Airfoil file names (NumAFfiles
lines) (quoted strings)
37 "Airfoils/Cylinder2.dat"
38 "Airfoils/DU40_A17.dat"
39 "Airfoils/DU35_A17.dat"
40 "Airfoils/DU30_A17.dat"

```

```

40 "Airfoils/DU25_A17.dat"
41 "Airfoils/DU21_A17.dat"
42 "Airfoils/NACA64_A17.dat"
43 ===== Rotor/Blade Properties
=====
44 True          UseBlCm          - Include aerodynamic pitching moment in
calculations? (flag)
45 "NRELOffshrBslne10MWopt_AeroDyn_blade.dat"  ADBlFile(1)      - Name of file
containing distributed aerodynamic properties for Blade #1 (-)
46 "NRELOffshrBslne10MWopt_AeroDyn_blade.dat"  ADBlFile(2)      - Name of file
containing distributed aerodynamic properties for Blade #2 (-) [unused if NumBl < 2]
47 "NRELOffshrBslne10MWopt_AeroDyn_blade.dat"  ADBlFile(3)      - Name of file
containing distributed aerodynamic properties for Blade #3 (-) [unused if NumBl < 3]
48 ===== Tower Influence and Aerodynamics
===== [used only when
TwrPotent/=0, TwrShadow=True, or TwrAero=True]
49 12 NumTwrNds          - Number of tower nodes used in the analysis (-)
[used only when TwrPotent/=0, TwrShadow=True, or TwrAero=True]
50 TwrElev          TwrDiam          TwrCd
51 (m)              (m)              (-)
52 0.000000E+00    6.000000E+00    1.000000E+00
53 8.526100E+00    5.787000E+00    1.000000E+00
54 1.705300E+01    5.574000E+00    1.000000E+00
55 2.557900E+01    5.361000E+00    1.000000E+00
56 3.410500E+01    5.148000E+00    1.000000E+00
57 4.263300E+01    4.935000E+00    1.000000E+00
58 5.115800E+01    4.722000E+00    1.000000E+00
59 5.968500E+01    4.509000E+00    1.000000E+00
60 6.821100E+01    4.296000E+00    1.000000E+00
61 7.673800E+01    4.083000E+00    1.000000E+00
62 8.526800E+01    3.870000E+00    1.000000E+00
63 8.760000E+01    3.870000E+00    1.000000E+00
64 ===== Outputs
=====
65 True          SumPrint          - Generate a summary file listing input options
and interpolated properties to "<rootname>.AD.sum"? (flag)
66 3 NBlOuts          - Number of blade node outputs [0 - 9] (-)
67 1, 9, 16 BlOutNd          - Blade nodes whose
values will be output (-)
68 0 NTwOuts          - Number of tower node outputs [0 - 9] (-)
69 1, 2, 6 TwOutNd          - Tower nodes whose
values will be output (-)
70 OutList          - The next line(s) contains a list of output
parameters. See OutListParameters.xlsx for a listing of
available output channels, (-)
71
72 "RtAeroCp,RtAeroPwr,RtAeroCt"
73 END of input file (the word "END" must appear in the first 3 columns of this last
OutList line)
74 -----
-
75

```

Figure A. 2 Aerodyn Input File for 10 MW Optimized Blade

```

1 ----- ELASTODYN v1.03.* INPUT FILE -----
2 NREL 10.0 MW Baseline Wind Turbine for Use in Offshore Analysis. Properties from
  Dutch Offshore Wind Energy Converter (DOWEC) 6MW Pre-Design (10046_009.pdf) and
  REpower 5M 5MW (5m_uk.pdf)
3 ----- SIMULATION CONTROL -----
4 False      Echo      - Echo input data to "<RootName>.ech" (flag)
5           3 Method    - Integration method: {1: RK4, 2: AB4, or 3: ABM4} (-)
6 "DEFAULT"  DT         - Integration time step (s)
7 ----- ENVIRONMENTAL CONDITION -----
8           9.80665 Gravity - Gravitational acceleration (m/s^2)
9 ----- DEGREES OF FREEDOM -----
10 True      FlapDOF1   - First flapwise blade mode DOF (flag)
11 True      FlapDOF2   - Second flapwise blade mode DOF (flag)
12 True      EdgeDOF    - First edgewise blade mode DOF (flag)
13 False     TeetDOF    - Rotor-teeter DOF (flag) [unused for 3 blades]
14 True      DrTrDOF    - Drivetrain rotational-flexibility DOF (flag)
15 True      GenDOF     - Generator DOF (flag)
16 True      YawDOF     - Yaw DOF (flag)
17 True      TwFADOF1   - First fore-aft tower bending-mode DOF (flag)
18 True      TwFADOF2   - Second fore-aft tower bending-mode DOF (flag)
19 True      TwSSDOF1   - First side-to-side tower bending-mode DOF (flag)
20 True      TwSSDOF2   - Second side-to-side tower bending-mode DOF (flag)
21 False     PtfmSgDOF  - Platform horizontal surge translation DOF (flag)
22 False     PtfmSwDOF  - Platform horizontal sway translation DOF (flag)
23 False     PtfmHvDOF  - Platform vertical heave translation DOF (flag)
24 False     PtfmRDOF   - Platform roll tilt rotation DOF (flag)
25 False     PtfmPDOF   - Platform pitch tilt rotation DOF (flag)
26 False     PtfmYDOF   - Platform yaw rotation DOF (flag)
27 ----- INITIAL CONDITIONS -----
28           0 OoPDefl   - Initial out-of-plane blade-tip displacement (meters)
29           0 IPDefl    - Initial in-plane blade-tip deflection (meters)
30           0 BLPitch(1) - Blade 1 initial pitch (degrees)
31           0 BLPitch(2) - Blade 2 initial pitch (degrees)
32           0 BLPitch(3) - Blade 3 initial pitch (degrees) [unused for 2 blades]
33           0 TeetDefl  - Initial or fixed teeter angle (degrees) [unused for 3
  blades]
34           0 Azimuth   - Initial azimuth angle for blade 1 (degrees)
35           8.56 RotSpeed - Initial or fixed rotor speed (rpm)
36           0 NacYaw    - Initial or fixed nacelle-yaw angle (degrees)
37           0 TTDspFA   - Initial fore-aft tower-top displacement (meters)
38           0 TTDspSS   - Initial side-to-side tower-top displacement (meters)
39           0 PtfmSurge - Initial or fixed horizontal surge translational
  displacement of platform (meters)
40           0 PtfmSway  - Initial or fixed horizontal sway translational
  displacement of platform (meters)
41           0 PtfmHeave - Initial or fixed vertical heave translational
  displacement of platform (meters)
42           0 PtfmRoll  - Initial or fixed roll tilt rotational displacement of
  platform (degrees)
43           0 PtfmPitch - Initial or fixed pitch tilt rotational displacement of
  platform (degrees)
44           0 PtfmYaw   - Initial or fixed yaw rotational displacement of platform
  (degrees)
45 ----- TURBINE CONFIGURATION -----
46           3 NumBl    - Number of blades (-)
47           89 TipRad   - The distance from the rotor apex to the blade tip (meters)
48           2.0 HubRad  - The distance from the rotor apex to the blade root
  (meters)
49           -2.5 PreCone(1) - Blade 1 cone angle (degrees)
50           -2.5 PreCone(2) - Blade 2 cone angle (degrees)
51           -2.5 PreCone(3) - Blade 3 cone angle (degrees) [unused for 2 blades]
52           0 HubCM    - Distance from rotor apex to hub mass [positive downwind]
  (meters)
53           0 UndSling  - Undersling length [distance from teeter pin to the rotor
  apex] (meters) [unused for 3 blades]
54           0 Delta3    - Delta-3 angle for teetering rotors (degrees) [unused for
  3 blades]
55           0 AzimBlUp - Azimuth value to use for I/O when blade 1 points up
  (degrees)
56           -5.0191 OverHang - Distance from yaw axis to rotor apex [3 blades] or
  teeter pin [2 blades] (meters)

```

```

57      1.912  ShftGagL   - Distance from rotor apex [3 blades] or teeter pin [2
      blades] to shaft strain gages [positive for upwind rotors] (meters)
58      -5    ShftTilt   - Rotor shaft tilt angle (degrees)
59      1.9    NacCMxn    - Downwind distance from the tower-top to the nacelle CM
      (meters)
60      0     NacCMyn    - Lateral distance from the tower-top to the nacelle CM
      (meters)
61      1.75   NacCMzn    - Vertical distance from the tower-top to the nacelle CM
      (meters)
62      -3.09528 NcIMUxn   - Downwind distance from the tower-top to the nacelle IMU
      (meters)
63      0     NcIMUyn   - Lateral distance from the tower-top to the nacelle IMU
      (meters)
64      2.23336 NcIMUzn   - Vertical distance from the tower-top to the nacelle IMU
      (meters)
65      1.96256 Twr2Shft  - Vertical distance from the tower-top to the rotor shaft
      (meters)
66      127.3  TowerHt    - Height of tower above ground level [onshore] or MSL
      [offshore] (meters)
67      0     TowerBsHt - Height of tower base above ground level [onshore] or MSL
      [offshore] (meters)
68      0     PtfmCMxt  - Downwind distance from the ground level [onshore] or MSL
      [offshore] to the platform CM (meters)
69      0     PtfmCMyt  - Lateral distance from the ground level [onshore] or MSL
      [offshore] to the platform CM (meters)
70      0     PtfmCMzt  - Vertical distance from the ground level [onshore] or MSL
      [offshore] to the platform CM (meters)
71      0     PtfmRefzt - Vertical distance from the ground level [onshore] or MSL
      [offshore] to the platform reference point (meters)
72      ----- MASS AND INERTIA -----
73      0     TipMass(1) - Tip-brake mass, blade 1 (kg)
74      0     TipMass(2) - Tip-brake mass, blade 2 (kg)
75      0     TipMass(3) - Tip-brake mass, blade 3 (kg) [unused for 2 blades]
76      56780  HubMass   - Hub mass (kg)
77      115926 HubIner   - Hub inertia about rotor axis [3 blades] or teeter axis
      [2 blades] (kg m^2)
78      534.116 GenIner   - Generator inertia about HSS (kg m^2)
79      240000  NacMass   - Nacelle mass (kg)
80      2.60789E+06 NacYIner - Nacelle inertia about yaw axis (kg m^2)
81      0     YawBrMass - Yaw bearing mass (kg)
82      0     PtfmMass  - Platform mass (kg)
83      0     PtfmRIner - Platform inertia for roll tilt rotation about the
      platform CM (kg m^2)
84      0     PtfmPIner - Platform inertia for pitch tilt rotation about the
      platform CM (kg m^2)
85      0     PtfmYIner - Platform inertia for yaw rotation about the platform CM
      (kg m^2)
86      ----- BLADE -----
87      49    BldNodes  - Number of blade nodes (per blade) used for analysis (-)
88      "NRELOffshrbSline10Mwopt_Blade.dat" BldFile(1) - Name of file containing
      properties for blade 1 (quoted string)
89      "NRELOffshrbSline10Mwopt_Blade.dat" BldFile(2) - Name of file containing
      properties for blade 2 (quoted string)
90      "NRELOffshrbSline10Mwopt_Blade.dat" BldFile(3) - Name of file containing
      properties for blade 3 (quoted string) [unused for 2 blades]
91      ----- ROTOR-TEETER -----
92      0     TeetMod    - Rotor-teeter spring/damper model {0: none, 1: standard,
      2: user-defined from routine UserTeet} (switch) [unused for 3 blades]
93      0     TeetDmpP   - Rotor-teeter damper position (degrees) [used only for 2
      blades and when TeetMod=1]
94      0     TeetDmp    - Rotor-teeter damping constant (N-m/(rad/s)) [used only
      for 2 blades and when TeetMod=1]
95      0     TeetCDmp   - Rotor-teeter rate-independent Coulomb-damping moment
      (N-m) [used only for 2 blades and when TeetMod=1]
96      0     TeetSStP   - Rotor-teeter soft-stop position (degrees) [used only for
      2 blades and when TeetMod=1]
97      0     TeetHStP   - Rotor-teeter hard-stop position (degrees) [used only for
      2 blades and when TeetMod=1]
98      0     TeetSSSp   - Rotor-teeter soft-stop linear-spring constant (N-m/rad)
      [used only for 2 blades and when TeetMod=1]
99      0     TeetHSSp   - Rotor-teeter hard-stop linear-spring constant (N-m/rad)

```

```

[used only for 2 blades and when TeetMod=1]
----- DRIVETRAIN -----
100
101      100  GBoxEff - Gearbox efficiency (%)
102      97   GBRatio - Gearbox ratio (-)
103  8.67637E+08  DTTorSpr - Drivetrain torsional spring (N-m/rad)
104  6.215E+06   DTTorDmp - Drivetrain torsional damper (N-m/(rad/s))
105
----- FURLING -----
106 False      Furling - Read in additional model properties for furling turbine
(flag) [must currently be FALSE]
107 "unused"     FurlFile - Name of file containing furling properties (quoted
string) [unused when Furling=False]
108
----- TOWER -----
109      20   TwrNodes - Number of tower nodes used for analysis (-)
110 "NRELOffshrbSline5MW_Onshore_ElastoDyn_Tower.dat" TwrFile - Name of file
containing tower properties (quoted string)
111
----- OUTPUT -----
112 True       SumPrint - Print summary data to "<RootName>.sum" (flag)
113      1   OutFile - Switch to determine where output will be placed: {1: in
module output file only; 2: in glue code output file only; 3: both}
(currently unused)
114 True       TabDelim - Use tab delimiters in text tabular output file? (flag)
(currently unused)
115 "ES10.3E2"  OutFmt - Format used for text tabular output (except time).
Resulting field should be 10 characters. (quoted string) (currently unused)
116      0   TStart - Time to begin tabular output (s) (currently unused)
117      1   DecFact - Decimation factor for tabular output {1: output every
time step} (-) (currently unused)
118      0   NTwGages - Number of tower nodes that have strain gages for output
[0 to 9] (-)
119      10, 19, 28   TwrGagNd - List of tower nodes that have
strain gages [1 to TwrNodes] (-) [unused if NTwGages=0]
120      3   NBlGages - Number of blade nodes that have strain gages for output
[0 to 9] (-)
121      5, 9, 13   BldGagNd - List of blade nodes that have
strain gages [1 to BldNodes] (-) [unused if NBlGages=0]
122      OutList - The next line(s) contains a list of output parameters.
See OutListParameters.xlsx for a listing of available output channels,
(-)
123 "OoPDefl1" twist - Blade 1 out-of-plane and in-plane deflections and tip
124 "IPDefl1" twist - Blade 1 out-of-plane and in-plane deflections and tip
125 "TwstDefl1" twist - Blade 1 out-of-plane and in-plane deflections and tip
126 "BldPitch1" - Blade 1 pitch angle
127 "Azimuth" - Blade 1 azimuth angle
128 "RotSpeed" - Low-speed shaft and high-speed shaft speeds
129 "GenSpeed" - Low-speed shaft and high-speed shaft speeds
130 "TTDspFA" twist - Tower fore-aft and side-to-side displacements and top
131 "TTDspSS" twist - Tower fore-aft and side-to-side displacements and top
132 "TTDspTwst" twist - Tower fore-aft and side-to-side displacements and top
133 "Spn2MLxb1" - Blade 1 local edgewise and flapwise bending moments at
span station 2 (approx. 50% span)
134 "Spn2MLyb1" - Blade 1 local edgewise and flapwise bending moments at
span station 2 (approx. 50% span)
135 "RootFxb1" - Out-of-plane shear, in-plane shear, and axial forces at
the root of blade 1
136 "RootFyb1" - Out-of-plane shear, in-plane shear, and axial forces at
the root of blade 1
137 "RootFzc1" - Out-of-plane shear, in-plane shear, and axial forces at
the root of blade 1
138 "RootMxb1" - In-plane bending, out-of-plane bending, and pitching
moments at the root of blade 1
139 "RootMyb1" - In-plane bending, out-of-plane bending, and pitching
moments at the root of blade 1
140 "RootMzb1" - In-plane bending, out-of-plane bending, and pitching
moments at the root of blade 1
141 "RotTorq" - Rotor torque and low-speed shaft 0- and 90-bending

```

```

moments at the main bearing
142 "LSSGagMya" - Rotor torque and low-speed shaft 0- and 90-bending
moments at the main bearing
143 "LSSGagMza" - Rotor torque and low-speed shaft 0- and 90-bending
moments at the main bearing
144 "YawBrFxp" - Fore-aft shear, side-to-side shear, and vertical forces
at the top of the tower (not rotating with nacelle yaw)
145 "YawBrFyp" - Fore-aft shear, side-to-side shear, and vertical forces
at the top of the tower (not rotating with nacelle yaw)
146 "YawBrFzp" - Fore-aft shear, side-to-side shear, and vertical forces
at the top of the tower (not rotating with nacelle yaw)
147 "YawBrMxp" - Side-to-side bending, fore-aft bending, and yaw moments
at the top of the tower (not rotating with nacelle yaw)
148 "YawBrMyp" - Side-to-side bending, fore-aft bending, and yaw moments
at the top of the tower (not rotating with nacelle yaw)
149 "YawBrMzp" - Side-to-side bending, fore-aft bending, and yaw moments
at the top of the tower (not rotating with nacelle yaw)
150 "TwrBsFxt" - Fore-aft shear, side-to-side shear, and vertical forces
at the base of the tower (mudline)
151 "TwrBsFyt" - Fore-aft shear, side-to-side shear, and vertical forces
at the base of the tower (mudline)
152 "TwrBsFzt" - Fore-aft shear, side-to-side shear, and vertical forces
at the base of the tower (mudline)
153 "TwrBsMxt" - Side-to-side bending, fore-aft bending, and yaw moments
at the base of the tower (mudline)
154 "TwrBsMyt" - Side-to-side bending, fore-aft bending, and yaw moments
at the base of the tower (mudline)
155 "TwrBsMzt" - Side-to-side bending, fore-aft bending, and yaw moments
at the base of the tower (mudline)
156 "TipDxbl"
157 "TipDybl"
158 END of input file (the word "END" must appear in the first 3 columns of this last
OutList line)
159 -----
160 -

```

Figure A. 3 Elastodyn Input File for 10 MW Optimized Rotor

```

1 ----- AERODYN v15.00.* BLADE DEFINITION INPUT FILE
-----
2 NREL 10.0 MW opt offshore baseline aerodynamic blade input properties; note that we
need to add the aerodynamic center to this file
3 ===== Blade Properties
=====
4 48 NumBLNds - Number of blade nodes used in the analysis (-)
5 BlSpn BlCrvAC BlSwpAC BlCrvAng BlTwist
6 BlChord BlAFID
7 (m) (m) (-) (m) (deg) (deg)
8 0.000000E+00 0.000000E+00 0.000000E+00 0.000000E+00 1.8073119E+01
9 5.810000E+00 1 1.8073119E+01
10 4.7602041E+00 0.000000E+00 0.000000E+00 0.000000E+00 1.8073119E+01
11 5.9665681E+00 1 1.8073119E+01
12 6.5336735E+00 0.000000E+00 0.000000E+00 0.000000E+00 1.8073119E+01
13 6.3454510E+00 1 1.8073119E+01
14 8.3071429E+00 0.000000E+00 0.000000E+00 0.000000E+00 1.8073119E+01
15 6.8262030E+00 1 1.8073119E+01
16 1.0080612E+01 0.000000E+00 0.000000E+00 0.000000E+00 1.8073119E+01
17 7.3311544E+00 2 1.8073119E+01
18 1.1854082E+01 0.000000E+00 0.000000E+00 0.000000E+00 1.8073119E+01
19 7.8064059E+00 2 1.8073119E+01
20 1.3627551E+01 0.000000E+00 0.000000E+00 0.000000E+00 1.8073119E+01
21 8.2134727E+00 2 1.8073119E+01
22 1.5401020E+01 0.000000E+00 0.000000E+00 0.000000E+00 1.8073119E+01
23 8.5272336E+00 2 1.8073119E+01
24 1.7174490E+01 0.000000E+00 0.000000E+00 0.000000E+00 1.8073119E+01
25 8.7323661E+00 3 1.8073119E+01
26 1.8947959E+01 0.000000E+00 0.000000E+00 0.000000E+00 1.8073119E+01
27 8.8271665E+00 3 1.8073119E+01
28 2.0721429E+01 0.000000E+00 0.000000E+00 0.000000E+00 1.8073119E+01
29 8.8285474E+00 4 1.6810407E+01
30 2.2494898E+01 0.000000E+00 0.000000E+00 0.000000E+00 1.6810407E+01
31 8.7495146E+00 4 1.6810407E+01
32 2.4268367E+01 0.000000E+00 0.000000E+00 0.000000E+00 1.5637824E+01
33 8.6073994E+00 4 1.5637824E+01
34 2.6041837E+01 0.000000E+00 0.000000E+00 0.000000E+00 1.4546069E+01
35 8.4218663E+00 4 1.4546069E+01
36 2.7815306E+01 0.000000E+00 0.000000E+00 0.000000E+00 1.3528396E+01
37 8.2079471E+00 5 1.3528396E+01
38 2.9588776E+01 0.000000E+00 0.000000E+00 0.000000E+00 1.2578100E+01
39 7.9738053E+00 5 1.2578100E+01
40 3.1362245E+01 0.000000E+00 0.000000E+00 0.000000E+00 1.1688140E+01
41 7.7307305E+00 5 1.1688140E+01
42 3.3135714E+01 0.000000E+00 0.000000E+00 0.000000E+00 1.0858113E+01
43 7.4840590E+00 5 1.0858113E+01
44 3.4909184E+01 0.000000E+00 0.000000E+00 0.000000E+00 1.0078920E+01
45 7.2376723E+00 5 1.0078920E+01
46 3.6682653E+01 0.000000E+00 0.000000E+00 0.000000E+00 9.3494557E+00
47 6.9942074E+00 6 9.3494557E+00
48 3.8456122E+01 0.000000E+00 0.000000E+00 0.000000E+00 8.6635601E+00
49 6.7552963E+00 6 8.6635601E+00
50 4.0229592E+01 0.000000E+00 0.000000E+00 0.000000E+00 8.0236607E+00
51 6.5218064E+00 6 8.0236607E+00
52 4.2003061E+01 0.000000E+00 0.000000E+00 0.000000E+00 7.4211924E+00
53 6.2940596E+00 6 7.4211924E+00
54 4.3776531E+01 0.000000E+00 0.000000E+00 0.000000E+00 6.8545864E+00
55 6.0720206E+00 6 6.8545864E+00
56 4.5550000E+01 0.000000E+00 0.000000E+00 0.000000E+00 6.3272960E+00
57 5.8574248E+00 7 6.3272960E+00
58 4.7323469E+01 0.000000E+00 0.000000E+00 0.000000E+00 5.8321120E+00
59 5.6484117E+00 7 5.8321120E+00
60 4.9096939E+01 0.000000E+00 0.000000E+00 0.000000E+00 5.3674772E+00
61 5.4443059E+00 7 5.3674772E+00
62 5.0870408E+01 0.000000E+00 0.000000E+00 0.000000E+00 4.9319645E+00
63 5.2446203E+00 7 4.9319645E+00
64 5.2643878E+01 0.000000E+00 0.000000E+00 0.000000E+00 4.5241790E+00
65 5.0518960E+00 7 4.5241790E+00
66 5.4417347E+01 0.000000E+00 0.000000E+00 0.000000E+00 4.1427589E+00
67 4.8626730E+00 7 4.1427589E+00

```

```

37 5.6190816E+01 0.0000000E+00 0.0000000E+00 0.0000000E+00 3.7863763E+00
4.6765347E+00 7
38 5.7964286E+01 0.0000000E+00 0.0000000E+00 0.0000000E+00 3.4537381E+00
4.4964810E+00 8
39 5.9737755E+01 0.0000000E+00 0.0000000E+00 0.0000000E+00 3.1437252E+00
4.3187412E+00 8
40 6.1511224E+01 0.0000000E+00 0.0000000E+00 0.0000000E+00 2.8549184E+00
4.1443471E+00 8
41 6.3284694E+01 0.0000000E+00 0.0000000E+00 0.0000000E+00 2.5858868E+00
3.9739639E+00 8
42 6.5058163E+01 0.0000000E+00 0.0000000E+00 0.0000000E+00 2.3360008E+00
3.8050867E+00 8
43 6.6831633E+01 0.0000000E+00 0.0000000E+00 0.0000000E+00 2.1039240E+00
3.6411115E+00 8
44 6.8605102E+01 0.0000000E+00 0.0000000E+00 0.0000000E+00 1.8885759E+00
3.4784853E+00 8
45 7.0378571E+01 0.0000000E+00 0.0000000E+00 0.0000000E+00 1.6889111E+00
3.3195949E+00 8
46 7.2152041E+01 0.0000000E+00 0.0000000E+00 0.0000000E+00 1.5039188E+00
3.1630044E+00 8
47 7.3925510E+01 0.0000000E+00 0.0000000E+00 0.0000000E+00 1.3326231E+00
3.0094214E+00 8
48 7.5698980E+01 0.0000000E+00 0.0000000E+00 0.0000000E+00 1.1740823E+00
2.8590233E+00 8
49 7.7472449E+01 0.0000000E+00 0.0000000E+00 0.0000000E+00 1.0273885E+00
2.7112719E+00 8
50 7.9245918E+01 0.0000000E+00 0.0000000E+00 0.0000000E+00 8.9166730E-01
2.5675938E+00 8
51 8.1019388E+01 0.0000000E+00 0.0000000E+00 0.0000000E+00 7.6607765E-01
2.4265617E+00 8
52 8.2792857E+01 0.0000000E+00 0.0000000E+00 0.0000000E+00 6.4981118E-01
2.2904858E+00 8
53 8.4566327E+01 0.0000000E+00 0.0000000E+00 0.0000000E+00 5.4321822E-01
2.1574937E+00 8
54 8.6339796E+01 0.0000000E+00 0.0000000E+00 0.0000000E+00 4.4467107E-01
2.0302259E+00 8
55
56 !bjj: because of precision in the BD-AD coupling, 61.5m didn't work, so I changed it
to 61.4999m
57 6.1500000E+01 -3.2815226E-04 -1.7737470E-01 0.0000000E+00 1.0600000E-01
1.4190000E+00 8
58

```

Figure A. 4 Aerodyn Blade Input File for 10 MW Optimized Blade

```

1 ----- ELASTODYN V1.00.* INDIVIDUAL BLADE INPUT FILE -----
2 NREL 10.0 opt MW offshore baseline blade input properties.
3 ----- BLADE PARAMETERS -----
4         49  NBlInpSt   - Number of blade input stations (-)
5     0.477465  BldFlDmp(1) - Blade flap mode #1 structural damping in percent of
        critical (%)
6     0.477465  BldFlDmp(2) - Blade flap mode #2 structural damping in percent of
        critical (%)
7     0.477465  BldEdDmp(1) - Blade edge mode #1 structural damping in percent of
        critical (%)
8 ----- BLADE ADJUSTMENT FACTORS -----
9         1  FlStTunr(1) - Blade flapwise modal stiffness tuner, 1st mode (-)
10        1  FlStTunr(2) - Blade flapwise modal stiffness tuner, 2nd mode (-)
11    1.04536  AdjBlMs   - Factor to adjust blade mass density (-) !bjj: value for
        AD14=1.04536; value for AD15=1.057344 (it would be nice to enter the requested
        blade mass instead of a factor here)
12        1  AdjFlSt   - Factor to adjust blade flap stiffness (-)
13        1  AdjEdSt   - Factor to adjust blade edge stiffness (-)
14 ----- DISTRIBUTED BLADE PROPERTIES -----
15      BlFract      PitchAxis      StrcTwst      BMassDen      FlpStfff      EdgStfff
16      (-)          (-)            (deg)         (kg/m)        (Nm^2)        (Nm^2)
17    0.0000000E+00    3.7500000E-01    1.8073119E+01    8.3101103E+02    5.6877252E+10
        5.6919360E+10
18    5.3485439E-02    3.7500000E-01    1.8073119E+01    8.3865164E+02    5.6934350E+10
        6.0003338E+10
19    7.3412061E-02    3.7500000E-01    1.8073119E+01    8.5187159E+02    5.5149476E+10
        6.7053797E+10
20    9.3338684E-02    3.7500000E-01    1.8073119E+01    8.6730483E+02    5.1803379E+10
        7.6020577E+10
21    1.1326531E-01    3.7500000E-01    1.8073119E+01    8.8050297E+02    4.6476385E+10
        8.4965823E+10
22    1.3319193E-01    3.7500000E-01    1.8073119E+01    8.9006275E+02    3.9673672E+10
        9.2535005E+10
23    1.5311855E-01    3.7500000E-01    1.8073119E+01    8.9757544E+02    3.2840953E+10
        9.8405887E+10
24    1.7304517E-01    3.7500000E-01    1.8073119E+01    9.0034846E+02    2.5820198E+10
        1.0176736E+11
25    1.9297180E-01    3.7500000E-01    1.8073119E+01    9.0191799E+02    2.0344316E+10
        1.0368219E+11
26    2.1289842E-01    3.7500000E-01    1.8073119E+01    8.9638465E+02    1.7103584E+10
        1.0370408E+11
27    2.3282504E-01    3.7500000E-01    1.8073119E+01    8.8806771E+02    1.5153953E+10
        1.0189100E+11
28    2.5275166E-01    3.7500000E-01    1.6810407E+01    8.7586590E+02    1.3824159E+10
        9.8268132E+10
29    2.7267828E-01    3.7500000E-01    1.5637824E+01    8.5837241E+02    1.2493655E+10
        9.2886952E+10
30    2.9260491E-01    3.7500000E-01    1.4546069E+01    8.3706192E+02    1.1168253E+10
        8.6450044E+10
31    3.1253153E-01    3.7500000E-01    1.3528396E+01    8.1262863E+02    9.7885791E+09
        7.9417342E+10
32    3.3245815E-01    3.7500000E-01    1.2578100E+01    7.8619140E+02    8.4845310E+09
        7.2199042E+10
33    3.5238477E-01    3.7500000E-01    1.1688140E+01    7.5923122E+02    7.3514422E+09
        6.5243894E+10
34    3.7231140E-01    3.7500000E-01    1.0858113E+01    7.3144230E+02    6.2541189E+09
        5.8592772E+10
35    3.9223802E-01    3.7500000E-01    1.0078920E+01    7.0267817E+02    5.0671616E+09
        5.2376681E+10
36    4.1216464E-01    3.7500000E-01    9.3494557E+00    6.7498800E+02    4.1056365E+09
        4.6751909E+10
37    4.3209126E-01    3.7500000E-01    8.6635601E+00    6.4824050E+02    3.3067075E+09
        4.1672844E+10
38    4.5201789E-01    3.7500000E-01    8.0236607E+00    6.2429279E+02    2.8571986E+09
        3.7314451E+10
39    4.7194451E-01    3.7500000E-01    7.4211924E+00    6.0084013E+02    2.4446954E+09
        3.3359457E+10
40    4.9187113E-01    3.7500000E-01    6.8545864E+00    5.7807690E+02    2.0873973E+09
        2.9790807E+10
41    5.1179775E-01    3.7500000E-01    6.3272960E+00    5.5631942E+02    1.7950545E+09
        2.6610661E+10

```

42	5.3172438E-01	3.7500000E-01	5.8321120E+00	5.3505967E+02	1.5279073E+09
	2.3734779E+10				
43	5.5165100E-01	3.7500000E-01	5.3674772E+00	5.1439154E+02	1.2973036E+09
	2.1140100E+10				
44	5.7157762E-01	3.7500000E-01	4.9319645E+00	4.9418068E+02	1.0919137E+09
	1.8792496E+10				
45	5.9150424E-01	3.7500000E-01	4.5241790E+00	4.7422917E+02	9.4370532E+08
	1.6634483E+10				
46	6.1143086E-01	3.7500000E-01	4.1427589E+00	4.5402629E+02	7.9992082E+08
	1.4632209E+10				
47	6.3135749E-01	3.7500000E-01	3.7863763E+00	4.3461982E+02	6.8232900E+08
	1.2858278E+10				
48	6.5128411E-01	3.7500000E-01	3.4537381E+00	4.1556829E+02	5.7542870E+08
	1.1263755E+10				
49	6.7121073E-01	3.7500000E-01	3.1437252E+00	3.9424666E+02	4.8463415E+08
	9.7844816E+09				
50	6.9113735E-01	3.7500000E-01	2.8549184E+00	3.7335072E+02	4.0261273E+08
	8.4564814E+09				
51	7.1106398E-01	3.7500000E-01	2.5858868E+00	3.4318981E+02	3.3366823E+08
	7.1263624E+09				
52	7.3099060E-01	3.7500000E-01	2.3360008E+00	3.0976267E+02	2.7636429E+08
	5.9031694E+09				
53	7.5091722E-01	3.7500000E-01	2.1039240E+00	2.7587385E+02	2.2572404E+08
	4.8225767E+09				
54	7.7084384E-01	3.7500000E-01	1.8885759E+00	2.4391897E+02	1.8246087E+08
	3.8993353E+09				
55	7.9077047E-01	3.7500000E-01	1.6889111E+00	2.1172476E+02	1.4459883E+08
	3.0914774E+09				
56	8.1069709E-01	3.7500000E-01	1.5039188E+00	1.7944237E+02	1.1163408E+08
	2.3881184E+09				
57	8.3062371E-01	3.7500000E-01	1.3326231E+00	1.4946627E+02	8.4487758E+07
	1.8086943E+09				
58	8.5055033E-01	3.7500000E-01	1.1740823E+00	1.2173768E+02	6.2364665E+07
	1.3362835E+09				
59	8.7047695E-01	3.7500000E-01	1.0273885E+00	9.4245202E+01	4.3647099E+07
	9.3647664E+08				
60	8.9040358E-01	3.7500000E-01	8.9166730E-01	7.0904836E+01	2.9599616E+07
	6.3613089E+08				
61	9.1033020E-01	3.7500000E-01	7.6607765E-01	4.9582071E+01	1.8588806E+07
	4.0051574E+08				
62	9.3025682E-01	3.7500000E-01	6.4981118E-01	3.1901152E+01	1.0711384E+07
	2.3160735E+08				
63	9.5018344E-01	3.7500000E-01	5.4321822E-01	1.7474706E+01	5.2322596E+06
	1.1355104E+08				
64	9.7011007E-01	3.7500000E-01	4.4467107E-01	7.5032086E+00	1.9974573E+06
	4.3499994E+07				
65	1.0000000E+00	3.7500000E-01	3.5292274E-01	7.0464604E+00	1.6548561E+06
	3.6030011E+07				
66	----- BLADE MODE SHAPES -----				
67	0.1322	BldFl1Sh(2) - Flap mode 1,	coeff of x^2		
68	1.5533	BldFl1Sh(3) -	, coeff of x^3		
69	-1.7077	BldFl1Sh(4) -	, coeff of x^4		
70	1.9130	BldFl1Sh(5) -	, coeff of x^5		
71	-0.8906	BldFl1Sh(6) -	, coeff of x^6		
72	-11.5974	BldFl2Sh(2) - Flap mode 2,	coeff of x^2		
73	-27.6383	BldFl2Sh(3) -	, coeff of x^3		
74	-143.4659	BldFl2Sh(4) -	, coeff of x^4		
75	343.6117	BldFl2Sh(5) -	, coeff of x^5		
76	-159.9102	BldFl2Sh(6) -	, coeff of x^6		
77	0.2644	BldEdgSh(2) - Edge mode 1,	coeff of x^2		
78	2.2095	BldEdgSh(3) -	, coeff of x^3		
79	-3.3362	BldEdgSh(4) -	, coeff of x^4		
80	2.7203	BldEdgSh(5) -	, coeff of x^5		
81	-0.8580	BldEdgSh(6) -	, coeff of x^6		
82					
83					
84					

Figure A. 5 Elastodyn Blade Input File for 10 MW Optimized Blade

```

1 ----- AERODYN v15.00.* BLADE DEFINITION INPUT FILE
-----
2 NREL 15.0 MW opt offshore baseline aerodynamic blade input properties; note that we
need to add the aerodynamic center to this file
3 ===== Blade Properties
=====
4          48 NumBLNds          - Number of blade nodes used in the analysis (-)
5      BlSpn      BlCrvAC      BlSwpAC      BlCrvAng      BlTwist
6      BlChord      BlAFID
7      (m)          (m)          (m)          (deg)          (deg)
8      (m)          (-)
9      0.000000E+00 0.000000E+00 0.000000E+00 0.000000E+00 1.9730421E+01
10     7.100000E+00 1
11     5.7806122E+00 0.000000E+00 0.000000E+00 0.000000E+00 1.9730421E+01
12     7.2643158E+00 1
13     7.9010204E+00 0.000000E+00 0.000000E+00 0.000000E+00 1.9730421E+01
14     7.6413339E+00 1
15     1.0021429E+01 0.000000E+00 0.000000E+00 0.000000E+00 1.9730421E+01
16     8.1177042E+00 1
17     1.2141837E+01 0.000000E+00 0.000000E+00 0.000000E+00 1.9730421E+01
18     8.6179853E+00 2
19     1.4262245E+01 0.000000E+00 0.000000E+00 0.000000E+00 1.9730421E+01
20     9.0904836E+00 2
21     1.6382653E+01 0.000000E+00 0.000000E+00 0.000000E+00 1.9730421E+01
22     9.4975315E+00 2
23     1.8503061E+01 0.000000E+00 0.000000E+00 0.000000E+00 1.9730421E+01
24     9.8136596E+00 2
25     2.0623469E+01 0.000000E+00 0.000000E+00 0.000000E+00 1.9730421E+01
26     1.0024440E+01 2
27     2.2743878E+01 0.000000E+00 0.000000E+00 0.000000E+00 1.9730421E+01
28     1.0121833E+01 3
29     2.4864286E+01 0.000000E+00 0.000000E+00 0.000000E+00 1.9730421E+01
30     1.0123360E+01 3
31     2.6984694E+01 0.000000E+00 0.000000E+00 0.000000E+00 1.7796843E+01
32     1.0042247E+01 4
33     2.9105102E+01 0.000000E+00 0.000000E+00 0.000000E+00 1.6224815E+01
34     9.8920119E+00 4
35     3.1225510E+01 0.000000E+00 0.000000E+00 0.000000E+00 1.4884786E+01
36     9.6951313E+00 4
37     3.3345918E+01 0.000000E+00 0.000000E+00 0.000000E+00 1.3715801E+01
38     9.4655295E+00 4
39     3.5466327E+01 0.000000E+00 0.000000E+00 0.000000E+00 1.2678659E+01
40     9.2127962E+00 5
41     3.7586735E+01 0.000000E+00 0.000000E+00 0.000000E+00 1.1745506E+01
42     8.9490067E+00 5
43     3.9707143E+01 0.000000E+00 0.000000E+00 0.000000E+00 1.0904134E+01
44     8.6803149E+00 5
45     4.1827551E+01 0.000000E+00 0.000000E+00 0.000000E+00 1.0135411E+01
46     8.4113786E+00 5
47     4.3947959E+01 0.000000E+00 0.000000E+00 0.000000E+00 9.4312562E+00
48     8.1455170E+00 6
49     4.6068367E+01 0.000000E+00 0.000000E+00 0.000000E+00 8.7815124E+00
50     7.8849149E+00 6
51     4.8188776E+01 0.000000E+00 0.000000E+00 0.000000E+00 8.1845900E+00
52     7.6308460E+00 6
53     5.0309184E+01 0.000000E+00 0.000000E+00 0.000000E+00 7.6290729E+00
54     7.3838945E+00 6
55     5.2429592E+01 0.000000E+00 0.000000E+00 0.000000E+00 7.1120926E+00
56     7.1441609E+00 6
57     5.4550000E+01 0.000000E+00 0.000000E+00 0.000000E+00 6.6347725E+00
58     6.9138464E+00 7
59     5.6670408E+01 0.000000E+00 0.000000E+00 0.000000E+00 6.1888116E+00
60     6.6910742E+00 7
61     5.8790816E+01 0.000000E+00 0.000000E+00 0.000000E+00 5.7718768E+00
62     6.4747632E+00 7
63     6.0911224E+01 0.000000E+00 0.000000E+00 0.000000E+00 5.3818354E+00
64     6.2642411E+00 7
65     6.3031633E+01 0.000000E+00 0.000000E+00 0.000000E+00 5.0167323E+00
66     6.0627615E+00 7
67     6.5152041E+01 0.000000E+00 0.000000E+00 0.000000E+00 4.6747710E+00
68     5.8658302E+00 7

```

```

37 6.7272449E+01 0.0000000E+00 0.0000000E+00 0.0000000E+00 4.3542960E+00
5.6727871E+00 7
38 6.9392857E+01 0.0000000E+00 0.0000000E+00 0.0000000E+00 4.0537786E+00
5.4868274E+00 8
39 7.1513265E+01 0.0000000E+00 0.0000000E+00 0.0000000E+00 3.7721454E+00
5.3033371E+00 8
40 7.3633673E+01 0.0000000E+00 0.0000000E+00 0.0000000E+00 3.5074405E+00
5.1232153E+00 8
41 7.5754082E+01 0.0000000E+00 0.0000000E+00 0.0000000E+00 3.2584938E+00
4.9463523E+00 8
42 7.7874490E+01 0.0000000E+00 0.0000000E+00 0.0000000E+00 3.0244748E+00
4.7706006E+00 8
43 7.9994898E+01 0.0000000E+00 0.0000000E+00 0.0000000E+00 2.8044404E+00
4.5971587E+00 8
44 8.2115306E+01 0.0000000E+00 0.0000000E+00 0.0000000E+00 2.5972384E+00
4.4238288E+00 8
45 8.4235714E+01 0.0000000E+00 0.0000000E+00 0.0000000E+00 2.4019458E+00
4.2507937E+00 8
46 8.6356122E+01 0.0000000E+00 0.0000000E+00 0.0000000E+00 2.2176986E+00
4.0769468E+00 8
47 8.8476531E+01 0.0000000E+00 0.0000000E+00 0.0000000E+00 2.0436871E+00
3.9020737E+00 8
48 9.0596939E+01 0.0000000E+00 0.0000000E+00 0.0000000E+00 1.8791518E+00
3.7248196E+00 8
49 9.2717347E+01 0.0000000E+00 0.0000000E+00 0.0000000E+00 1.7233797E+00
3.5456399E+00 8
50 9.4837755E+01 0.0000000E+00 0.0000000E+00 0.0000000E+00 1.5757009E+00
3.3621749E+00 8
51 9.6958163E+01 0.0000000E+00 0.0000000E+00 0.0000000E+00 1.4354855E+00
3.1759852E+00 8
52 9.9078571E+01 0.0000000E+00 0.0000000E+00 0.0000000E+00 1.3021411E+00
2.9836195E+00 8
53 1.0119898E+02 0.0000000E+00 0.0000000E+00 0.0000000E+00 1.1759364E+00
2.7874668E+00 8
54 1.0331939E+02 0.0000000E+00 0.0000000E+00 0.0000000E+00 1.0557451E+00
2.5836448E+00 8
55
56 !bjj: because of precision in the BD-AD coupling, 61.5m didn't work, so I changed it
to 61.4999m
57 6.1500000E+01 -3.2815226E-04 -1.7737470E-01 0.0000000E+00 1.0600000E-01
1.4190000E+00 8
58

```

Figure A. 6 Aerodyn Blade Input File for 15 MW Optimized Blade

```

1 ----- ELASTODYN V1.00.* INDIVIDUAL BLADE INPUT FILE -----
2 NREL 15.0 MW opt offshore baseline blade input properties.
3 ----- BLADE PARAMETERS -----
4         49  NBlInpSt  - Number of blade input stations (-)
5     0.477465  BldFlDmp(1) - Blade flap mode #1 structural damping in percent of
        critical (%)
6     0.477465  BldFlDmp(2) - Blade flap mode #2 structural damping in percent of
        critical (%)
7     0.477465  BldEdDmp(1) - Blade edge mode #1 structural damping in percent of
        critical (%)
8 ----- BLADE ADJUSTMENT FACTORS -----
9         1  FlStTunr(1) - Blade flapwise modal stiffness tuner, 1st mode (-)
10        1  FlStTunr(2) - Blade flapwise modal stiffness tuner, 2nd mode (-)
11    1.04536  AdjBlMs  - Factor to adjust blade mass density (-) !bjj: value for
        AD14=1.04536; value for AD15=1.057344 (it would be nice to enter the requested
        blade mass instead of a factor here)
12        1  AdjFlSt  - Factor to adjust blade flap stiffness (-)
13        1  AdjEdSt  - Factor to adjust blade edge stiffness (-)
14 ----- DISTRIBUTED BLADE PROPERTIES -----
15      BlFract      PitchAxis      StrcTwst      BMassDen      FlpStfff      EdgStfff
16      (-)          (-)          (deg)          (kg/m)          (Nm^2)          (Nm^2)
17    0.0000000E+00    3.7500000E-01    1.9730421E+01    1.3008566E+03    1.3290486E+11
18    1.3300321E+11    3.7500000E-01    1.9730421E+01    1.3086416E+03    1.3188316E+11
19    5.4278049E-02    3.7500000E-01    1.9730421E+01    1.3197446E+03    1.2592672E+11
20    1.3876937E+11    3.7500000E-01    1.9730421E+01    1.3305123E+03    1.1583263E+11
21    7.4187985E-02    3.7500000E-01    1.9730421E+01    1.3377576E+03    1.0206562E+11
22    1.5099080E+11    3.7500000E-01    1.9730421E+01    1.3383142E+03    8.4972852E+10
23    9.4097921E-02    3.7500000E-01    1.9730421E+01    1.3372620E+03    6.8484255E+10
24    1.6571787E+11    3.7500000E-01    1.9730421E+01    1.3311464E+03    5.2208364E+10
25    1.1400786E-01    3.7500000E-01    1.9730421E+01    1.3275340E+03    4.0149467E+10
26    1.7971720E+11    3.7500000E-01    1.9730421E+01    1.3167657E+03    3.3161603E+10
27    1.3391779E-01    3.7500000E-01    1.9730421E+01    1.3038414E+03    2.9195073E+10
28    1.9016861E+11    3.7500000E-01    1.7796843E+01    1.2870958E+03    2.6707058E+10
29    1.5382773E-01    3.7500000E-01    1.6224815E+01    1.2628398E+03    2.4229464E+10
30    1.9731957E+11    3.7500000E-01    1.4884786E+01    1.2331845E+03    2.1767441E+10
31    1.7373766E-01    3.7500000E-01    1.3715801E+01    1.1987123E+03    1.9177750E+10
32    1.9995524E+11    3.7500000E-01    1.2678659E+01    1.1614026E+03    1.6715089E+10
33    1.9364760E-01    3.7500000E-01    1.1745506E+01    1.1235022E+03    1.4564493E+10
34    2.0127121E+11    3.7500000E-01    1.0904134E+01    1.0844095E+03    1.2461399E+10
35    2.1355754E-01    3.7500000E-01    1.0135411E+01    1.0438055E+03    1.0155184E+10
36    2.0014348E+11    3.7500000E-01    9.4312562E+00    1.0043868E+03    8.2221742E+09
37    2.3346747E-01    3.7500000E-01    8.7815124E+00    9.6693764E+02    6.7108382E+09
38    1.9643475E+11    3.7500000E-01    8.1845900E+00    9.3350483E+02    5.8402229E+09
39    2.5337741E-01    3.7500000E-01    7.6290729E+00    9.0086954E+02    5.0362837E+09
40    1.8996733E+11    3.7500000E-01    7.1120926E+00    8.6931930E+02    4.3374206E+09
41    2.7328734E-01    3.7500000E-01    6.6347725E+00    8.3933865E+02    3.7657827E+09
42    1.8018548E+11    3.7500000E-01    6.6347725E+00    8.3933865E+02    3.7657827E+09
43    2.9319728E-01    3.7500000E-01    6.6347725E+00    8.3933865E+02    3.7657827E+09
44    1.6839525E+11    3.7500000E-01    6.6347725E+00    8.3933865E+02    3.7657827E+09
45    3.1310721E-01    3.7500000E-01    6.6347725E+00    8.3933865E+02    3.7657827E+09
46    1.5529413E+11    3.7500000E-01    6.6347725E+00    8.3933865E+02    3.7657827E+09
47    3.3301715E-01    3.7500000E-01    6.6347725E+00    8.3933865E+02    3.7657827E+09
48    1.4180454E+11    3.7500000E-01    6.6347725E+00    8.3933865E+02    3.7657827E+09
49    3.5292709E-01    3.7500000E-01    6.6347725E+00    8.3933865E+02    3.7657827E+09
50    1.2880959E+11    3.7500000E-01    6.6347725E+00    8.3933865E+02    3.7657827E+09
51    3.7283702E-01    3.7500000E-01    6.6347725E+00    8.3933865E+02    3.7657827E+09
52    1.1633198E+11    3.7500000E-01    6.6347725E+00    8.3933865E+02    3.7657827E+09
53    3.9274696E-01    3.7500000E-01    6.6347725E+00    8.3933865E+02    3.7657827E+09
54    1.0460564E+11    3.7500000E-01    6.6347725E+00    8.3933865E+02    3.7657827E+09
55    4.1265689E-01    3.7500000E-01    6.6347725E+00    8.3933865E+02    3.7657827E+09
56    9.3893483E+10    3.7500000E-01    6.6347725E+00    8.3933865E+02    3.7657827E+09
57    4.3256683E-01    3.7500000E-01    6.6347725E+00    8.3933865E+02    3.7657827E+09
58    8.4275833E+10    3.7500000E-01    6.6347725E+00    8.3933865E+02    3.7657827E+09
59    4.5247677E-01    3.7500000E-01    6.6347725E+00    8.3933865E+02    3.7657827E+09
60    7.6019481E+10    3.7500000E-01    6.6347725E+00    8.3933865E+02    3.7657827E+09
61    4.7238670E-01    3.7500000E-01    6.6347725E+00    8.3933865E+02    3.7657827E+09
62    6.8515518E+10    3.7500000E-01    6.6347725E+00    8.3933865E+02    3.7657827E+09
63    4.9229664E-01    3.7500000E-01    6.6347725E+00    8.3933865E+02    3.7657827E+09
64    6.1733673E+10    3.7500000E-01    6.6347725E+00    8.3933865E+02    3.7657827E+09
65    5.1220657E-01    3.7500000E-01    6.6347725E+00    8.3933865E+02    3.7657827E+09
66    5.5686770E+10    3.7500000E-01    6.6347725E+00    8.3933865E+02    3.7657827E+09

```

42	5.3211651E-01	3.7500000E-01	6.1888116E+00	8.1022915E+02	3.2397506E+09
	5.0217600E+10				
43	5.5202644E-01	3.7500000E-01	5.7718768E+00	7.8208122E+02	2.7833648E+09
	4.5272122E+10				
44	5.7193638E-01	3.7500000E-01	5.3818354E+00	7.5468496E+02	2.3731290E+09
	4.0781988E+10				
45	5.9184632E-01	3.7500000E-01	5.0167323E+00	7.2768031E+02	2.0806083E+09
	3.6619516E+10				
46	6.1175625E-01	3.7500000E-01	4.6747710E+00	7.0033013E+02	1.7912494E+09
	3.2720423E+10				
47	6.3166619E-01	3.7500000E-01	4.3542960E+00	6.6628534E+02	1.5364470E+09
	2.8927142E+10				
48	6.5157612E-01	3.7500000E-01	4.0537786E+00	6.3334465E+02	1.3043913E+09
	2.5521262E+10				
49	6.7148606E-01	3.7500000E-01	3.7721454E+00	5.9835016E+02	1.1087727E+09
	2.2383126E+10				
50	6.9139600E-01	3.7500000E-01	3.5074405E+00	5.6077444E+02	9.2501925E+08
	1.9432544E+10				
51	7.1130593E-01	3.7500000E-01	3.2584938E+00	5.1253687E+02	7.7363046E+08
	1.6527615E+10				
52	7.3121587E-01	3.7500000E-01	3.0244748E+00	4.6076022E+02	6.4813533E+08
	1.3850657E+10				
53	7.5112580E-01	3.7500000E-01	2.8044404E+00	4.0524537E+02	5.3083972E+08
	1.1349380E+10				
54	7.7103574E-01	3.7500000E-01	2.5972384E+00	3.5566932E+02	4.3255963E+08
	9.2524274E+09				
55	7.9094567E-01	3.7500000E-01	2.4019458E+00	3.0576309E+02	3.4446132E+08
	7.3725511E+09				
56	8.1085561E-01	3.7500000E-01	2.2176986E+00	2.5864128E+02	2.6897095E+08
	5.7610119E+09				
57	8.3076555E-01	3.7500000E-01	2.0436871E+00	2.1431339E+02	2.0493707E+08
	4.3933646E+09				
58	8.5067548E-01	3.7500000E-01	1.8791518E+00	1.7274257E+02	1.5113334E+08
	3.2435342E+09				
59	8.7058542E-01	3.7500000E-01	1.7233797E+00	1.3400953E+02	1.0670454E+08
	2.2934077E+09				
60	8.9049535E-01	3.7500000E-01	1.5757009E+00	1.0050855E+02	7.2263591E+07
	1.5560661E+09				
61	9.1040529E-01	3.7500000E-01	1.4354855E+00	6.9731467E+01	4.4934342E+07
	9.7034179E+08				
62	9.3031522E-01	3.7500000E-01	1.3021411E+00	4.3839243E+01	2.5039705E+07
	5.4239993E+08				
63	9.5022516E-01	3.7500000E-01	1.1759364E+00	2.2614239E+01	1.1323093E+07
	2.4608211E+08				
64	9.7013510E-01	3.7500000E-01	1.0557451E+00	9.5566015E+00	4.1231906E+06
	8.9876828E+07				
65	1.0000000E+00	3.7500000E-01	9.4066839E-01	8.7798682E+00	3.1983233E+06
	6.9695497E+07				
66	----- BLADE MODE SHAPES -----				
67	0.1322	BldFl1Sh(2) -	Flap mode 1,	coeff of x^2	
68	1.5533	BldFl1Sh(3) -		, coeff of x^3	
69	-1.7077	BldFl1Sh(4) -		, coeff of x^4	
70	1.9130	BldFl1Sh(5) -		, coeff of x^5	
71	-0.8906	BldFl1Sh(6) -		, coeff of x^6	
72	-11.5974	BldFl2Sh(2) -	Flap mode 2,	coeff of x^2	
73	-27.6383	BldFl2Sh(3) -		, coeff of x^3	
74	-143.4659	BldFl2Sh(4) -		, coeff of x^4	
75	343.6117	BldFl2Sh(5) -		, coeff of x^5	
76	-159.9102	BldFl2Sh(6) -		, coeff of x^6	
77	0.2644	BldEdgSh(2) -	Edge mode 1,	coeff of x^2	
78	2.2095	BldEdgSh(3) -		, coeff of x^3	
79	-3.3362	BldEdgSh(4) -		, coeff of x^4	
80	2.7203	BldEdgSh(5) -		, coeff of x^5	
81	-0.8580	BldEdgSh(6) -		, coeff of x^6	
82					
83					
84					

Figure A. 7 Elastodyn Blade Input File for 15 MW Optimized Blade

```

1 ----- AERODYN v15.00.* BLADE DEFINITION INPUT FILE
-----
2 NREL 20.0 MW offshore baseline aerodynamic blade input properties; note that we need
to add the aerodynamic center to this file
3 ===== Blade Properties
=====
4          48 NumBLNds          - Number of blade nodes used in the analysis (-)
5      BlSpn      BlCrvAC      BlSwpAC      BlCrvAng      BlTwist
6      BlChord      BlAFID
7      (m)          (m)          (m)          (deg)          (deg)
8      (m)          (-)
9      0.000000E+00 0.000000E+00 0.000000E+00 0.000000E+00 1.2727133E+01
10     8.300000E+00 1
11     6.6734694E+00 0.000000E+00 0.000000E+00 0.000000E+00 1.2727133E+01
12     8.4107678E+00 1
13     9.1224490E+00 0.000000E+00 0.000000E+00 0.000000E+00 1.2727133E+01
14     8.6648214E+00 1
15     1.1571429E+01 0.000000E+00 0.000000E+00 0.000000E+00 1.2727133E+01
16     8.9838933E+00 1
17     1.4020408E+01 0.000000E+00 0.000000E+00 0.000000E+00 1.2727133E+01
18     9.3152886E+00 2
19     1.6469388E+01 0.000000E+00 0.000000E+00 0.000000E+00 1.2727133E+01
20     9.6221936E+00 2
21     1.8918367E+01 0.000000E+00 0.000000E+00 0.000000E+00 1.2727133E+01
22     9.8774115E+00 2
23     2.1367347E+01 0.000000E+00 0.000000E+00 0.000000E+00 1.2727133E+01
24     1.0062411E+01 2
25     2.3816327E+01 0.000000E+00 0.000000E+00 0.000000E+00 1.2727133E+01
26     1.0166655E+01 3
27     2.6265306E+01 0.000000E+00 0.000000E+00 0.000000E+00 1.2727133E+01
28     1.0184426E+01 3
29     2.8714286E+01 0.000000E+00 0.000000E+00 0.000000E+00 1.2347565E+01
30     1.0129262E+01 4
31     3.1163265E+01 0.000000E+00 0.000000E+00 0.000000E+00 1.1830481E+01
32     1.0011393E+01 4
33     3.3612245E+01 0.000000E+00 0.000000E+00 0.000000E+00 1.1234935E+01
34     9.8414237E+00 4
35     3.6061224E+01 0.000000E+00 0.000000E+00 0.000000E+00 1.0599111E+01
36     9.6365505E+00 4
37     3.8510204E+01 0.000000E+00 0.000000E+00 0.000000E+00 9.9472569E+00
38     9.4075690E+00 4
39     4.0959184E+01 0.000000E+00 0.000000E+00 0.000000E+00 9.2944483E+00
40     9.1620024E+00 5
41     4.3408163E+01 0.000000E+00 0.000000E+00 0.000000E+00 8.6524090E+00
42     8.9090359E+00 5
43     4.5857143E+01 0.000000E+00 0.000000E+00 0.000000E+00 8.0259430E+00
44     8.6534292E+00 5
45     4.8306122E+01 0.000000E+00 0.000000E+00 0.000000E+00 7.4227078E+00
46     8.3987762E+00 5
47     5.0755102E+01 0.000000E+00 0.000000E+00 0.000000E+00 6.8417926E+00
48     8.1476250E+00 6
49     5.3204082E+01 0.000000E+00 0.000000E+00 0.000000E+00 6.2896006E+00
50     7.9016357E+00 6
51     5.5653061E+01 0.000000E+00 0.000000E+00 0.000000E+00 5.7642363E+00
52     7.6617533E+00 6
53     5.8102041E+01 0.000000E+00 0.000000E+00 0.000000E+00 5.2655813E+00
54     7.4283796E+00 6
55     6.0551020E+01 0.000000E+00 0.000000E+00 0.000000E+00 4.7961546E+00
56     7.2015342E+00 6
57     6.3000000E+01 0.000000E+00 0.000000E+00 0.000000E+00 4.3561164E+00
58     6.9831592E+00 6
59     6.5448980E+01 0.000000E+00 0.000000E+00 0.000000E+00 3.9430178E+00
60     6.7715523E+00 7
61     6.7897959E+01 0.000000E+00 0.000000E+00 0.000000E+00 3.5565423E+00
62     6.5657627E+00 7
63     7.0346939E+01 0.000000E+00 0.000000E+00 0.000000E+00 3.1962200E+00
64     6.3651944E+00 7
65     7.2795918E+01 0.000000E+00 0.000000E+00 0.000000E+00 2.8614530E+00
66     6.1728571E+00 7
67     7.5244898E+01 0.000000E+00 0.000000E+00 0.000000E+00 2.5515385E+00
68     5.9847168E+00 7

```

37	7.7693878E+01	0.0000000E+00	0.0000000E+00	0.0000000E+00	2.2656881E+00
	5.8001709E+00	7			
38	8.0142857E+01	0.0000000E+00	0.0000000E+00	0.0000000E+00	2.0032994E+00
	5.6223293E+00	8			
39	8.2591837E+01	0.0000000E+00	0.0000000E+00	0.0000000E+00	1.7633128E+00
	5.4469169E+00	8			
40	8.5040816E+01	0.0000000E+00	0.0000000E+00	0.0000000E+00	1.5443157E+00
	5.2748232E+00	8			
41	8.7489796E+01	0.0000000E+00	0.0000000E+00	0.0000000E+00	1.3453600E+00
	5.1061830E+00	8			
42	8.9938776E+01	0.0000000E+00	0.0000000E+00	0.0000000E+00	1.1657553E+00
	4.9387472E+00	8			
43	9.2387755E+01	0.0000000E+00	0.0000000E+00	0.0000000E+00	1.0048017E+00
	4.7742358E+00	8			
44	9.4836735E+01	0.0000000E+00	0.0000000E+00	0.0000000E+00	8.6116196E-01
	4.6101335E+00	8			
45	9.7285714E+01	0.0000000E+00	0.0000000E+00	0.0000000E+00	7.3381268E-01
	4.4471105E+00	8			
46	9.9734694E+01	0.0000000E+00	0.0000000E+00	0.0000000E+00	6.2173598E-01
	4.2839654E+00	8			
47	1.0218367E+02	0.0000000E+00	0.0000000E+00	0.0000000E+00	5.2392390E-01
	4.1206658E+00	8			
48	1.0463265E+02	0.0000000E+00	0.0000000E+00	0.0000000E+00	4.3938232E-01
	3.9561395E+00	8			
49	1.0708163E+02	0.0000000E+00	0.0000000E+00	0.0000000E+00	3.6713429E-01
	3.7906203E+00	8			
50	1.0953061E+02	0.0000000E+00	0.0000000E+00	0.0000000E+00	3.0622291E-01
	3.6224429E+00	8			
51	1.1197959E+02	0.0000000E+00	0.0000000E+00	0.0000000E+00	2.5571375E-01
	3.4525745E+00	8			
52	1.1442857E+02	0.0000000E+00	0.0000000E+00	0.0000000E+00	2.1469699E-01
	3.2785675E+00	8			
53	1.1687755E+02	0.0000000E+00	0.0000000E+00	0.0000000E+00	1.8338224E-01
	3.1020218E+00	8			
54	1.1932653E+02	0.0000000E+00	0.0000000E+00	0.0000000E+00	1.6001893E-01
	2.9201144E+00	8			
55					
56					
57	!bjj: because of precision in the BD-AD coupling, 61.5m didn't work, so I changed it to 61.4999m				
58	6.1500000E+01	-3.2815226E-04	-1.7737470E-01	0.0000000E+00	1.0600000E-01
	1.4190000E+00	8			
59					

Figure A. 8 Aerdoyn Blade Input File for 20 MW Optimized Blade

```

1 ----- ELASTODYN V1.00.* INDIVIDUAL BLADE INPUT FILE -----
2 NREL 20.0 MW opt offshore baseline blade input properties.
3 ----- BLADE PARAMETERS -----
4         49  NBlInpSt   - Number of blade input stations (-)
5         0.477465  BldFlDmp(1) - Blade flap mode #1 structural damping in percent of
          critical (%)
6         0.477465  BldFlDmp(2) - Blade flap mode #2 structural damping in percent of
          critical (%)
7         0.477465  BldEdDmp(1) - Blade edge mode #1 structural damping in percent of
          critical (%)
8 ----- BLADE ADJUSTMENT FACTORS -----
9         1  FlStTunr(1) - Blade flapwise modal stiffness tuner, 1st mode (-)
10        1  FlStTunr(2) - Blade flapwise modal stiffness tuner, 2nd mode (-)
11        1.04536  AdjBlMs   - Factor to adjust blade mass density (-) !bjj: value for
          AD14=1.04536; value for AD15=1.057344 (it would be nice to enter the requested
          blade mass instead of a factor here)
12        1  AdjFlSt   - Factor to adjust blade flap stiffness (-)
13        1  AdjEdSt   - Factor to adjust blade edge stiffness (-)
14 ----- DISTRIBUTED BLADE PROPERTIES -----
15        BFract      PitchAxis      StrcTwst      BMassDen      FlpStfff      EdgStfff
16        (-)         (-)           (deg)         (kg/m)         (Nm^2)         (Nm^2)
17        0.0000000E+00  3.7500000E-01  1.2727133E+01  2.6550998E+03  3.4408205E+11
          3.4433556E+11
18        5.4255849E-02  3.7500000E-01  1.2727133E+01  2.6524565E+03  3.3576396E+11
          3.5049430E+11
19        7.4166252E-02  3.7500000E-01  1.2727133E+01  2.6281760E+03  3.0606854E+11
          3.6018460E+11
20        9.4076655E-02  3.7500000E-01  1.2727133E+01  2.5899268E+03  2.6454500E+11
          3.6870015E+11
21        1.1398706E-01  3.7500000E-01  1.2727133E+01  2.5388129E+03  2.1600630E+11
          3.7165850E+11
22        1.3389746E-01  3.7500000E-01  1.2727133E+01  2.4760769E+03  1.6468546E+11
          3.6627801E+11
23        1.5380786E-01  3.7500000E-01  1.2727133E+01  2.4190927E+03  1.2095217E+11
          3.5666703E+11
24        1.7371827E-01  3.7500000E-01  1.2727133E+01  2.3661185E+03  8.4042517E+10
          3.4339190E+11
25        1.9362867E-01  3.7500000E-01  1.2727133E+01  2.3256328E+03  6.1944278E+10
          3.3140253E+11
26        2.1353907E-01  3.7500000E-01  1.2727133E+01  2.2889375E+03  5.2134797E+10
          3.2134945E+11
27        2.3344948E-01  3.7500000E-01  1.2347565E+01  2.2562658E+03  4.6822894E+10
          3.1016684E+11
28        2.5335988E-01  3.7500000E-01  1.1830481E+01  2.2162396E+03  4.2329117E+10
          2.9555399E+11
29        2.7327028E-01  3.7500000E-01  1.1234935E+01  2.1680684E+03  3.8134963E+10
          2.7790158E+11
30        2.9318069E-01  3.7500000E-01  1.0599111E+01  2.1134155E+03  3.4134234E+10
          2.5837888E+11
31        3.1309109E-01  3.7500000E-01  9.9472569E+00  2.0524601E+03  3.0034954E+10
          2.3766178E+11
32        3.3300149E-01  3.7500000E-01  9.2944483E+00  1.9880898E+03  2.6196704E+10
          2.1689612E+11
33        3.5291190E-01  3.7500000E-01  8.6524090E+00  1.9234769E+03  2.2871948E+10
          1.9714072E+11
34        3.7282230E-01  3.7500000E-01  8.0259430E+00  1.8571140E+03  1.9623006E+10
          1.7825309E+11
35        3.9273270E-01  3.7500000E-01  7.4227078E+00  1.7879328E+03  1.6035789E+10
          1.6046075E+11
36        4.1264311E-01  3.7500000E-01  6.8417926E+00  1.7205633E+03  1.3021986E+10
          1.4415425E+11
37        4.3255351E-01  3.7500000E-01  6.2896006E+00  1.6564388E+03  1.0662089E+10
          1.2948457E+11
38        4.5246391E-01  3.7500000E-01  5.7642363E+00  1.6022697E+03  9.3173384E+09
          1.1748156E+11
39        4.7237432E-01  3.7500000E-01  5.2655813E+00  1.5494675E+03  8.0669935E+09
          1.0654461E+11
40        4.9228472E-01  3.7500000E-01  4.7961546E+00  1.4983059E+03  6.9750854E+09
          9.6596800E+10
41        5.1219512E-01  3.7500000E-01  4.3561164E+00  1.4494180E+03  6.0797957E+09
          8.7641434E+10

```

```

42 5.3210553E-01 3.7500000E-01 3.9430178E+00 1.4019753E+03 5.2496198E+09
7.9513766E+10
43 5.5201593E-01 3.7500000E-01 3.5565423E+00 1.3559939E+03 4.5260781E+09
7.2117511E+10
44 5.7192633E-01 3.7500000E-01 3.1962200E+00 1.3112237E+03 3.8716743E+09
6.5371972E+10
45 5.9183673E-01 3.7500000E-01 2.8614530E+00 1.2621643E+03 3.3970625E+09
5.8811786E+10
46 6.1174714E-01 3.7500000E-01 2.5515385E+00 1.2171307E+03 2.9347620E+09
5.2858355E+10
47 6.3165754E-01 3.7500000E-01 2.2656881E+00 1.1625634E+03 2.5323324E+09
4.7121561E+10
48 6.5156794E-01 3.7500000E-01 2.0032994E+00 1.1136030E+03 2.1689024E+09
4.2084513E+10
49 6.7147835E-01 3.7500000E-01 1.7633128E+00 1.0487481E+03 1.8431767E+09
3.7015792E+10
50 6.9138875E-01 3.7500000E-01 1.5443157E+00 9.8954371E+02 1.5511654E+09
3.2546913E+10
51 7.1129915E-01 3.7500000E-01 1.3453600E+00 9.0417293E+02 1.3043806E+09
2.7868491E+10
52 7.3120956E-01 3.7500000E-01 1.1657553E+00 8.0726597E+02 1.0945641E+09
2.3376671E+10
53 7.5111996E-01 3.7500000E-01 1.0048017E+00 7.1199178E+02 9.0706484E+08
1.9365198E+10
54 7.7103036E-01 3.7500000E-01 8.6116196E-01 6.2126267E+02 7.4229721E+08
1.5843301E+10
55 7.9094077E-01 3.7500000E-01 7.3381268E-01 5.3211845E+02 5.9554918E+08
1.2709704E+10
56 8.1085117E-01 3.7500000E-01 6.2173598E-01 4.4758629E+02 4.6814194E+08
9.9923512E+09
57 8.3076157E-01 3.7500000E-01 5.2392390E-01 3.6766881E+02 3.5845320E+08
7.6559093E+09
58 8.5067198E-01 3.7500000E-01 4.3938232E-01 2.9502427E+02 2.6708797E+08
5.7111972E+09
59 8.7058238E-01 3.7500000E-01 3.6713429E-01 2.2939433E+02 1.9209131E+08
4.1134305E+09
60 8.9049278E-01 3.7500000E-01 3.0622291E-01 1.6789784E+02 1.2943253E+08
2.7771092E+09
61 9.1040319E-01 3.7500000E-01 2.5571375E-01 1.1562938E+02 8.1587965E+07
1.7552375E+09
62 9.3031359E-01 3.7500000E-01 2.1469699E-01 7.2013385E+01 4.6131193E+07
9.9651687E+08
63 9.5022399E-01 3.7500000E-01 1.8338224E-01 3.8808583E+01 2.2384834E+07
4.8557860E+08
64 9.7013440E-01 3.7500000E-01 1.6001893E-01 1.5110373E+01 7.7602398E+06
1.6901825E+08
65 1.0000000E+00 3.7500000E-01 1.4319419E-01 1.0115785E+01 4.5588422E+06
9.9391979E+07
66 ----- BLADE MODE SHAPES -----
67 0.0622 BldFl1Sh(2) - Flap mode 1, coeff of x^2
68 1.7254 BldFl1Sh(3) - , coeff of x^3
69 -3.2452 BldFl1Sh(4) - , coeff of x^4
70 4.7131 BldFl1Sh(5) - , coeff of x^5
71 -2.2555 BldFl1Sh(6) - , coeff of x^6
72 -0.5809 BldFl2Sh(2) - Flap mode 2, coeff of x^2
73 1.2067 BldFl2Sh(3) - , coeff of x^3
74 -15.5349 BldFl2Sh(4) - , coeff of x^4
75 29.7347 BldFl2Sh(5) - , coeff of x^5
76 -13.8255 BldFl2Sh(6) - , coeff of x^6
77 0.3627 BldEdgSh(2) - Edge mode 1, coeff of x^2
78 2.5337 BldEdgSh(3) - , coeff of x^3
79 -3.5772 BldEdgSh(4) - , coeff of x^4
80 2.376 BldEdgSh(5) - , coeff of x^5
81 -0.6952 BldEdgSh(6) - , coeff of x^6
82
83
84

```

Figure A. 9 Elastodyn Blade Input File for 20 MW Optimized Blade

